ABSTRACT

Title of Thesis:	UNDERSTANDING THE RELEVANCE OF EXTENDED AMYGDALA REACTIVITY TO DISPOSITIONAL NEGATIVITY
	Shannon E. Grogans, Master of Science, 2021
Thesis Directed By:	Dr. Alexander J. Shackman, Associate Professor, Department of Psychology

Elevated dispositional negativity (DN; i.e., neuroticism/negative emotionality) is associated with a range of deleterious outcomes, including mental illness. Yet, DN's neurobiology remains incompletely understood. Prior work suggests that DN reflects heightened threat-elicited reactivity in the extended amygdala (EAc), a circuit encompassing the central nucleus (Ce) and the bed nucleus of the stria terminalis (BST), and that this association may be intensified for *uncertain* threat. We utilized a multi-trait, multi-occasion DN composite and neuroimaging assays of threat anticipation and perception to demonstrate that individuals with elevated DN show heightened BST activation during threat anticipation. Analyses revealed that DN is uniquely predicted by BST reactivity to uncertain threat. DN was unrelated to Ce activation during threat anticipation or EAc activation during 'threatening'-face presentation. Follow-up analyses revealed that the threat paradigms are not interchangeable probes of EAc function. These observations lay the foundation for future studies necessary to determine causation and improve interventions.

UNDERSTANDING THE RELEVANCE OF EXTENDED AMYGDALA REACTIVITY TO DISPOSITIONAL NEGATIVITY

by

Shannon E. Grogans

Thesis submitted to the Faculty of the Graduate School of the
University of Maryland, College Park, in partial fulfillment
of the requirements for the degree of
Master of Science
2021

Advisory Committee:
Professor Alexander Shackman, Chair
Professor Lea Dougherty
Professor Arianna Gard

Table of Contents

This Table of Contents is automatically generated by MS Word, linked to the Heading formats used within the Chapter text.

List of Tables

List of Figures

Introduction

Dispositional negativity (i.e., neuroticism or negative emotionality)—the propensity to experience and express more intense, frequent, or persistent negative affect—is a fundamental dimension of mammalian temperament (Boissy, 1995; Hur, Stockbridge, Fox, & Shackman, 2019; Shackman, Stockbridge, LeMay, & Fox, 2018; Shackman et al., 2016). Elevated levels of dispositional negativity are associated with a wide range of practically important outcomes, from marital stability and socioeconomic attainment to mental illness and premature death. Despite this, our understanding of the brain bases of dispositional negativity remains far from complete.

The Nature of Dispositional Negativity

Dispositional negativity encompasses a range of overlapping measures and traits, including neuroticism, negative affectivity/emotionality, anxious temperament, behavioral inhibition, harm avoidance, and trait anxiety (Caspi, Roberts, & Shiner, 2005; Knowles & Olatunji, in press; Shackman et al., 2016; Watson, Stanton, & Clark, 2017; Zentner & Shiner, 2012). This extended family of distress-promoting phenotypes first emerges early in development, persists into adulthood, and reflects a combination of genetic and environmental factors (Cheesman et al., 2020; Hur et al., 2019; Kendler et al., 2019; Valk et al., 2020). The structure of dispositional negativity is relatively invariant across cultures, languages, and ages—at least from elementary school onward (Hur et al., 2019). Core features of this family of traits, including hypervigilance and behavioral inhibition, manifest similarly across mammalian species, enabling mechanistic (e.g., focal perturbation) research to be performed in rodents and monkeys

(Fox & Kalin, 2014; Fox & Shackman, 2019; Fox et al., in press; Kalin et al., 2016; Kenwood & Kalin, 2020; Oler, Fox, Shackman, & Kalin, 2016). Individual differences in dispositional negativity are highly reliable, show substantial agreement across instruments and informants, and are lawfully associated with behavior in the laboratory and in the real world (Geukes et al., 2019; Gross, Sutton, & Ketelaar, 1998; Hur et al., 2019; Lenhausen, van Scheppingen, & Bleidorn, 2020; Oltmanns, Jackson, & Oltmanns, 2020; Thake & Zelenski, 2013).

The Deleterious Consequences of Dispositional Negativity

Individual differences in dispositional negativity have important consequences for health, wealth, and wellbeing—drawing the attention of social scientists, biomedical researchers, clinicians, and policy makers (Barlow, Sauer-Zavala, Carl, Bullis, & Ellard, 2013; Bleidorn et al., 2019; Lahey, 2009; Rapee & Bayer, 2018; Tackett & Lahey, 2017; Widiger & Oltmanns, 2017).

General Wellbeing and Health. Elevated dispositional negativity is prospectively associated with lower levels of educational attainment, occupational success, and annual income (Beck, 2020; Hoff, Einarsdóttir, Chu, Briley, & Rounds, in press; Hur et al., 2019; Kajonius & Carlander, 2017; Leckelt et al., 2019; C. J. Soto, in press; von Soest, Wagner, Hansen, & Gerstorf, 2018). Individuals with a more negative disposition report lower levels of social support and decreased well-being, and they are less satisfied with their jobs, sexual experiences, friends, romantic partners, family members, and lives (M. S. Allen & E. E. Walter, 2018; Anglim, Horwood, Smillie, Marrero, & Wood, 2020; Barelds, 2005; Baselmans et al., 2019; Bolger & Eckenrode,

1991; Caughlin, Huston, & Houts, 2000; Finn, Mitte, & Neyer, 2013; Hansson et al., 2020; Hanzal & Segrin, 2009; Heller, Watson, & Ilies, 2004; Hur et al., 2019; Joel et al., in press; Judge, Heller, & Mount, 2002; Kajonius & Carlander, 2017; Lavner, Weiss, Miller, & Karney, 2018; Leskela et al., 2009; Li et al., 2019; McHugh & Lawlor, 2012; Mueller, Wagner, Smith, Voelkle, & Gerstorf, 2018; Newton-Howes, Horwood, & Mulder, 2015; O'Meara & South, 2019; Roohafza et al., 2016; Røysamb, Nes, Czajkowski, & Vassend, 2018; Shaver & Brennan, 1992; Slatcher & Vazire, 2009; C. J. Soto, 2019, in press; Swickert, Hittner, & Foster, 2010). Cross-sectional and longitudinal studies show that dispositionally negative individuals are prone to experiences that confer risk for emotional illness, including heightened feelings of loneliness, burnout, and emotional exhaustion; greater difficulties adjusting to major life transitions, such as college, moving abroad, and retirement; and more frequent work-family conflict, marital discord, unemployment, and divorce (Abdellaoui, Chen, et al., 2019; Abdellaoui et al., 2018; Abdellaoui, Sanchez-Roige, et al., 2019; T. D. Allen et al., 2012; Altschul, Iveson, & Deary, in press; Asselmann & Specht, 2020; Baselmans et al., 2019; Beck, 2020; Brock, Dindo, Simms, & Clark, 2016; Buecker, Maes, Denissen, & Luhmann, 2020; Credé & Niehorster, 2012; Day, Ong, & Perry, 2018; Hansson et al., 2020; Harari, Reaves, Beane, Laginess, & Viswesvaran, 2018; Hur et al., 2019; Klimstra, Noftle, Luyckx, Goossens, & Robins, 2018; C. J. Soto, in press; Swider & Zimmerman, 2010; You, Huang, Wang, & Bao, 2015). They are more likely to engage in unhealthy behaviors; to suffer from sleep problems, chronic pain, and subjective health complaints; to develop physical illnesses; and to die prematurely (Adams et al., in press; M. S. Allen & Robson, 2018; M. S. Allen & Emma E. Walter,

2018; Baselmans et al., 2019; B. P. Chapman & Goldberg, 2017; B. P Chapman et al., 2019; B. P. Chapman et al., 2020; Charles, Gatz, Kato, & Pedersen, 2008; Gale et al., 2017; E. K. Graham et al., 2017; Huang et al., 2017; Hur et al., 2019; Jokela, Airaksinen, Kivimaki, & Hakulinen, 2018; Jokela et al., in press; Kööts-Ausmees et al., 2016; Kornadt, Hagemeyer, Neyer, & Kandler, 2018; M. Liu et al., 2019; Meng et al., 2020; Puterman et al., 2020; Quach et al., 2020; Sallis, Davey Smith, & Munafo, 2019; Spengler, Roberts, Ludtke, Martin, & Brunner, 2016; Sutin et al., 2016; Tackman et al., in press; Valk et al., 2020; Weston & Jackson, 2018; Wettstein, Wahl, & Siebert, in press).

Mental Illness. There is ample cross-sectional, longitudinal, and genetic evidence that individuals with a negative disposition are more likely to develop a variety of psychiatric illnesses—including anxiety disorders, depression, and alcohol abuse—and, among those who do, to experience more severe, recurrent, and treatment-resistant symptoms (Adams et al., in press; Akingbuwa et al., 2020; Beck, 2020; Boe, Holgersen, & Holen, 2011; Brislin et al., 2020; Brouwer et al., 2019; Bucher, Suzuki, & Samuel, 2019; Class et al., 2019b; Cohen, Thakur, Young, & Hankin, in press; Coryell, Mills, Dindo, & Calarge, in press; du Pont, Rhee, Corley, Hewitt, & Friedman, 2019; Ejova, Milojev, Worthington, Bulbulia, & Sibley, 2020; Fullana et al., 2020; B. L. Goldstein, Greg Perlman, Nicholas R. Eaton, Roman Kotov, & D. N. Klein, in press; B. L. Goldstein, G. Perlman, N. R. Eaton, R. Kotov, & D. N. Klein, in press; Hur et al., 2019; Jones et al., 2018; Katz, Matanky, Aviram, & Yovel, 2020; Khoo, Stanton, Clark, & Watson, 2020; Kostyrka-Allchorne, Wass, & Sonuga-Barke, 2020; Kroencke, Kuper, Bleidorn, & Denissen, in press; Levin-Aspenson, Khoo, & Kotelnikova, 2019;

Michelini et al., 2020; Mineka et al., in press; Mumper, Dyson, Finsaas, Olino, & Klein, 2020; Sadeh, Miller, Wolf, & Harkness, 2015; Sen et al., 2010; A. Tang et al., 2020; Thorp et al., 2020; van Eeden et al., 2019). Likewise, dimensional approaches to psychopathology indicate that dispositional negativity is associated with the *p*-factor, a superordinate dimension that encompasses both internalizing and externalizing symptoms (Brandes, Herzhoff, Smack, & Tackett, 2019; Caspi & Moffitt, 2018; Jones et al., 2018; Levin-Aspenson et al., 2019; Mann, Atherton, DeYoung, Krueger, & Robins, in press). Furthermore, there is evidence that relations between dispositional negativity and mental illness remain evident, albeit attenuated, after eliminating overlapping item content (Class et al., 2019a; Uliaszek et al., 2009) or controlling for baseline symptomatology (Jeronimus, Kotov, Riese, & Ormel, 2016). Given this panoply of adverse, often co-morbid outcomes, dispositional negativity imposes a tremendous burden on healthcare providers and the global economy (Cuijpers et al., 2010; Goodwin, Hoven, Lyons, & Stein, 2002; ten Have, Oldehinkel, Vollebergh, & Ormel, 2005). Despite its profound consequences for wellbeing and disease, the neural systems underlying trait-like individual differences in dispositional negativity remain incompletely understood.

Relevance of the Extended Amygdala to Dispositional Negativity

Theoretical Foundations. The neural circuits governing trait-like individual differences in dispositional negativity have only recently started to come into focus. Decades ago, the influential personality theorist, Gordon Allport, wrote that, *"traits are cortical [or] subcortical … dispositions having the capacity to gate or guide*

specific phasic reactions" (Allport, 1966, p. 3). Today, most models remain firmly rooted in the idea that dispositional negativity reflects a neurobiological tendency to overreact to conflict, criticism, novelty, punishment, threat, and other kinds of acute 'trait-relevant' challenges (Eysenck, 1967; Goldsmith et al., 1987; Kagan, Reznick, & Snidman, 1988; Lahey, 2009; Reiss, 1997; Shackman et al., 2016; Spielberger, 1966; Zuckerman, 1976). This tendency has been linked to altered function in a number of brain regions—including the anterior insula/frontal operculum, extended amygdala, mid-cingulate cortex, and periaqueductal gray (Cavanagh & Shackman, 2015; Fox & Kalin, 2014; Hur et al., 2019; Kalin, 2017; Kirlic et al., 2019; Lowery-Gionta, DiBerto, Mazzone, & Kash, 2018; Shackman et al., 2011; Shackman et al., 2016; Sjouwerman, Scharfenort, & Lonsdorf, 2020; Somerville, Whalen, & Kelley, 2010). Among these, the extended amygdala has received the most intense empirical scrutiny and occupies the most privileged position in neurobiological models of dispositional negativity and pathological fear and anxiety (e.g., Davis, Walker, Miles, & Grillon, 2010; Fox, Oler, Tromp, Fudge, & Kalin, 2015; Grupe & Nitschke, 2013; Kagan et al., 1988; Kalin, 2017; Shackman et al., 2016).

Anatomy of the Extended Amygdala. The extended amygdala encompasses a heterogeneous collection of subcortical nuclei along the borders of the amygdala and the ventral striatum (Yilmazer-Hanke, 2012). Classical studies of anatomical connectivity first suggested that the central division of the extended amygdala—including the dorsal amygdala in the region of the central nucleus (Ce) and the lateral division of the neighboring bed nucleus of the stria terminalis (BST)—represents an integrative macrocircuit (Alheid & Heimer, 1988). More recent axonal tracing studies

in monkeys have confirmed that the Ce and BST are densely interconnected (deCampo & Fudge, 2013; Fudge et al., 2017; Oler et al., 2017). In parallel, magnetic resonance imaging (MRI) studies in humans have revealed evidence of robust anatomical (Avery et al., 2014; Kamali et al., 2016; Kamali et al., 2015) and functional connectivity between the Ce and BST (Avery et al., 2014; Berry, Wise, Lawrence, & Lancaster, 2021; R. M. Birn et al., 2014; Cano et al., 2018; Gorka, Torrisi, Shackman, Grillon, & Ernst, 2018; Oler et al., 2012; Oler et al., 2017; Pedersen et al., 2020; Tillman et al., 2018; Torrisi et al., 2018; Torrisi et al., 2015), reinforcing the hypothesis that they represent a functionally meaningful circuit (Alheid & Heimer, 1988; Fox, Oler, Tromp, et al., 2015).

From an anatomical perspective, the extended amygdala is poised to integrate divergent sources of potentially threat-relevant information and assemble states of fear and anxiety. The Ce and BST receive direct and indirect projections from brain regions that encode sensory, contextual, and regulatory information (Freese & Amaral, 2009), and both regions are anatomically poised to trigger somatomotor and neuroendocrine responses via dense projections to brainstem and subcortical effector regions (Fox, Oler, Tromp, et al., 2015; Freese & Amaral, 2009; Fudge et al., 2017). Other work shows that the Ce and BST contain cells with similar architectonic and neurochemical features and that the two regions show similar patterns of gene expression (for a detailed review, see Fox, Oler, Tromp, et al., 2015). Collectively, these anatomical observations suggest that the Ce and the BST represent an evolutionarily conserved circuit that is poised to use potentially threat-relevant information to trigger a range of fear- and anxiety-related defensive responses.

Mechanistic Evidence. A growing body of perturbation and recording studies in rodents demonstrates that the extended amygdala is critical for orchestrating adaptive defensive responses to a wide variety of threatening stimuli (Ahrens et al., 2018; Calhoon & Tye, 2015; Fadok, Markovic, Tovote, & Lüthi, 2018; Fox & Shackman, 2019; Glover et al., 2020; Griessner et al., in press; Gungor & Paré, 2016; Pomrenze, Giovanetti, et al., 2019; Pomrenze, Tovar-Diaz, et al., 2019; Ressler, Goode, Evemy, & Maren, 2020; Tovote, Fadok, & Luthi, 2015). Other work suggests a role in dispositional negativity (Ahrens et al., 2018; Glover et al., 2020). For example, Ahrens and colleagues showed that anxious, behaviorally inhibited mice are marked by tonically elevated activity in a specific type of Ce neurons—cells within the lateral division that express somatostatin and project to the BST (Ahrens et al., 2018)—consistent with the much coarser results revealed by positron emission tomography (PET) and perfusion fMRI studies of tonic amygdala activity in humans and monkeys (Abercrombie et al., 1998; Canli et al., 2006; Fox, Oler, Shackman, et al., 2015; Fox, Shelton, Oakes, Davidson, & Kalin, 2008; Kaczkurkin et al., 2016). In an elegant series of experiments, Ahrens and colleagues demonstrated that these neurons are sensitive to uncertain danger (i.e., unpredictable shock) and that they are both necessary and sufficient for heightened defensive responses (e.g., freezing) to novelty and diffuse threat (e.g., a brightly lit open field).

While our understanding of the primate extended amygdala lags far behind that of rodents, work in monkeys and humans motivates the hypothesis that the dorsal amygdala (Ce) is crucial for dispositional negativity. In monkeys, fiber-sparing excitotoxic lesions of the Ce have been shown to attenuate defensive behaviors and

neuroendocrine responses to a range of learned and innate threats (Davis, Antoniadis, Amaral, & Winslow, 2008; Kalin et al., 2016; Oler et al., 2016). These findings are well aligned with observations of humans with circumscribed amygdala damage (Bechara et al., 1995; Feinstein, Adolphs, Damasio, & Tranel, 2011; Feinstein, Adolphs, & Tranel, 2016; Klumpers, Morgan, Terburg, Stein, & van Honk, 2015; Korn et al., 2017). Patient SM, for example, shows a profound lack of fear and anxiety—whether measured objectively or subjectively—to both diffusely threatening contexts (e.g., a haunted house) and acute threat cues, including exotic spiders and snakes, horror film clips, and conditioned threat cues (Feinstein et al., 2011). Notably, she also endorses atypically low levels of dispositional negativity on standard psychometric measures (Feinstein et al., 2011), consistent with clinical assessments of her temperament (Tranel, Gullickson, Koch, & Adolphs, 2006).

Other research has examined the consequences of amplifying extended amygdala activity. Work in monkeys shows that genetic manipulations that increase dorsal amygdala (Ce) metabolism potentiate defensive responses to uncertain threat (Kalin et al., 2016), consistent with rodent studies (Ahrens et al., 2018). Electrical stimulation work in humans has revealed a broadly consistent pattern of results, with stimulation delivered in the region of the dorsal amygdala (Ce) eliciting intense feelings of fear and anxiety and elevated signs of arousal (Inman et al., 2020). Although the causal contribution of the BST to individual differences in fear and anxiety has yet to be explored in humans or other primates, the existing body of mechanistic work reinforces the hypothesis that circuits centered on the extended amygdala are a critical substrate for trait-like individual differences in dispositional negativity.

Functional Neuroimaging Findings. Functional neuroimaging studies in monkeys and humans demonstrate that the dorsal amygdala and the BST both respond to a broad spectrum of fear- and anxiety-eliciting challenges, including intruder threat (Fox, Oler, Shackman, et al., 2015), aversive photographs (Brinkmann et al., 2018; Sabatinelli et al., 2011), an unpredictably approaching tarantula (Mobbs et al., 2010), horror film clips (Hudson et al., in press; https://neurovault.org/collections/6237), and the anticipation of noxious stimuli (Hur, Smith, et al., 2020). Furthermore, there is evidence that extended amygdala responses to such challenges are associated with concurrent changes in subjective experience and objective arousal (Fox & Shackman, 2019; Hur et al., 2019; Orem et al., 2019).

Despite this progress, it remains remarkably unclear whether more trait-like individual differences in dispositional negativity reflect heightened extended amygdala reactivity to threat. To date, the vast majority of human neuroimaging studies have relied on emotional-face paradigms. While faces are potent triggers of amygdala activity (Hur et al., 2019) and are widely used in a variety of on-going biobank projects[1], they do not elicit robust negative affect and, as such, do not represent a 'trait-relevant' challenge in the traditional sense. In emotional-face paradigms, 'threat' is operationalized as the difference in activity elicited by negative expressions (e.g., anger, fear) and either neutral expressions or simple control stimuli (e.g., geometric shapes, houses). While there is some evidence that dispositionally negative individuals show increased

[1] Emotional-face paradigms are used in the ABCD Study (Casey et al., 2018), Duke Neurogenetics Study (Elliott et al., 2019), Human Connectome Project and follow-up studies (Barch et al., 2013; Siless et al., 2020; Somerville et al., 2018; Tozzi et al., 2020), IMAGEN (Albaugh et al., 2019), Philadelphia Neurodevelopmental Cohort (Satterthwaite et al., 2016), and UK Biobank (Miller et al., 2016).

amygdala reactivity to negative expressions (Calder, Ewbank, & Passamonti, 2011; Fonzo et al., 2015; Fox & Kalin, 2014; Stein, Simmons, Feinstein, & Paulus, 2007), recent large-scale studies of middle-aged (Minnesota Twin Study: n = 548) and young adults (Duke Neurogenetics Study: n = 1,256) failed to detect credible relations (MacDuffie, Knodt, Radtke, Strauman, & Hariri, 2019; Silverman et al., 2019). On balance, this body of research suggests that relations between dispositional negativity and amygdala reactivity to emotional faces are negligible in magnitude, conditional on moderator variables[2], or simply non-existent.

To date, comparatively few human studies have used demonstrably distress-eliciting challenges to examine relations between dispositional negativity and extended amygdala function, and most of these have predominantly focused on the role of the amygdala (**Table 1**). Studies using aversive photographs have not found evidence of heightened amygdala reactivity in convenience samples of either young (Brinkmann et al., 2018; West, Burgess, Dust, Kandala, & Barch, 2021) or middle-aged adults (Schuyler et al., 2012). Studies of Pavlovian threat conditioning provide mixed evidence, with some reporting a positive association between dispositional negativity and dorsal amygdala reactivity to cues or contexts predictive of shock delivery (CS+; Indovina, Robbins, Núñez-Elizalde, Dunn, & Bishop, 2011; Sjouwerman et al., 2020), and others reporting null effects (Kirlic et al., 2019; Klumpers, Kroes, Baas, &

[2] Potentially important moderators include the degree to which the faces are task-relevant or masked (Calder et al., 2011; Günther et al., 2020; D. M. Stout, A. J. Shackman, W. S. Pedersen, T. A. Miskovich, & C. L. Larson, 2017), the control condition (Ball et al., 2012), the analytic approach (Blackford, Avery, Cowan, Shelton, & Zald, 2011; Blackford, Avery, Shelton, & Zald, 2009), the degree of ambient stress (Everaerd, Klumpers, van Wingen, Tendolkar, & Fernández, 2015), and the range of dispositional negativity (Ball et al., 2012; Greenberg et al., 2017).

Fernandez, 2017). Much less is known about the role of the BST, the other major division of the extended amygdala. To date, only one human neuroimaging study has directly addressed this question, showing that individuals with a more negative disposition show heightened engagement of the BST during the anticipation of temporally uncertain shock (Somerville et al., 2010). Taken with the available strands of mechanistic work, these observations motivate the hypothesis that dispositional negativity reflects heightened recruitment of the BST, and possibly the dorsal amygdala, during the anticipation of genuinely threatening stimuli, and that this association may be more evident when threat is uncertain.

Convergent Validity Across Threat Assays

The extended amygdala is exquisitely sensitive to a broad spectrum of emotionally and motivationally salient stimuli (Chase, Eickhoff, Laird, & Hogarth, 2011; Costafreda, Brammer, David, & Fu, 2008; Fried, MacDonald, & Wilson, 1997; Fusar-Poli et al., 2009; Gothard, Battaglia, Erickson, Spitler, & Amaral, 2007; Hoffman, Gothard, Schmid, & Logothetis, 2007; Hur, Smith, et al., 2020; Kuhn & Gallinat, 2011; Lindquist, Wager, Kober, Bliss-Moreau, & Barrett, 2012; Sabatinelli et al., 2011; Sergerie, Chochol, & Armony, 2008; Sescousse, Caldu, Segura, & Dreher, 2013; D. W. Tang, Fellows, Small, & Dagher, 2012; Wang et al., 2014), and there is ample evidence that it plays a mechanistically critical role in orchestrating defensive responses to a variety of threats (Fox & Shackman, 2019; Hur et al., 2019). This makes it tempting to treat a variety of so-called 'threat' paradigms—from viewing photographs of fearful faces to anticipating the delivery of a painful electric shock—as interchangeable probes of individual differences in extended amygdala reactivity.

Although this muddling of emotion perception and expression is common (e.g., Tozzi et al., in press), the underlying assumption of convergent validity has rarely been examined empirically. In the only study aimed at addressing this fundamental question, Villalta-Gill and colleagues reported negligible relations ($r < 0.17$) between amygdala reactivity to threat-related faces and aversive scenes in 32 young adults (Villalta-Gil et al., 2017)—a sample much too small to allow decisive inferences (i.e., the 95% CI for $r = 0.17$ ranges from -0.19 to +0.49).

Overview of the Present Approach

Here, we used a suite of neuroimaging techniques to determine the degree to which trait-like individual differences in dispositional negativity are associated with extended amygdala reactivity to well-established 'threat-of-shock' and emotional-face paradigms in an existing longitudinal sample of more than 200 young adults (**Table 1**). We focused on young adulthood because it is a time of profound, often stressful developmental transitions (e.g., moving away from home, forging new identities and relationships; Alloy & Abramson, 1999; Arnett, 2000; Hays & Oxley, 1986; Pancer, Hunsberger, Pratt, & Alisat, 2000). In fact, more than half of undergraduate students report overwhelming feelings of anxiety and more than a third report severe feelings of depression (American College Health Association, 2019), with many experiencing the first onset of anxiety disorders and depression during this period (Auerbach et al., 2016; Auerbach et al., 2018; Beesdo, Pine, Lieb, & Wittchen, 2010; Binkley & Fenn, 2019; Fava et al., 2010; Global Burden of Disease Collaborators, 2016; Kessler et al., 2007; Kessler, Petukhova, Sampson, Zaslavsky, & Wittchen, 2012; Lipson, Lattie, &

Eisenberg, 2019; Liu, Stevens, Wong, Yasui, & Chen, 2019; Slee, Nazareth, Freemantle, & Horsfall, in press; Substance Abuse and Mental Health Services Administration, 2019; Twenge, Cooper, Joiner, Duffy, & Binau, 2019). Subjects were selectively recruited from a much larger pool of previously screened individuals (N = 6,594), enabling us to examine a broad spectrum of dispositional negativity. A multiband pulse sequence, advanced co-registration and spatial normalization techniques, and anatomically-defined regions-of-interest (ROIs) made it possible to examine variation in Ce and BST reactivity to the two tasks in an unbiased manner (J. F. Smith, Hur, Kaplan, & Shackman, 2018; Theiss, Ridgewell, McHugo, Heckers, & Blackford, 2017; Tillman et al., 2018). To further enhance anatomical specificity, analyses were conducted using spatially unsmoothed data and newly developed extended amygdala seeds. To facilitate open and reproducible science, the study hypotheses and approach were pre-registered using tools provided by the Open Science Foundation (Botvinik-Nezer et al., 2020; Fox, Lapate, Davidson, & Shackman, 2018; Munafò et al., 2017; Shackman & Fox, 2018).

Understanding the neural systems underlying individual differences in dispositional negativity and determining the degree to which different experimental probes of threat reactivity are interchangeable is conceptually and practically important. Dispositional negativity is a central dimension of childhood temperament and adult personality, and individuals with a more negative disposition are at risk for a range of adverse outcomes. Although a range of mechanistic and observational evidence suggests that the extended amygdala mediates the heightened threat reactivity that characterizes individuals with a negative disposition, this hypothesis has rarely been subjected to a stringent test.

Likewise, emotional-face paradigms are widely used to probe the neural systems that orchestrate responses to threat, but the degree to which 'threatening' faces adequately capture individual differences in extended amygdala reactivity to a genuinely distress-eliciting challenge remains largely unknown. In short, addressing these aims has the potential to significantly refine scientific theory and practice, and accelerate the development of improved intervention strategies for extreme dispositional negativity (Barlow et al., 2017; S. E. Sauer-Zavala et al., in press).

Specific Aims

Aim 1: Leverage a large sample and cutting-edge neuroimaging techniques to determine the relevance of trait-like individual differences in dispositional negativity to extended amygdala activation during an anxiety-eliciting experimental challenge ('threat-of-shock'). We anticipated that individuals with a more negative disposition would show heighted reactivity in the dorsal amygdala (Ce) and BST, and explored the possibility that this association would be most evident during the anticipation of uncertain threat. To clarify specificity, we performed a parallel set of analyses using data from an emotional-faces paradigm that, while widely used as a probe of individual differences in amygdala reactivity, does not elicit robust anxiety. Whole-brain voxelwise analyses enabled us to explore the potential relevance of other, less intensively scrutinized regions.

Aim 2: Determine whether neuroimaging probes of 'threat' reactivity are interchangeable. It is widely assumed that different experimental tasks that target a common function (e.g., 'emotion') are quasi-interchangeable probes of individual

differences in regional function (e.g., amygdala). Yet this has rarely been examined empirically, never in a large sample, and never in the BST. Here, we tested whether assays of emotion perception (fearful and angry emotional faces) and emotion elicitation ('threat-of-shock') show evidence of 'convergent validity' in the extended amygdala. Based on prior work (Villalta-Gil et al., 2017), we anticipated that measures of dorsal amygdala (Ce) and BST reactivity to the two tasks would show little-to-no evidence of convergence, as indexed by negligible between-assay correlations and moderate-to-strong Bayesian evidence for the null hypothesis (i.e., Bayes Factor <.33) (Kelter, 2020; Quintana & Williams, 2018; van Doorn et al., in press).

Methods

Overview of the Larger Longitudinal Study

As part of an on-going prospective-longitudinal study focused on individuals at risk for the development of internalizing disorders, we used a well-established psychometric measure of dispositional negativity to screen 6,594 first-year university students (57.1% female; 59.0% White, 19.0% Asian, 9.9% African American, 6.3% Hispanic, 5.8% Multiracial/Other; *M*=19.2 years, *SD*=1.1 years) (Shackman, Weinstein, et al., 2018). Screening data were stratified into quartiles (top quartile, middle quartiles, bottom quartile), separately for males and females. Individuals who met preliminary inclusion criteria were independently and randomly recruited via email from each of the resulting six strata. Because of our focus on psychiatric risk, approximately half the participants were recruited from the top quartile, with the remainder split between the middle and bottom quartiles (i.e., 50% high, 25% medium, and 25% low). This enabled us to sample a broad spectrum of dispositional negativity without gaps or discontinuities, while balancing the inclusion of men and women. Simulation work suggests that this over-sampling ('enrichment') approach does not bias statistical tests to a degree that would compromise their validity (Hauner, Zinbarg, & Revelle, 2014). All subjects had normal or corrected-to-normal color vision, and reported the absence of lifetime neurological symptoms, pervasive developmental disorder, very premature birth, medical conditions that would contraindicate MRI, and prior experience with noxious electrical stimulation. All subjects were free from a lifetime history of psychotic and bipolar disorders; a current diagnosis of a mood, anxiety, or trauma

disorder (past 2 months); severe substance abuse; active suicidality; and on-going psychiatric treatment as determined by an experienced, masters-level diagnostician using the Structured Clinical Interview for DSM-5 (First, Williams, Karg, & Spitzer, 2015). Subjects provided informed written consent and all procedures were approved by the Institutional Review Board at the University of Maryland, College Park. Data from this study were featured in prior work focused on the development and validation of the threat-anticipation paradigm (Hur, Smith, et al., 2020) and relations between social anxiety and momentary mood (Hur, DeYoung, et al., 2020), but have not yet been used to address the two central aims proposed here.

Power Analyses

Sample size was determined *a priori* as part of the application for the award that supported this research (R01-MH107444). The target sample size ($N \approx 240$) was chosen to afford acceptable power and precision given available resources. At the time of study design, G-power 3.1.9.2 (http://www.gpower.hhu.de) indicated >99% power to detect a benchmark medium-sized effect ($r = 0.30$) with up to 20% planned attrition (N = 192 usable datasets) using $\alpha = 0.05$ (two-tailed).

Participants

A total of 241 subjects were recruited and scanned. Of these, 6 withdrew due to excess distress in the scanner, 1 withdrew from the study after the imaging session, and 4 were excluded due to incidental neurological findings.

Threat-anticipation task. One subject was excluded from fMRI analyses due to gross susceptibility artifacts in the echoplanar imaging (EPI) data, 2 were excluded due to insufficient usable data (<2 usable scans; see below), 6 were excluded due to excessive movement artifact (i.e., the variance of the volume-to-volume displacement of a selected voxel at the center of the brain was >2 *SDs* above the mean), and 1 was excluded due to task timing issues, yielding a final sample of 220 subjects (49.5% female; 61.4% White, 18.2% Asian, 8.6% African American, 4.1% Hispanic, 7.3% Multiracial/Other; *M* = 18.8 years, *SD* = 0.4 years). Of these, 2 individuals were excluded from skin conductance analyses due to insufficient usable data (<2 usable 'scans'; see below).

Emotional faces task. Three subjects were excluded due to gross susceptibility artifacts in the EPI data, 1 was excluded due to insufficient usable data (<2 scans), 7 were excluded due to excessive motion artifact, and 6 subjects for inadequate behavioral performance (i.e., both runs had accuracy less than 2 *SD* from the mean), yielding a final sample of 213 subjects (49.3% female; 61.0% White, 17.8% Asian, 8.5% African American, 4.2% Hispanic, 7.0% Multiracial/Other; *M* = 18.8 years, *SD* = 0.3 years).

Dispositional Negativity

As in prior work (Hur, DeYoung, et al., 2020*;* Hur, Smith, et al., 2020; Shackman, Weinstein, et al., 2018), we used psychometrically sound measures of neuroticism (Big Five Inventory-Neuroticism; John, Naumann, & Soto, 2008) and trait anxiety (International Personality Item Pool-Trait Anxiety; Goldberg, 1999; Goldberg et al., 2006) to quantify individual differences in dispositional negativity. Participants used a

1 (*disagree strongly*) to 5 (*agree strongly*) scale to rate themselves on a total of 18 items (e.g., *depressed or blue, tense, worry, nervous, get distressed easily, fear for the worst, afraid of many things*). At screening, the neuroticism and anxiety scales were strongly correlated (rs > .85) and reliable (αs > .85, ω_hs > .80). To minimize the influence of occasion-specific fluctuations in responding, hypothesis testing employed a composite measure of dispositional negativity. The composite was created by standardizing the neuroticism and trait anxiety scales (z-transformation using the mean and *SD* from the screening sample), and then averaging across the 2 scales and 3 assessments (screening, enrollment, and 6-month follow-up). The resulting composite is intended to capture a sizable range of the dispositional negativity spectrum.

Threat-Anticipation Paradigm

Paradigm Structure and Design Considerations. The Maryland Threat Countdown paradigm is a well-established, fMRI-optimized version of temporally uncertain-threat assays that have been validated using fear-potentiated startle and acute anxiolytic administration (e.g., benzodiazepine) in mice (Daldrup et al., 2015; Lange et al., 2017), rats (Miles, Davis, & Walker, 2011), and humans (Hefner, Moberg, Hachiya, & Curtin, 2013), enhancing its translational relevance. The MTC paradigm takes the form of a 2 (*Valence:* Threat/Safety) × 2 (*Temporal Certainty:* Uncertain/Certain) randomized event-related design (3 scans; 6 trials/condition/scan). Simulations were used to optimize the detection and deconvolution of task-related hemodynamic signals (variance inflation factors <1.54). Stimulus presentation and ratings acquisition were

controlled using Presentation software (version 19.0, Neurobehavioral Systems, Berkeley, CA).

On Certain Threat trials, subjects saw a descending stream of integers ('count-down;' e.g., 30, 29, 28...3, 2, 1) for 18.75 s. To ensure robust emotion, this anticipatory epoch always culminated with the delivery of a noxious electric shock, unpleasant photographic image (e.g., mutilated body), and thematically related audio clip (e.g., scream, gunshot). Uncertain Threat trials were similar, but the integer stream was randomized and presented for an uncertain and variable duration (8.75-30.00 s; M = 18.75 s). Here, subjects knew that something aversive was going to occur, but they had no way of knowing precisely when it would occur. Consistent with recent recommendations (Shackman & Fox, 2016), the average duration of the anticipatory epoch was identical across conditions, ensuring an equal number of measurements (TRs/condition). Mean duration was chosen to enhance detection of task-related differences in the blood oxygen level-dependent (BOLD) signal (Henson, 2007b), and to enable dissection of onset from genuinely sustained responses. Safety trials were similar, but terminated with the delivery of benign reinforcers (see below). Valence was continuously signaled during the anticipatory epoch by the background color of the display. Temporal certainty was signaled by the nature of the integer stream. Certain trials always began with the presentation of the number 30 (**Fig. 1**). On Uncertain trials, integers were randomly drawn from a near-uniform distribution ranging from 1 to 45 to reinforce the impression that Uncertain trials could be much longer than Certain ones and to minimize incidental temporal learning ('time-keeping'). To mitigate potential confusion and eliminate mnemonic demands, a lower-case 'c' or 'u' was presented at

the lower edge of the display throughout the anticipatory epoch. White-noise visual masks (3.2 s) were presented between trials to minimize persistence of the visual reinforcers in iconic memory. Subjects provided ratings of anticipatory fear/anxiety for each trial type during each scan using an MRI-compatible response pad (MRA, Washington, PA). Subjects were instructed to rate the intensity of the fear/anxiety experienced during the prior anticipatory ('countdown') epoch using a 1 (*minimal*) to 4 (*maximal*) scale. Subjects were prompted to rate each trial type once per scan. Premature ratings (< 300 ms) were censored. All subjects provided at least 6 usable ratings, and rated each condition at least once. A total of 6 additional echo-planar imaging (EPI) volumes were acquired at the beginning and end of each scan.

Procedures. Prior to scanning, subjects practiced an abbreviated version of the paradigm—without electrical stimulation—until they indicated and staff confirmed that they understood the task. Benign and aversive electrical stimulation levels were individually titrated. *Benign Stimulation.* Subjects were asked whether they could "reliably detect" a 20 V stimulus and whether it was "at all unpleasant." If the subject could not detect the stimulus, the voltage was increased by 4 V and the process repeated. If the subject indicated that the stimulus was unpleasant, the voltage was reduced by 4V and the process was repeated. The final level chosen served as the benign electrical stimulation during the imaging assessment (M = 21.06 V, SD = 4.98 V). *Aversive Stimulation.* Subjects received a 100 V stimulus and were asked whether it was "as unpleasant as you are willing to tolerate." If the subject indicated that they were willing to tolerate more intense stimulation, the voltage was increased by 10 V and the process repeated. If the subject indicated that the stimulus was too intense, the

voltage was reduced by 5 V and the process repeated. The final level chosen served as the aversive electrical stimulation during the imaging assessment (M = 118.02, SD = 26.09). Following each scan of the MTC paradigm, we re-assessed whether stimulation was sufficiently intense and re-calibrated as necessary.

Electrical Stimuli. Electrical stimuli (100 ms; 2 ms pulses every 10 ms) were generated using an MRI-compatible constant-voltage stimulator system (STMEPM-MRI; Biopac Systems, Inc., Goleta, CA). Stimuli were delivered using MRI-compatible, disposable carbon electrodes (Biopac) attached to the fourth and fifth phalanges of the non-dominant hand.

Visual Stimuli. Visual stimuli (1.8 s) were digitally back-projected (Powerlite Pro G5550, Epson America, Inc., Long Beach, CA) onto a semi-opaque screen mounted at the head-end of the scanner bore and viewed using a mirror mounted on the head-coil. A total of 72 photographs were selected from the International Affective Picture System (IAPS identification numbers)—*Benign:* 1670, 2026, 2038, 2102, 2190, 2381, 2393, 2397, 2411, 2850, 2870, 2890, 5390, 5471, 5510, 5740, 7000, 7003, 7004, 7014, 7020, 7026, 7032, 7035, 7050, 7059, 7080, 7090, 7100, 7140, 7187, 7217, 7233, 7235, 7300, 7950. *Aversive:* 1300, 3000, 3001, 3010, 3015, 3030, 3051, 3053, 3061, 3062, 3063, 3069, 3100, 3102, 3150, 3168, 3170, 3213, 3400, 3500, 6022, 6250, 6312, 6540, 8230, 9042, 9140, 9253, 9300, 9405, 9410, 9414, 9490, 9570, 9584, 9590 (Lang, Bradley, & Cuthbert, 2008). Based on normative ratings, the aversive images were significantly more negative and arousing than the benign images, $t(70) > 24.3$, $p < 0.001$. On a 1 (*negative/low-arousal*) to 9 (*positive/high-arousal*) scale, the mean

valence and arousal scores were 2.2 (*SD* = 0.6) and 6.3 (*SD* = 0.6) for the aversive images, and 5.2 (*SD* = 0.4) and 2.8 (*SD* = 0.3) for the benign images.

Auditory Stimuli. Auditory stimuli (0.80 s) were delivered using an amplifier (PA-1 Whirlwind) with in-line noise-reducing filters and ear buds (S14; Sensimetrics, Gloucester, MA) fitted with noise-reducing ear plugs (Hearing Components, Inc., St. Paul, MN). A total of 72 auditory stimuli (half aversive, half benign) were adapted from open-access online sources.

Skin Conductance Data Collection. To confirm the validity of the threat-anticipation paradigm, skin conductance was continuously assessed during each scan of the task using a Biopac system (MP-150; Biopac Systems, Inc., Goleta, CA). Skin conductance (250 Hz; 0.05 Hz high-pass) was measured using MRI-compatible disposable electrodes (EL507) attached to the second and third fingers of the non-dominant hand.

Emotional Faces Paradigm

Building on work by our group (Daniel M Stout, Alexander J Shackman, Walker S Pedersen, Tara A Miskovich, & Christine L Larson, 2017) and many others (Albaugh et al., 2019; Barch et al., 2013; Casey et al., 2018; Elliott et al., 2019; Miller et al., 2016; Satterthwaite et al., 2016; Siless et al., 2020; Somerville et al., 2018; Tozzi et al., 2020) demonstrating the utility of emotional-faces paradigms for probing extended amygdala reactivity, subjects viewed alternating blocks of either faces (21 blocks) or places (7 blocks) in a pseudo-randomized order. The use of a block design mitigates potential concerns about alcohol-induced changes in the shape of the hemodynamic response function (HRF). Block length (20 s) was chosen to maximize our power to

detect a difference in the blood oxygen level-dependent (BOLD) signal elicited by the two conditions (Henson, 2007a; Maus, van Breukelen, Goebel, & Berger, 2010). To maximize signal strength and homogeneity and minimize potential neural habituation (Henson, 2007a; Maus et al., 2010; Plichta et al., 2014), each block consisted of 10 brief photographs of faces or places (1.5 s/image) separated by a fixation cross (0.5 s) Face blocks included photographs of prototypical angry, fearful, or happy facial expressions (7 blocks/expression). Face stimuli were taken from prior work by Gamer and colleagues (Gamer, Schmitz, Tittgemeyer, & Schilbach, 2013; Scheller, Büchel, & Gamer, 2012) and included standardized images of unfamiliar male and female adults displaying unambiguous fearful or neutral expressions. To maximize the number of models and mitigate potential habituation, images were derived from several well-established databases: Ekman and Friesen's Pictures of Facial Affect (Ekman & Friesen, 1976), the FACES database (Ebner, Riediger, & Lindenberger, 2010), the Karolinska Directed Emotional Faces database (http://www.emotionlab.se/resources/kdef), and the NimStim Face Stimulus Set (https://www.macbrain.org/resources.htm). Colored images were converted to grayscale, brightness normalized, and masked to occlude non-facial features (e.g., ears, hair). Place blocks included photographs of residential and commercial buildings. Grayscale building stimuli were adapted from prior work (Choi, Padmala, & Pessoa, 2012, 2015). To ensure engagement, subjects indicated whether each image matched that presented on the prior trial (i.e., a 1-back continuous performance task).

MRI Data Acquisition

MRI data were acquired using a Siemens Magnetom TIM Trio 3 Tesla scanner (32-channel head-coil). Foam inserts were used to immobilize the participant's head within the head-coil and mitigate potential motion artifact. Subjects were continuously monitored from the control room using an MRI-compatible eye-tracker (Eyelink 1000; SR Research, Ottawa, Ontario, Canada). Head motion was monitored using the AFNI real-time plugin (Cox, 1996). Sagittal T1-weighted anatomical images were acquired using a magnetization prepared rapid acquisition gradient echo (MPRAGE) sequence (TR=2,400 ms; TE=2.01 ms; inversion time=1060 ms; flip angle=8°; sagittal slice thickness=0.8 mm; in-plane=0.8 × 0.8 mm; matrix=300 × 320; field-of-view=240 × 256). A T2-weighted image was collected co-planar to the T1-weighted image (TR=3,200 ms; TE=564 ms; flip angle=120°). To enhance resolution, a multi-band sequence was used to collect oblique-axial echo planar imaging (EPI) volumes (multiband acceleration=6; TR=1,250 ms; TE=39.4 ms; flip angle=36.4°; slice thickness=2.2 mm, number of slices=60; in-plane resolution=2.1875 × 2.1875 mm; matrix=96 × 96). Images were collected in the oblique axial plane (approximately −20° relative to the AC-PC plane) to minimize potential susceptibility artifacts. For the threat-anticipation task, three 478-volume EPI scans were acquired. For the emotional-faces task, two 454-volume EPI scans were acquired. The scanner automatically discarded 7 volumes prior to the first recorded volume. To enable fieldmap correction, two oblique-axial spin echo (SE) images were collected in each of two opposing phase-encoding directions (rostral-to-caudal and caudal-to-rostral) at the same location and resolution as the functional volumes (i.e., co-planar; TR=7,220 ms; TE=73 ms).

Following the last scan, subjects were removed from the scanner, debriefed, compensated, and discharged.

Skin Conductance Pipeline

Skin conductance data were processed using PsPM (version 4.0.2) and in-house MATLAB code (Dominik R Bach et al., 2018; Dominik R Bach, Friston, & Dolan, 2013). For those subjects with usable fMRI data for the threat-anticipation task, skin conductance data from each scan were outlier-interpolated (>3 median absolute deviations; linear-interpolation), regressed to remove pulse and respiration signals, band-pass filtered (0.008-0.2 Hz), resampled to match the TR used for fMRI data acquisition (1.25 s), and median-centered. Subject-specific SCR functions were derived using a four-parameter model (D. R. Bach, Flandin, Friston, & Dolan, 2010) and a boxcar function corresponding to the period of reinforcer presentation and the subsequent visual white noise mask. A robust regression framework was used to residualize signals associated with the presentation of reinforcers, the white noise mask, and the rating prompts for each subject. Skin conductance levels were computed for the anticipatory epoch of each condition by averaging the studentized residuals, separately for each scan.

To ensure data validity, scans that did not show numerically positive skin conductance responses to reinforcer delivery were censored. Subjects with <2 usable scans were excluded from analyses (n = 2).

MRI Data Pipeline

Methods have been optimized to minimize spatial normalization error and other potential sources of noise. Structural and functional MRI data were visually inspected before and after processing for quality assurance.

Anatomical Data Processing. Methods are similar to those described in other recent reports by our group (Hur et al., 2018; Hur, Smith, et al., 2020; Tillman et al., 2018). T1-weighted images were inhomogeneity corrected using N4 (Tustison et al., 2010) and filtered using the denoise function in ANTS (Avants et al., 2011). The brain was then be extracted using a variant of the BEaST algorithm (Eskildsen et al., 2012) with brain-extracted and normalized reference brains from the IXI database (https://brain-development.org/ixi-dataset). Brain-extracted T1 images were normalized to a version of the brain-extracted 1-mm T1-weighted MNI152 (version 6) template (Grabner et al., 2006) modified to remove extracerebral tissue. This was motivated by evidence that brain-extracted T1 images and a brain-extracted template enhance the quality of spatial normalization (Acosta-Cabronero, Williams, Pereira, Pengas, & Nestor, 2008; Fein et al., 2006; Fischmeister et al., 2013). Normalization was performed using the diffeomorphic approach implemented in SyN (version 1.9.x.2017-09.11; Avants et al., 2011; Klein et al., 2009). T2-weighted images were rigidly co-registered with the corresponding T1 prior to normalization and the brain extraction mask from the T1 were then applied. Tissue priors (Lorio et al., 2016) were unwarped to the native space of each T1 using the inverse of the diffeomorphic transformation. Brain-extracted T1 and T2 images were simultaneously segmented using native-space priors generated using FAST (FSL version 5.0.9) (Zhang, Brady, & Smith, 2001) for use in T1-EPI co-registration (see below).

Fieldmap Data Processing. SE images were used to create a fieldmap in topup (Andersson, Skare, & Ashburner, 2003; Graham, Drobnjak, & Zhang, 2017; S. M. Smith et al., 2004). Fieldmaps were converted to radians, median-filtered, and smoothed (2-mm). The average of the distortion-corrected SE images was inhomogeneity corrected using N4, and brain-masked using 3dSkullStrip in AFNI (version 17.2.10; Cox, 1996).

Functional Data Processing. EPI files were de-spiked using 3dDespike and slice-time corrected (to the center of the TR) using 3dTshift, and motion corrected to the first volume using a 12-parameter affine transformation implemented in ANTs. During motion correction, data were inhomogeneity corrected using N4. Recent work indicates that de-spiking is more effective than 'scrubbing' for attenuating motion-related artifacts (Jo et al., 2013; Power, Schlaggar, & Petersen, 2015; Siegel et al., 2014). Transformations were saved in ITK-compatible format for subsequent use. The first volume was extracted for EPI-T1 co-registration. The reference EPI volume was simultaneously co-registered with the corresponding T1-weighted image in native space and corrected for geometric distortions using boundary-based registration (Greve & Fischl, 2009). This step incorporated the previously created fieldmap, undistorted SE, T1, white matter (WM) image, and masks. The spatial transformations necessary to transform each EPI volume from native space to the reference EPI, from the reference EPI to the T1, and from the T1 to the template were concatenated and applied to the processed (de-spiked and slice-time corrected) EPI data in a single step to minimize incidental spatial blurring. Normalized EPI data were resampled to 2-mm isotopic voxels using fifth-order b-splines. To maximize spatial resolution, no

additional spatial filters were applied, consistent with recent recommendations (Stelzer, Lohmann, Mueller, Buschmann, & Turner, 2014; Turner & Geyer, 2014).

Data Exclusions. To assess residual motion artifact, we computed the variance of volume-to-volume displacement of a selected voxel in the center of the brain (x = 5, y = 34, z = 28) using the motion-corrected EPI data. Scans with excess artifact (>2 *SD* above the mean) were discarded. Subjects who lacked sufficient usable fMRI data (<2 scans of the threat-anticipation task or <1 scan of the emotional-faces task) or showed inadequate performance on the emotional-faces task (see above; accuracy >2 *SD*) were excluded from analyses.

Canonical First-Level (Single-Subject) fMRI Modeling. First-level modeling was performed using SPM12 (version 6678; https://www.fil.ion.ucl.ac.uk/spm), with the band-pass set to the hemodynamic response function (HRF) and 128 s for low and high pass, respectively. Regressors were convolved with a canonical HRF and its temporal derivative. The autoregressive model at the first level was set to the default of AR 0.2. EPI volumes collected before the first trial, during intertrial intervals, and following the final trial were unmodeled, and contributed to the baseline estimate. Clusters and local maxima were labeled using a combination of the Allen Institute, Harvard–Oxford, and Mai atlases (Desikan et al., 2006; Frazier et al., 2005; Hawrylycz et al., 2012; Mai, Majtanik, & Paxinos, 2015; Makris et al., 2006) and a recently established consensus nomenclature (ten Donkelaar, Tzourio-Mazoyer, & Mai, 2018). Brain figures were created using MRIcroGL (version 1.2; https://www.nitrc.org/projects/mricrogl).

Threat-Anticipation Task. The threat-anticipation paradigm was modeled using variable-duration rectangular ('box-car') regressors time-locked to the anticipation epochs of the Uncertain Threat, Certain Threat, and Uncertain Safety trials. The anticipation epochs of Certain Safety trials were treated as the implicit baseline. The periods corresponding to the delivery of each of the four reinforcer types, the white noise mask following each trial, and rating trials were modeled using a similar approach (**Fig. 1**). Volume-to-volume displacement and motion parameters (including 1- and 2-volume lagged versions) were be included, similar to other recent work (Reddan, Wager, & Schiller, 2018). To further attenuate potential noise, cerebrospinal fluid (CSF) time-series, instantaneous pulse and respiration rates, and their estimated effect on the BOLD time-series were also be included as nuisance variates (R. M. Birn, Smith, Jones, & Bandettini, 2008; Chang, Cunningham, & Glover, 2009). ICA-AROMA (Pruim et al., 2015) was used to model several other potential sources of noise (e.g., brain-edge, CSF-edge, WM). These and the single ICA component showing the strongest correlation with motion estimates were included as additional nuisance variates. EPI volumes with excessive volume-to-volume displacement (>0.5 mm), as well as those during and immediately following the delivery of aversive reinforcers, were also censored.

Emotional-Faces Task. Hemodynamic activity associated with each emotional expression (angry, fearful, and happy) was modeled using rectangular functions time-locked to block on- and offset, with place blocks treated as an implicit baseline.

Extended Amygdala Regions of Interest (ROIs). Consistent with past work by our group (Tillman et al., 2018), task-related Ce and BST activity was quantified using well-established anatomically-defined ROIs and spatially unsmoothed functional data (Theiss et al., 2017; Tillman et al., 2018) (**Fig. 2**). Analyses were performed using standardized regression coefficients extracted and averaged for each combination of task contrast (e.g., Threat vs. Safety anticipation, 'Threatening' Faces vs. Places), ROI, and subject.

Data Analytic Plan

All analyses were performed in R version 4.0.2 (Team, 2020). As a precursor to hypothesis testing, we first confirmed that the threat-anticipation paradigm had the intended effects on subjective distress (in-scanner fear/anxiety ratings) and anxious arousal (skin conductance response).

To do so, we used 2 (Valence: Threat, Safety) x 2 (Certainty: Uncertain, Certain) repeated-measures generalized linear models, implemented using the 'lme4' package (Bates, Mächler, Bolker, & Walker, 2015). To inform interpretation of predicted brain-behavior associations, dispositional negativity was included in the model. dispositional negativity was indexed using the mean-centered, multi-assessment composite. Preliminary analyses indicated that the ratings data for the Safety condition were positively skewed. Accordingly, we modelled the data with a gamma distribution using a log link function. For skin conductance analyses, we used an ordinary least-squares model. For simplicity, non-significant three-way interaction terms were pruned from the final model. Significance was determined using a parametric bootstrapping

approach (1,000 samples), implemented using the 'afex' package (Singmann, Bolker, Westfall, & Aust, 2021). Significant interactions were then decomposed using simple slopes, implemented using the 'interactions' package (Long, 2019).

Next, we confirmed that the threat-anticipation and emotional-faces tasks had the predicted consequences for brain function.

A series of whole-brain voxelwise GLMs was used to confirm significant BST and dorsal amygdala activation during threat anticipation (Threat vs. Safety). The same approach was used to examine extended amygdala reactivity to temporally *Uncertain* Threat (vs. Baseline) and *Certain* Threat (vs. Baseline) anticipation. For the emotional-faces task, a parallel approach was used to confirm significant extended amygdala reactivity to 'threatening' faces (Angry and Fearful Faces vs. Places) presentation. Significance was assessed using FDR $q < .05$, whole-brain corrected. All analyses employed unsmoothed data to maximize spatial resolution.

The first major aim of the present study was to test whether individuals with a more negative disposition show heightened extended amygdala reactivity to threat. To do so, we extracted regression coefficients for the Threat vs. Safety contrast, separately for the anatomically-defined BST and Ce ROIs. Exploratory one-sample *t*-tests, implemented using the 'stats' package (Team, 2020), confirmed significant activation in both ROIs ($ps < 0.001$).

To maximize power and ensure strong inferences, brain-disposition relations were tested using robust regression models (Tukey's bi-weight), which mitigate the

influence of outliers and other departures from conventional model assumptions (Wager, Keller, Lacey, & Jonides, 2005).

To provide an unbiased estimate of model performance, we used a repeated cross-validation approach (5-fold, 1,000 repetitions) (Yarkoni & Westfall, 2017). The dataset was randomly subdivided into 5 'folds' of approximately equal size. Then, the regression model was trained using 4 folds of the data (80%) and tested on the 'held-out' fold (20%). This was iteratively repeated 4 times using a different fold for testing each time. This method was then repeated 1,000 times, randomly re-allocating the data to a new set of 5 folds on each repetition. Model estimates were averaged across repetitions.

A similar analytic framework was used to test whether relations between dispositional negativity and extended amygdala reactivity are more evident during the anticipation of *Uncertain* Threat (vs. Baseline) compared to *Certain* Threat (vs. Baseline). To determine the unique contribution of each contrast, this was tested using a simultaneous model. Follow-up analyses—focused on relations with concurrent measures of anxious distress and arousal—were used to inform the interpretation of significant brain-disposition associations. To clarify specificity, we performed parallel analyses using data acquired during the presentation of 'threatening' faces (Angry and Fearful Faces vs. Places). Again, exploratory one-sample *t*-tests confirmed significant activation in both ROIs ($ps < 0.001$).

Hypothesis testing used spatially unsmoothed data, and significance was assessed using $p = 0.05$ (two-tailed, uncorrected). To inform the interpretation of significant brain-

disposition associations, we performed follow-up tests to explore potential relations between brain function and concurrent measures of in-scanner distress and arousal. Finally, standard voxelwise GLMs (random effects) were used to explore relations between mean-centered dispositional negativity and activation in less intensely scrutinized regions.

The second major aim of the present study was to determine whether the threat-anticipation and emotional-faces tasks are interchangeable probes of extended amygdala reactivity (i.e., show 'convergent validity').

Using the analytic framework described above, we computed the correlation between individual differences in threat-anticipation and emotional-faces activation, separately for the BST and Ce ROIs. To quantify the strength of the evidence for the null and alternative hypotheses, Bayes Factors were computed using the 'bayesTestR' package (Makowski, Ben Shachar, & Lüdecke, 2019). This approach quantified the odds in favor of one hypothesis (e.g., alternative hypothesis, $\boldsymbol{H_1; \rho > 0}$; tasks show evidence of convergence) relative to another (i.e., null hypothesis, $\boldsymbol{H_0; \rho = 0}$; tasks show no evidence of convergence). This approach integrates prior parameter information with model likelihood to obtain the posterior distribution of the parameters of interest (e.g., the between-task correlation coefficient for BST reactivity). Here, the Bayes Factor ($\boldsymbol{BF_{10}}$) quantifies the change in relative belief in favor of a given hypothesis, using the following equation (Kelter, 2020; Quintana & Williams, 2018; van Doorn et al., in press):

$$\underbrace{\frac{p(x|H_1)}{p(x|H_0)}}_{BF_{10}} = \underbrace{\frac{\mathbb{P}(H_1|x)}{\mathbb{P}(H_0|x)}}_{\textit{Posterior Odds}} \cdot \underbrace{\frac{\mathbb{P}(H_0)}{\mathbb{P}(H_1)}}_{\textit{Prior Odds}}$$

A $\boldsymbol{BF_{10}} < .33$ is often interpreted as moderate-to-strong support for the null, whereas a $\boldsymbol{BF_{10}} > 3$ is often interpreted as moderate-to-strong support for the alternative.

Results

Threat anticipation increases anxious distress and arousal

As a precursor to hypothesis testing, we used a series of repeated-measures generalized linear models to confirm that the threat-anticipation task had the intended effects on behavior (**Fig. 3**). To inform interpretation of predicted brain-behavior associations, dispositional negativity was included in the model.

Results revealed that subjects experienced significantly greater distress when anticipating aversive outcomes (Valence: $t = 56.65$, $p < 0.001$), and when anticipating outcomes with uncertain timing (Certainty: $t = 11.54$, $p < 0.001$). Furthermore, individuals with higher levels of dispositional negativity showed indiscriminately elevated distress across conditions (dispositional negativity: $t = 4.12$, $p < 0.001$). None of the interactions were significant, ps > 0.126.

A similar pattern was evident for anxious arousal. Skin conductance levels were significantly elevated when anticipating aversive outcomes (Valence: $t = 38.00$, $p < 0.001$), and when anticipating outcomes with uncertain timing (Certainty: $t = 8.84$, $p < 0.001$). The impact of threat on skin conductance was potentiated by temporal uncertainty (Valence x Certainty: $t = 20.54$, $p < 0.001$), such that the difference in skin conductance levels during Threat and Safety conditions was significantly greater when timing was uncertain ($\beta = 0.09$, $t = 41.24$, $p < 0.001$) than when it was predictable ($\beta = 0.03$, $t = 12.30$, $p < 0.001$).

Taken together, these observations confirm that the threat-anticipation task elicits robust anxiety across multiple response channels.

Threat anticipation and 'threatening' faces recruit the extended amygdala

We used a series of whole-brain voxelwise GLMs to confirm that the threat-anticipation and the emotional-faces tasks both engaged the extended amygdala. Results revealed significant BST and dorsal amygdala activation during threat anticipation (FDR $q < 0.05$, whole-brain corrected; see **Fig. 4** and **Supplementary Table 1**). The same general pattern was evident for the anticipation of Uncertain Threat and Certain Threat, relative to the implicit baseline (see **Fig. 4** and **Supplementary Tables 2-3**). Analyses focused on the presentation of 'threatening' faces also revealed significant activation in the BST and the dorsal amygdala (see **Fig. 4** and **Supplementary Table 4**).

Collectively, these findings demonstrate that both threat anticipation and emotional-face presentation are valid probes of extended amygdala function.

Dispositionally negative individuals show increased BST reactivity to Uncertain Threat

The first major aim of the present study was to test whether individuals with a more negative disposition show heightened extended amygdala reactivity during threat anticipation. To test this, we extracted contrast coefficients (Threat vs. Safety), separately for each subject and ROI, and computed robust regressions with dispositional negativity. Models were trained and tested using a repeated cross-validation approach, providing unbiased estimates of brain-disposition relations (5-folds, 1,000 repetitions).

Results revealed that individuals with a more negative disposition exhibited significantly greater activation in the BST during threat anticipation (β = 0.12, t(218) = 1.67, p = 0.049; see **Fig. 5**). This association was marginally significant when controlling for Ce reactivity (β = 0.11, t(217) = 1.58, p = 0.057). Ce activation during threat anticipation was not significantly related to individual differences in dispositional negativity (β = 0.02, t(218) = 0.34, p = 0.366; see **Fig. 5**).

Prior work raises the possibility that relations between dispositional negativity and extended amygdala function will be magnified when threat is uncertain. To test this, we computed robust regressions between dispositional negativity and extended amygdala reactivity to temporally *uncertain* threat, separately for each ROI. To clarify specificity, models controlled for activation during the anticipation of *certain* threat. Results revealed that individuals with a more negative disposition showed significantly greater activation in the BST during Uncertain-Threat anticipation, controlling for Certain-Threat (β = 0.24, t(217) = 2.71, p = 0.004; see **Fig. 5**). This association remained significant in models that *included* Ce reactivity to *Uncertain* Threat (β = 0.26, t(216) = 2.84, p = 0.002), or *excluded* BST reactivity to *Certain* Threat (β = 0.19, t(218) = 2.73, p = 0.003). Individual differences in dispositional negativity were not significantly related to BST reactivity to Certain Threat (β = -0.09, t(217) = -1.04, p = 0.151; see **Fig. 5**). Dispositional negativity was also unrelated to Ce reactivity for both types of Threat (Uncertain: β = -0.10, t(217) = -1.04, p = 0.150; Certain: β = 0.04, t(217) = 0.48, p = 0.317; see **Fig. 5**). In short, relations between dispositional negativity and extended amygdala reactivity are only evident for the BST and unique to Uncertain-Threat anticipation.

To inform interpretation of the observed association between dispositional negativity and BST function, we performed a series of follow-up analyses. The first examined relations between BST reactivity to Uncertain-Threat anticipation and concurrent measures of anxious distress and arousal. BST activation was associated with elevated levels of physiological arousal during Uncertain-Threat anticipation (β = 0.16, t(216) = 2.31, p = 0.011), but was unrelated to the intensity of subjective anxiety (β = 0.07, t(218) = 1.03, p = 0.152). A second set of analyses examined relations between dispositional negativity and threat-elicited distress and arousal. Results mirrored the first set. Here, higher levels of dispositional negativity were associated with more intense anxiety (β = 0.35, t(218) = 5.27, p < 0.001), but were unrelated to the degree of physiological arousal elicited by Uncertain-Threat anticipation (β = 0.00, t(216)=0.05, p = 0.482). Individual differences in anxious distress and arousal were marginally associated, β = 0.095, t(216) = 1.36, p = 0.087. These results suggest that relations between dispositional negativity—the propensity to experience heightened negative affect—and BST reactivity to Uncertain Threat are indirect. BST reactivity to Uncertain Threat is associated with heightened physiological arousal, consistent with prior work, but not increased feelings of distress.

To date, the vast majority of human neuroimaging studies of dispositional negativity have relied on emotional-face paradigms. While emotional faces are widely used and evoke robust extended amygdala activation, they do not elicit meaningful distress or arousal in typical populations. Here, we leveraged the same ROI-based analytic approach used to interrogate relations with threat anticipation to test relations between dispositional negativity and extended amygdala reactivity to 'threatening' faces (Angry

and Fearful Faces vs. Places). Results failed to reveal significant relations with either the BST (β = 0.03, t(211) = 0.41, p = 0.342) or Ce (β = 0.03, t(211) = 0.39, p = 0.348). Likewise, a series of exploratory voxelwise analyses did not detect significant relations between (mean-centered) dispositional negativity and extended amygdala reactivity to either the threat-anticipation or the emotional-faces tasks (FDR q < .05, whole-brain corrected).

Individual differences in extended amygdala reactivity to the threat-anticipation and emotional-faces tasks show inconsistent evidence of convergent validity

Implicit in much of the literature is the assumption that different fMRI paradigms targeting a common function (e.g., 'emotion') are exchangeable probes of individual differences in brain function (e.g., amygdala). Yet, this assumption of 'convergent validity' has rarely been examined. Here, we used robust regressions with repeated cross-validation to test whether individual differences in BST and Ce reactivity to the anticipation of threat and the presentation of 'threatening' faces co-vary.

Consistent with prior work (Villalta-Gil et al., 2017), robust regression showed no evidence of convergence in Ce reactivity between tasks, β = -0.01, t(207) = -0.19, p = 0.424. From a Bayesian perspective, this corresponds to inconclusive evidence of convergent validity (BF_{10} = 1.02). In contrast to the Ce, robust regression yielded marginally significant evidence of between-task convergence in the BST, β = 0.11, t(207) = 1.57, p = 0.059, with moderate Bayesian evidence of convergent validity, BF_{10} = 3.47.

Discussion

Elevated levels of dispositional negativity confer increased risk for anxiety disorders, depression, and a variety of other adverse outcomes, but the underlying neurobiology has remained incompletely understood (Boissy, 1995; Hur, Stockbridge, Fox, & Shackman, 2019; Shackman, Stockbridge, LeMay, & Fox, 2018; Shackman et al., 2016). The present results demonstrate that individuals with a more negative disposition show heightened BST activation during threat anticipation, and this association is uniquely evident when threat is temporally uncertain. In fact, BST reactivity to Uncertain Threat remained predictive of dispositional negativity after controlling for either BST reactivity to Certain Threat or Ce reactivity to Uncertain Threat. Our results further suggest that relations between dispositional negativity—the propensity to experience heightened negative affect—and BST function are indirect. BST reactivity to Uncertain Threat was associated with heightened signs of threat-elicited arousal, but not increased feelings of distress. Dispositional negativity was unrelated to Ce activation during threat anticipation and to extended amygdala (BST/Ce) activation during 'threatening' face presentation. While it is tempting to treat different 'threat' paradigms—from viewing photographs of 'threatening' faces to anticipating the delivery of aversive stimulation—as interchangeable probes of individual differences in extended amygdala function, the underlying assumption of convergent validity has rarely been examined. The present results provide no evidence of between-task convergence in the Ce, consistent with prior work (Villalta-Gil et al., 2017), and marginal evidence in the BST.

The present study provides new evidence that individual differences in dispositional negativity are associated with heightened BST activation during Uncertain-Threat anticipation. This is consistent with anatomical evidence that the BST sends dense projections to the subcortical and brainstem regions that proximally mediate behavioral and physiological signs of negative affect (Hur et al., 2019). While the mechanistic relevance of the BST to dispositional negativity remains under-explored, perturbation studies in rodents suggest that it is crucial for some forms of anxiety (Duvarci, Bauer, & Paré, 2009; Glover et al., 2020). For example, excitotoxic lesions of the BST attenuate defensive responses (freezing) to diffuse, uncertain threat (elevated-plus maze; Duvarci, Bauer, & Paré, 2009). These mechanistic observations are consistent with neuroimaging evidence that the BST is sensitive to a range of noxious and threatening stimuli, including aversive photographs (Brinkmann et al., 2018; Sabatinelli et al., 2011), horror film clips (Hudson et al., in press; https://neurovault.org/collections/6237), and the uncertain anticipation of aversive stimuli (Hur, Smith, et al., 2020; Mobbs et al., 2010). With regard to dispositional negativity, PET studies in monkeys demonstrate that BST metabolism is phenotypically and genetically correlated with trait anxiety and behavioral inhibition (Fox, Oler, Shackman, et al., 2015; Shackman et al., 2017). Likewise, fMRI work in humans shows that individuals with a more negative disposition are characterized by heightened BST engagement during the anticipation of temporally uncertain shock (Somerville et al., 2010). The present results reinforce and extend this work by showing that BST reactivity to Uncertain-Threat anticipation is uniquely associated with individual differences in dispositional negativity, over and above variation in BST

reactivity to Certain Threat, and dorsal amygdala (Ce) reactivity to Uncertain Threat. Together, these observations reinforce the hypothesis that the BST is a central component of the distributed neural system governing dispositional negativity. A key challenge for the future will be to clarify causation. There is compelling evidence that dispositional negativity can be dampened through both psychological and pharmacological interventions (Roberts et al., 2017; S. Sauer-Zavala et al., 2020; Stieger et al., 2021; Zemestani, Ommati, Rezaei, & Gallagher, 2021). It would be fruitful to test whether these effects reflect attenuated BST reactivity to uncertain threat.

The present results have implications for understanding how dispositional negativity confers risk for anxiety disorders and depression. Our findings show that individuals who, by virtue of their more negative disposition, are at risk for developing internalizing disorders are marked by heightened BST reactivity to Uncertain Threat. This observation is consistent with conceptual models that emphasize the central role of threat uncertainty to the development and maintenance of pathological anxiety (Davis et al., 2010; Grupe & Nitschke, 2013; Shackman et al., 2016). It is also consistent with recent meta-analytic evidence that individuals with anxiety disorders show exaggerated BST reactivity to threat (Chavanne & Robinson, 2021; Shackman & Fox, 2021). Collectively, this work motivates the hypothesis that exaggerated BST reactivity to uncertain threat is an active ingredient (i.e., diathesis) that helps mediate the association between dispositional negativity and internalizing illnesses. Prospective-longitudinal studies in more nationally representative, diverse populations will be a key step to addressing this hypothesis.

Our findings also demonstrate that BST reactivity to Uncertain-Threat anticipation is associated with elevated physiological arousal, but not the intensity of threat-elicited anxiety. This result is broadly consistent with the theoretical model articulated by LeDoux and colleagues, who argue that the BST is primarily responsible for orchestrating behavioral and physiological responses to uncertain threat, and that it only indirectly contributes to anxious feelings (LeDoux, 2015; LeDoux & Pine, 2016; Mobbs et al., 2019). The present results reinforce the possibility that relations between BST function and dispositional negativity—the tendency to experience heightened negative emotions—are implicit and indirect.

Our findings also have implications for the interpretation and design of neuroimaging studies of psychiatric risk and disease. Much of this work relies on emotional-faces tasks as the sole probe of negative valence systems. Yet, the present results demonstrate that extended amygdala reactivity to emotional faces is unrelated to the risk-conferring dispositional negativity phenotype. Moreover, analyses of convergent validity revealed modest between-task convergence in the BST, and negligible convergence in the dorsal amygdala (Ce), in broad accord with prior work (Villalta-Gil et al., 2017). These observations caution against relying on a single task to understand the role of individual differences in extended amygdala function in internalizing illness (Holmes & Patrick, 2018). To the extent that uncertain-threat anticipation is key, it may be necessary to devise new paradigms that are more suitable for community and biobank samples—for instance, using aversive auditory stimuli or film clips.

It is important to acknowledge the modest size of the BST-disposition associations observed in the present study. This is not surprising; it is, in fact, entirely consistent with theoretical expectation and prior work focused on the extended amygdala and other isolated brain regions (LeDoux & Pine, 2016; Shackman & Fox, 2018). In order to predict additional variance in dispositional negativity, it will be necessary to adopt multivoxel or multivariate machine learning approaches at the expense of neuroanatomical specificity (Woo, Chang, Lindquist, & Wager, 2017). In addition, recent psychometric work makes it clear that dispositional negativity can be fractionated into more specific facets (e.g., anxious, depressive, irritable) (Christopher J Soto & John, 2017). It will be fruitful to determine whether these specific facets are equally related to BST function.

Understanding the neural systems governing individual differences in dispositional negativity is important. Elevated dispositional negativity confers risk for a range of deleterious outcomes spanning health, wealth, and well-being. The present findings highlight the relevance of threat-elicited BST function to individual differences in dispositional negativity, particularly when threat is uncertain. A relatively large and carefully phenotyped sample, well-controlled tasks, and a pre-registered, best-practices approach (e.g., spatially unsmoothed data, *a priori* anatomical ROIs, and repeated cross-validation framework) bolster confidence in the robustness and translational relevance of these results. These observations lay the groundwork for the kinds of prospective-longitudinal and mechanistic studies that will be necessary to determine causation and, ultimately, to develop improved interventions for extreme dispositional negativity.

Tables

Study	*N* (% Male)	Dispositional Negativity	MRI Field Strength (T)	EPI Voxel Size (mm^3)	Normalization	Trait-Relevant Challenge	Relations Between Extended Amygdala Reactivity and Dispositional Negativity
Present Study	220 (49.5%), enriched for extreme dispositional negativity	Multi-Scale, Multi-Assessment Composite	3	10.5	BBR and Diffeomorphic	See the main report	See the main report
Brinkmann et al., 2018	93 (35.5%), screened to exclude any emotional illness in the past five years	STAI	3	15.3	Affine and Manual TT	Aversive Photographs	***N.S. ROI***
Indovina et al., 2011	23 (43.48%), screened to exclude l/t emotional illness	STAI	3	18.0	"SPM5"	Conditioned Aversive Cue	***Positive relations*** *between amygdala reactivity and dispositional negativity;* ***ROI & ROI-based FIR*** *BST not examined
Kirlic et al., 2019	83 (42.2%), 43 of whom had depression or anxiety disorder diagnoses	STAI	3	18.1	"AFNI" and Diffeomorphic	Conditioned Aversive Context (Instructed)	***N.S. Voxelwise***
Klumpers et al., 2017	108 (100%), screened to exclude l/t emotional illness	STAI	1.5	38.1	"SPM8"	Conditioned Aversive Cue	***N.S. Voxelwise***
Schuyler et al., 2011	127 (36.22%), screened to exclude emotional illness in the past year, & l/t serious mental illness	BFI-N	3	56.25	Affine	Aversive Photographs	***N.S. ROI*** ***Positive relations*** *between amygdala reactivity and dispositional negativity;* ***ROI-based FIR*** *BST not examined
Sjouwerman et al., 2020	113 (61.06%), screened to exclude l/t emotional illness	STAI	3	8.0	"SPM8"	Conditioned Aversive Cue	***Positive relations*** *between amygdala reactivity and dispositional negativity;* ***ROI*** *BST not examined
Somerville et al., 2010	50 (44%), screened to exclude l/t emotional illness	Multi-Scale Composite	3	31.5	"SPM2"	Anticipation of Temporally Uncertain Shock	***Positive relations*** *between BST reactivity and dispositional negativity;* ***ROI & Voxelwise*** ***N.S. Amygdala; ROI & Voxelwise***
West et al., 2021	319 (53.29%), screen to exclude l/t emotional illness	Multi-Scale Composite	3	8.0	"FNIRT"	Aversive Photographs	***N.S. ROI*** *BST not examined

Table 1. Human studies of dispositional negativity and distress-eliciting neuroimaging paradigms. [1]Older normalization techniques (e.g., affine, manual TT) can introduce substantial spatial smoothing and registration error, which is a concern for work focused on small subcortical structures, such as the Ce and BST. Abbreviations—BBR, boundary-based registration of the T1- and T2-weighted images; FIR, Finite Impulse Response modeling; l/t, lifetime; NR, not reported; NS, not significant; STAI, State-Trait Anxiety Inventory.

Figures

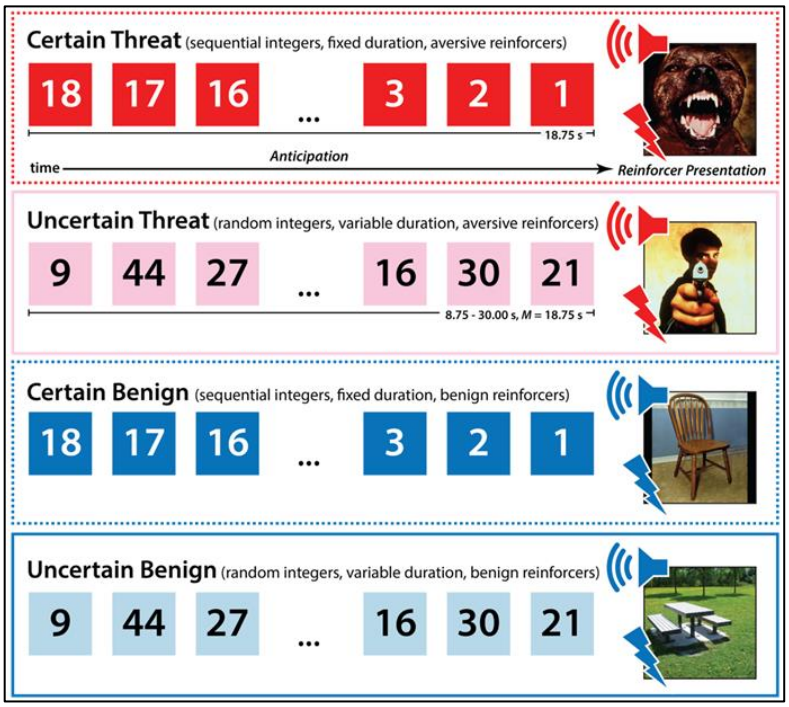

Figure 1. The 4 reinforcer conditions comprising the Maryland Threat Countdown (MTC) paradigm used in the present study. The task takes on a 2 × 2 design, using threat and benign reinforcers presented on a temporally certain or uncertain scale.

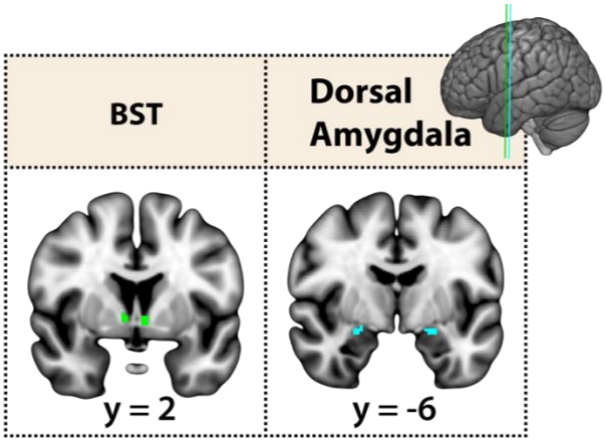

Figure 2. Coronal slices depicting the locations of the BST and Ce ROIs used in the present study. Analyses employed bilateral masks.

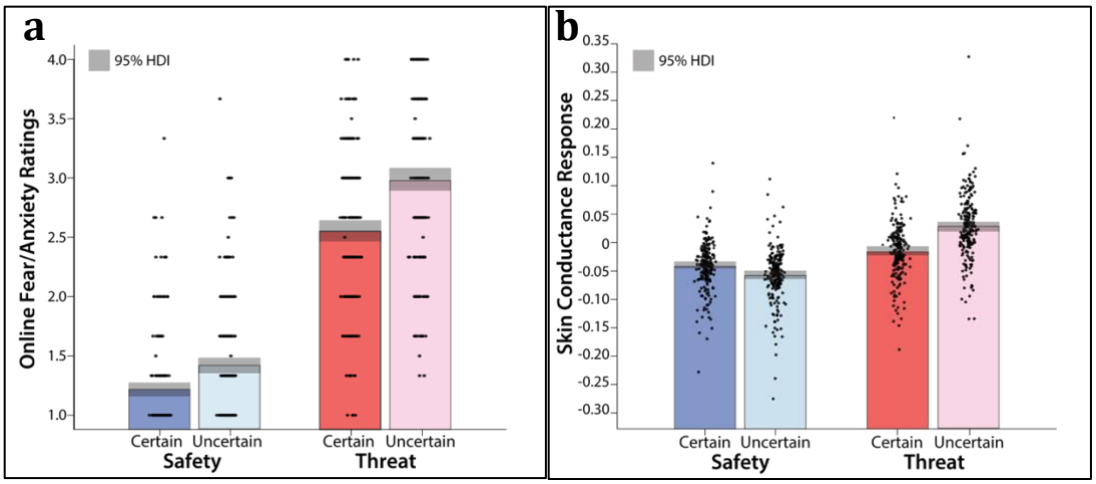

Figure 3. As shown in a and b, threat anticipation robustly increased subjective symptoms (in-scanner ratings) and objective signs (skin conductance) of anxiety, and this was particularly evident when the timing of aversive stimulation was uncertain (Threat > Safety, *p*s < 0.001; Uncertain Threat > Certain Threat, *p*s < 0.001). Skin conductance results also revealed a Valence x Certainty interaction, such that the difference in skin conductance levels during Threat and Safety conditions was significantly greater when timing was uncertain, $p < 0.001$. Data (black points; individual participants), Bayesian 95% highest density interval (gray bands), and mean (bars) for each condition. Highest density intervals permit population-generalizable visual inferences about mean differences and were estimated using 1000 samples from a posterior Gaussian distribution.

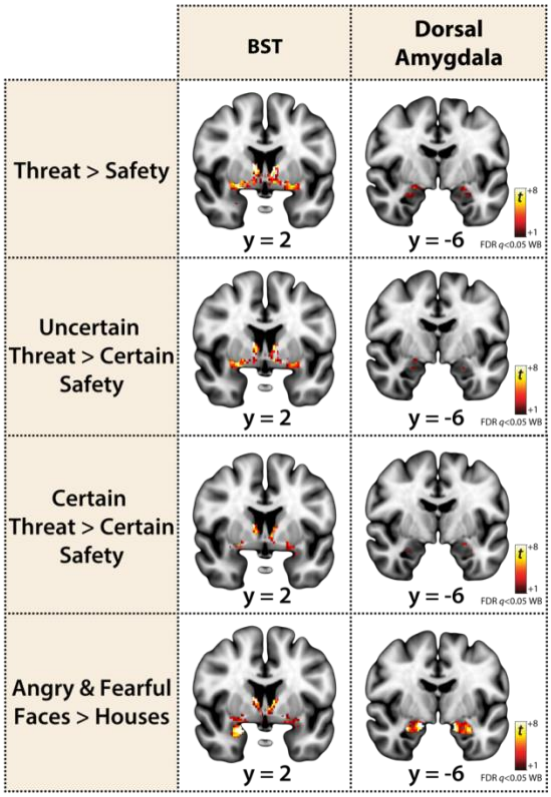

Figure 4. The coronal slices above depict voxels showing significantly increased activity within the BST (left column) and the dorsal amygdala/Ce (right column) for various contrasts of interest. All images are masked to highlight significant voxels in the extended amygdala. Together, these observations suggest that these regions are sensitive to both temporally certain and uncertain threat, as well as to threat-related face stimuli. For additional details, see Supplementary Tables 1-4; FDR, false discovery rate; WB, whole-brain-corrected.

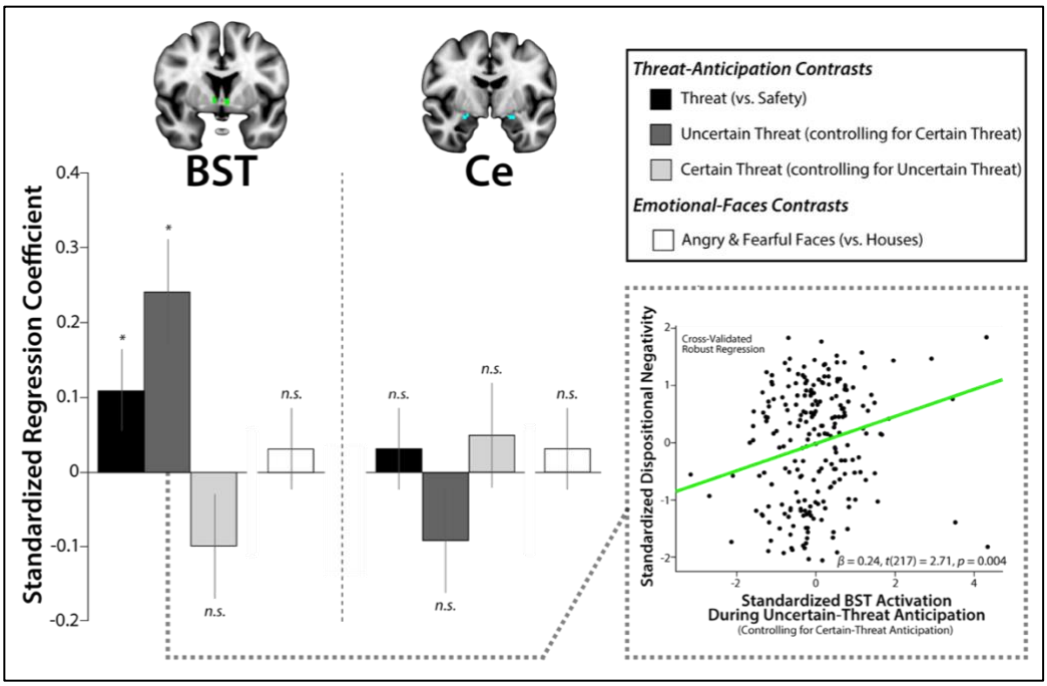

Figure 5. Individuals with a more negative disposition show increased BST reactivity to Uncertain Threat. Figure depicts standardized, cross-validated robust regression coefficients for threat-anticipation and emotional-faces contrasts of interest. The left side of the bar graph show findings for the BST. The right side of the bar graph show findings for the Ce. Error bars indicate the *SE*. Inset depicts the scatterplot corresponding to the key significant finding—that BST reactivity to Uncertain Threat is associated with heightened dispositional negativity when controlling for Certain Threat.

Supplement

Supplemental Table 1. Descriptive statistics for clusters and local extrema showing greater activity during the anticipation of Threat relative to Safety (FDR $q < 0.05$, whole-brain corrected).

		mm^3	*t*	x	y	z
	Cluster 1	666,016				
	L Frontal Operculum Cortex		13.64	-32	20	10
	L Frontal Orbital Cortex		11.77	-30	28	0
	L Paracingulate Gyrus		11.56	-8	12	38
	L Cingulate Gyrus, anterior division		11.50	-6	10	40
	L Central Opercular Cortex		11.10	-42	8	2
	L Caudate		11.05	-8	0	8
	L Putamen		10.88	-20	10	-2
	L Temporal Occipital Fusiform Cortex		10.67	-26	-60	-16
	L Brain-Stem		10.30	-2	-28	-2
	L Superior Frontal Gyrus		10.25	-14	-2	66
	L Precentral Gyrus		10.07	-32	-6	50
	L Juxtapositional Lobule Cortex		10.05	-2	6	46
	L Cingulate Gyrus, posterior division		10.04	-14	-28	38
	L Thalamus		10.01	-8	-4	12
	L Occipital Fusiform Gyrus		9.48	-30	-68	-18
	L Supramarginal Gyrus, posterior division		9.45	-56	-50	38
	L Bed Nucleus of the Stria Terminalis		9.43	-8	2	4
	L Middle Frontal Gyrus		9.16	-42	-2	60
	L Supramarginal Gyrus, anterior division		8.89	-54	-38	32
	L Inferior Frontal Gyrus, pars opercularis		8.85	-54	10	10
	L Lingual Gyrus		8.85	-4	-74	-12
	L Frontal Pole		8.83	-36	44	30
	L Bed Nucleus of the Stria Terminalis		8.55	-6	4	0
	L Parietal Operculum Cortex		7.71	-56	-34	24
	L Angular Gyrus		7.67	-56	-56	46
	L Superior Parietal Lobule		7.55	-18	-52	64
	L Precuneus Cortex		7.49	-10	-78	40
	L Lateral Occipital Cortex, superior division		7.35	-34	-60	60
	L Postcentral Gyrus		7.27	-42	-32	44

	L Cuneal Cortex		6.34	-16	-78	34
	L Occipital Pole		5.90	-20	-96	10
	L Hippocampus		5.56	-34	-28	-8
	L Insular Cortex		5.55	-34	18	-4
	L Lateral Occipital Cortex, inferior division		5.50	-56	-64	10
	L Pallidum		5.50	-20	-10	-4
	L Inferior Frontal Gyrus, pars triangularis		5.46	-54	22	6
	L Inferior Temporal Gyrus, temporooccipital part		5.46	-42	-56	-10
	L Heschls Gyrus (includes H1 and H2)		5.31	-38	-28	12
	L Middle Temporal Gyrus, temporooccipital part		5.13	-62	-56	6
	L Planum Polare		5.06	-40	-14	-8
	L Temporal Fusiform Cortex, posterior division		5.01	-30	-32	-28
	L Amygdala		4.74	-24	-14	-14
	L Superior Temporal Gyrus, posterior division		4.47	-54	-24	-4
	L Middle Temporal Gyrus, posterior division		4.44	-48	-28	-6
	L Planum Temporale		4.37	-62	-20	4
	L Intracalcarine Cortex		4.34	-18	-66	6
	L Amygdala (central nucleus)		4.14	-24	-12	-12
	L Subcallosal Cortex		4.12	-12	16	-14
	L Temporal Pole		4.04	-52	14	-12
	L Accumbens		3.65	-6	12	-6
	L Parahippocampal Gyrus, posterior division		3.33	-14	-36	-6
	L Superior Temporal Gyrus, anterior division		3.12	-54	2	-14
	L Amygdala (central nucleus)		2.92	-22	-6	-12
	L Inferior Temporal Gyrus, posterior division		2.34	-50	-38	-16
	L Supracalcarine Cortex		2.32	-22	-62	20
	R Cingulate Gyrus, anterior division		14.08	10	12	38
	R Paracingulate Gyrus		14.06	10	20	34
	R Frontal Operculum Cortex		13.18	34	24	8
	R Bed Nucleus of the Stria Terminalis/Caudate		12.87	10	2	8
	R Thalamus		12.44	10	-2	12
	R Precentral Gyrus		12.08	42	-2	46
	R Juxtapositional Lobule Cortex		11.49	10	6	44
	R Putamen		11.44	22	6	4

	R Brain-Stem		11.39	4	-28	-2
	R Supramarginal Gyrus, posterior division		11.32	60	-42	24
	R Central Opercular Cortex		11.15	44	8	2
	R Superior Temporal Gyrus, posterior division		10.61	48	-24	-4
	R Superior Frontal Gyrus		10.41	14	10	62
	R Pallidum		9.87	20	4	0
	R Superior Parietal Lobule		9.69	24	-46	62
	R Frontal Orbital Cortex		9.57	34	22	-8
	R Frontal Pole		9.56	34	46	30
	R Bed Nucleus of the Stria Terminalis/Caudate		9.51	8	6	0
	R Cingulate Gyrus, posterior division		9.49	10	-26	42
	R Parietal Operculum Cortex		9.40	56	-30	26
	R Supramarginal Gyrus, anterior division		9.33	56	-32	34
	R Angular Gyrus		9.16	64	-46	28
	R Precuneus Cortex		8.97	12	-54	54
	R Middle Frontal Gyrus		8.84	52	8	42
	R Postcentral Gyrus		8.43	48	-28	50
	R Inferior Frontal Gyrus, pars triangularis		8.05	50	22	2
	R Temporal Occipital Fusiform Cortex		8.03	26	-56	-16
	R Middle Temporal Gyrus, posterior division		7.83	52	-30	-4
	R Inferior Frontal Gyrus, pars opercularis		7.67	54	12	4
	R Lateral Occipital Cortex, superior division		7.50	18	-74	40
	R Middle Temporal Gyrus, temporooccipital part		6.94	56	-40	4
	R Inferior Temporal Gyrus, temporooccipital part		6.69	52	-60	-12
	R Occipital Fusiform Gyrus		6.45	20	-74	-16
	R Occipital Pole		6.41	28	-94	12
	R Hippocampus		6.38	34	-28	-6
	R Lateral Occipital Cortex, inferior division		6.29	42	-86	-8
	R Lingual Gyrus		6.27	0	-74	-8
	R Cuneal Cortex		6.00	14	-76	36
	R Amygdala		5.99	30	-8	-14
	R Insular Cortex		5.32	42	-2	-12
	R Temporal Pole		5.17	54	16	-10
	R Accumbens		4.77	6	10	-6

	R Planum Polare		4.50	44	-8	-6
	R Intracalcarine Cortex		4.35	24	-60	6
	R Amygdala (central nucleus)		4.16	22	-6	-12
	R Temporal Fusiform Cortex, posterior division		4.07	40	-32	-16
	R Inferior Temporal Gyrus, anterior division		3.99	42	-2	-38
	R Supracalcarine Cortex		3.89	22	-64	14
	R Parahippocampal Gyrus, anterior division		3.66	26	-4	-32
	R Planum Temporale		3.54	40	-28	12
	R Parahippocampal Gyrus, posterior division		3.32	16	-34	-6
	R Heschls Gyrus (includes H1 and H2)		2.95	48	-8	4
	R Superior Temporal Gyrus, anterior division		2.66	56	4	-14
	R Temporal Fusiform Cortex, anterior division		2.33	38	-8	-38
	Cluster 2	1,368				
	L Middle Temporal Gyrus, anterior division		4.11	-48	-2	-32
	L Inferior Temporal Gyrus, anterior division		3.97	-46	0	-34
	L Inferior Temporal Gyrus, posterior division		3.94	-56	-20	-32
	L Temporal Pole		3.61	-42	10	-34
	L Temporal Fusiform Cortex, anterior division		3.44	-34	-6	-34
	Cluster 3	920				
	R Frontal Pole		4.64	26	52	-12
	Cluster 4	392				
	R Frontal Pole		3.88	30	68	2
	Cluster 5	104				
	L Frontal Pole		3.22	-24	66	-6
	Cluster 6	96				
	R Occipital Pole		3.88	6	-96	-8
	Cluster 7	88				
	R Paracingulate Gyrus		3.14	12	46	-2
	Cluster 8	88				
	L Insular Cortex		4.28	-42	-14	2
	Cluster 9	80				
	L Hippocampus		3.51	-30	-14	-24
	L Parahippocampal Gyrus, anterior division		2.44	-30	-10	-30
	Cluster 10	80				

	R Frontal Pole		2.40	18	44	44
	Cluster 11	64				
	L Temporal Pole		3.21	-44	16	-26
	Cluster 12	64				
	L Temporal Pole		4.57	-50	16	-18
	Cluster 13	56				
	L Middle Temporal Gyrus, posterior division		2.61	-66	-34	-18
	Cluster 14	56				
	L Frontal Pole		2.95	-46	38	4
	L Inferior Frontal Gyrus, pars triangularis		2.32	-52	36	6
	Cluster 15	56				
	R Frontal Pole		3.45	10	62	10
	Cluster 16	56				
	L Postcentral Gyrus		3.97	-34	-26	52
	Cluster 17	48				
	L Frontal Medial Cortex		2.25	-6	40	-22
	Cluster 18	48				
	L Frontal Pole		3.18	-28	62	-10
	Cluster 19	48				
	L Middle Temporal Gyrus, posterior division		2.84	-68	-38	2
	Cluster 20	40				
	L Brain-Stem		3.26	-14	-26	-38
	Cluster 21	40				
	R Subcallosal Cortex		3.06	0	24	-4
	Cluster 22	40				
	L Planum Temporale		3.42	-52	-24	4

Supplemental Table 2. Descriptive statistics for clusters and local extrema showing greater activity during the anticipation of Uncertain Threat relative to Predictable Safety (FDR $q < 0.05$, whole-brain corrected).

	mm^3	***t***	**x**	**y**	**z**
Cluster 1	360,632				
L Frontal Operculum Cortex		12.24	-32	20	10
L Frontal Orbital Cortex		11.50	-30	28	0
L Cingulate Gyrus, anterior division		9.86	-2	22	34
L Central Opercular Cortex		9.53	-42	6	2

	L Paracingulate Gyrus		8.61	-8	22	32
	L Supramarginal Gyrus, posterior division		8.59	-56	-50	36
	L Superior Frontal Gyrus		8.58	-12	-6	68
	L Juxtapositional Lobule Cortex		8.35	-2	6	46
	L Angular Gyrus		8.33	-60	-54	36
	L Putamen		8.06	-24	6	-4
	L Brain-Stem		7.94	-2	-28	-2
	L Frontal Pole		7.58	-36	48	30
	L Cingulate Gyrus, posterior division		7.50	-12	-24	38
	L Precentral Gyrus		7.37	-32	-6	50
	L Occipital Fusiform Gyrus		7.37	-14	-90	-12
	L Bed Nucleus of the Stria Terminalis/Caudate		7.35	-8	2	6
	L Inferior Frontal Gyrus, pars opercularis		7.27	-56	14	0
	L Parietal Operculum Cortex		7.21	-62	-30	20
	L Temporal Occipital Fusiform Cortex		7.20	-34	-56	-22
	L Inferior Frontal Gyrus, pars triangularis		7.18	-54	22	4
	L Occipital Pole		7.01	-22	-98	14
	L Supramarginal Gyrus, anterior division		7.00	-56	-38	32
	L Precuneus Cortex		6.81	-10	-70	38
	L Lingual Gyrus		6.76	-8	-72	-12
	L Postcentral Gyrus		6.54	-66	-22	22
	L Middle Frontal Gyrus		6.49	-34	34	38
	L Superior Parietal Lobule		6.30	-18	-52	64
	L Thalamus		6.23	-8	-4	12
	L Lateral Occipital Cortex, superior division		6.12	-38	-58	58
	L Bed Nucleus of the Stria Terminalis/Anterior Commissure		5.99	-8	2	-6
	L Lateral Occipital Cortex, inferior division		5.42	-42	-84	-10
	L Insular Cortex		4.49	-38	2	-2
	L Temporal Pole		4.26	-58	6	-8
	L Temporal Fusiform Cortex, posterior division		4.20	-40	-42	-18
	L Inferior Temporal Gyrus, temporooccipital part		4.11	-46	-62	-10
	L Pallidum		4.05	-26	-16	-2
	L Bed Nucleus of the Stria Terminalis		3.95	-6	2	0
	R Frontal Operculum Cortex		11.68	34	24	10

	R Paracingulate Gyrus		11.60	10	20	34
	R Precentral Gyrus		11.14	40	-2	46
	R Thalamus		10.72	10	0	10
	R Cingulate Gyrus, anterior division		10.68	10	12	38
	R Juxtapositional Lobule Cortex		10.45	10	4	46
	R Frontal Orbital Cortex		10.30	32	22	-8
	R Putamen		10.12	32	-2	-6
	R Central Opercular Cortex		10.02	46	8	0
	R Parietal Operculum Cortex		9.85	52	-30	28
	R Brain-Stem		9.84	4	-28	-2
	R Lateral Occipital Cortex, inferior division		9.61	42	-86	-8
	R Middle Frontal Gyrus		9.37	46	2	56
	R Angular Gyrus		9.25	64	-46	28
	R Supramarginal Gyrus, posterior division		9.23	62	-46	34
	R Superior Parietal Lobule		9.02	22	-46	64
	R Supramarginal Gyrus, anterior division		8.94	54	-30	32
	R Occipital Pole		8.92	26	-94	12
	R Superior Frontal Gyrus		8.88	18	-8	70
	R Temporal Pole		8.87	50	10	-4
	R Occipital Fusiform Gyrus		8.62	38	-68	-12
	R Superior Temporal Gyrus, posterior division		8.19	48	-24	-4
	R Inferior Frontal Gyrus, pars triangularis		8.10	52	22	2
	R Cingulate Gyrus, posterior division		7.79	10	-20	42
	R Caudate		7.60	12	-2	16
	R Inferior Frontal Gyrus, pars opercularis		7.44	54	10	6
	R Postcentral Gyrus		7.40	34	-38	62
	R Frontal Pole		7.15	26	48	24
	R Bed Nucleus of the Stria Terminalis		6.87	8	2	4
	R Middle Temporal Gyrus, posterior division		6.61	54	-30	-4
	R Inferior Temporal Gyrus, temporooccipital part		6.50	46	-50	-14
	R Insular Cortex		6.49	38	4	0
	R Middle Temporal Gyrus, temporooccipital part		5.93	46	-56	6
	R Lingual Gyrus		5.68	10	-80	-4
	R Lateral Occipital Cortex, superior division		5.65	34	-66	28

	R Temporal Occipital Fusiform Cortex		5.63	38	-48	-18
	R Accumbens		5.11	10	6	-6
	R Pallidum		5.08	18	2	2
	R Precuneus Cortex		4.92	4	-48	54
	R Planum Polare		4.66	46	-8	-6
	R Thalamus		4.35	0	-10	0
	R Temporal Fusiform Cortex, posterior division		3.80	32	-34	-24
	R Hippocampus		3.79	34	-30	-6
	R Amygdala		3.66	18	-2	-14
	R Heschls Gyrus (includes H1 and H2)		3.08	48	-22	8
	Cluster 2	2,352				
	L Middle Temporal Gyrus, temporooccipital part		4.52	-62	-48	6
	L Supramarginal Gyrus, posterior division		4.23	-54	-48	14
	L Middle Temporal Gyrus, posterior division		3.97	-60	-26	-4
	L Angular Gyrus		3.19	-64	-50	10
	Cluster 3	1,432				
	R Precuneus Cortex		5.83	16	-64	36
	R Cuneal Cortex		2.71	12	-78	38
	Cluster 4	920				
	R Temporal Pole		4.24	42	8	-38
	R Middle Temporal Gyrus, anterior division		3.99	48	2	-32
	Cluster 5	448				
	L Inferior Temporal Gyrus, anterior division		3.76	-46	-6	-32
	L Temporal Pole		3.69	-38	4	-36
	L Middle Temporal Gyrus, anterior division		3.67	-50	0	-32
	L Middle Temporal Gyrus, posterior division		3.24	-58	-12	-28
	Cluster 6	256				
	L Frontal Pole		4.73	-32	54	-12
	Cluster 7	248				
	L Planum Polare		4.80	-40	-14	-8
	Cluster 8	224				
	R Right Hippocampus		4.60	30	-38	2
	Cluster 9	176				
	L Brain-Stem		3.86	-6	-46	-52
	Cluster 10	136				

	R Frontal Pole		3.93	40	46	6
	Cluster 11	128				
	L Thalamus		3.45	-22	-34	-2
	L Hippocampus		2.95	-28	-36	-2
	Cluster 12	120				
	L Precentral Gyrus		3.82	-36	-16	42
	L Postcentral Gyrus		3.51	-38	-18	40
	Cluster 13	112				
	L Frontal Pole		4.01	-16	52	-16
	Cluster 14	104				
	L Heschls Gyrus (includes H1 and H2)		4.35	-38	-28	12
	Cluster 15	96				
	L Middle Frontal Gyrus		4.42	-46	14	30
	Cluster 16	88				
	L Middle Temporal Gyrus, posterior division		3.06	-56	-34	-10
	Cluster 17	64				
	L Middle Temporal Gyrus, posterior division		2.96	-68	-42	-2
	Cluster 18	56				
	L Temporal Pole		3.13	-46	8	-34
	Cluster 19	56				
	L Paracingulate Gyrus		2.99	-12	50	6
	Cluster 20	56				
	L Inferior Frontal Gyrus, pars opercularis		2.83	-38	16	26
	L Middle Frontal Gyrus		2.48	-36	14	28
	Cluster 21	48				
	L Inferior Temporal Gyrus, posterior division		3.65	-56	-20	-30
	Cluster 22	48				
	L Hippocampus		3.60	-22	-34	-8
	Cluster 23	40				
	L Hippocampus		3.76	-28	-18	-12
	Cluster 24	40				
	L Precuneus Cortex		2.80	-8	-42	44

Note: Suprathreshold activation was also evident in the R Dorsal Amygdala in the region of the Ce.

Supplemental Table 3. Descriptive statistics for clusters and local extrema showing greater activity during the anticipation of Certain Threat relative to Predictable Safety (FDR $q < 0.05$, whole-brain corrected).

		mm^3	*t*	x	y	z
	Cluster 1	67,208				
	L Cingulate Gyrus, anterior division		8.15	-8	16	34
	L Superior Frontal Gyrus		7.25	-14	-2	68
	L Paracingulate Gyrus		6.75	-4	12	42
	L Juxtapositional Lobule Cortex		6.25	-6	4	56
	L Precentral Gyrus		5.97	-28	-8	46
	L Middle Frontal Gyrus		4.88	-40	0	50
	L Postcentral Gyrus		3.49	-40	-18	40
	R Cingulate Gyrus, anterior division		8.37	10	12	38
	R Paracingulate Gyrus		7.52	12	20	34
	R Superior Frontal Gyrus		7.07	14	-6	68
	R Juxtapositional Lobule Cortex		6.68	8	6	58
	R Precentral Gyrus		6.45	48	2	46
	R Supramarginal Gyrus, posterior division		6.14	64	-40	26
	R Lateral Occipital Cortex, superior division		6.00	18	-76	42
	R Superior Temporal Gyrus, posterior division		5.87	48	-24	-4
	R Postcentral Gyrus		5.82	44	-28	42
	R Superior Parietal Lobule		5.78	34	-42	58
	R Cingulate Gyrus, posterior division		5.68	14	-28	40
	R Angular Gyrus		5.46	60	-46	32
	R Precuneus Cortex		5.34	14	-78	42
	R Middle Temporal Gyrus, temporooccipital part		5.26	50	-42	8
	R Middle Frontal Gyrus		5.20	42	0	54
	R Parietal Operculum Cortex		5.15	56	-28	24
	R Middle Temporal Gyrus, posterior division		4.66	48	-22	-8
	R Supramarginal Gyrus, anterior division		4.59	58	-24	32
	R Occipital Pole		4.31	18	-90	34
	R Cuneal Cortex		4.13	12	-80	38
	R Planum Temporale		3.36	62	-32	20
	Cluster 2	41,944				
	L Putamen		6.71	-20	12	-2

	L Thalamus		5.98	-2	-2	4
	L Lingual Gyrus		5.83	-10	-72	-10
	L Bed Nucleus of the Stria Terminalis		5.81	-6	2	0
	L Pallidum		5.68	-20	2	-4
	L Occipital Fusiform Gyrus		5.57	-30	-68	-18
	L Temporal Occipital Fusiform Cortex		5.54	-26	-60	-16
	L Caudate		5.35	-8	0	8
	L Brain-Stem		5.18	-2	-28	-2
	L Insular Cortex		2.95	-32	6	8
	L Accumbens		2.83	-6	12	-6
	R Temporal Occipital Fusiform Cortex		5.86	24	-54	-16
	R Thalamus		5.83	2	-16	-2
	R Lingual Gyrus		5.46	12	-70	-12
	R Brain-Stem		5.24	4	-28	-2
	R Occipital Fusiform Gyrus		4.71	20	-68	-14
	R Thalamus		3.35	0	-10	2
	Cluster 3	20,704				
	L Supramarginal Gyrus, posterior division		6.43	-56	-50	40
	L Precuneus Cortex		5.43	-10	-70	36
	L Supramarginal Gyrus, anterior division		5.29	-58	-34	40
	L Lateral Occipital Cortex, superior division		5.08	-10	-64	62
	L Angular Gyrus		5.07	-60	-54	36
	L Cuneal Cortex		4.96	-12	-80	38
	L Parietal Operculum Cortex		4.88	-58	-36	22
	L Superior Parietal Lobule		4.80	-36	-48	48
	L Postcentral Gyrus		4.68	-40	-32	48
	L Superior Temporal Gyrus, posterior division		2.77	-66	-34	14
	Cluster 4	15,232				
	R Putamen		7.94	24	10	-4
	R Caudate		7.33	10	2	10
	R Pallidum		7.19	20	4	0
	R Bed Nucleus of the Stria Terminalis/Caudate		6.50	8	6	0
	R Bed Nucleus of the Stria Terminalis		6.36	8	2	4
	R Central Opercular Cortex		6.17	48	8	-2
	R Frontal Operculum Cortex		6.07	34	24	8
	R Precentral Gyrus		5.61	62	4	12

	R Thalamus		5.56	10	-2	12
	R Insular Cortex		5.47	34	16	8
	R Frontal Orbital Cortex		5.25	32	30	-2
	R Temporal Pole		4.38	54	10	-2
	R Accumbens		4.34	10	12	-6
	R Frontal Pole		4.32	50	34	-4
	R Inferior Frontal Gyrus, pars triangularis		4.17	54	26	6
	R Inferior Frontal Gyrus, pars opercularis		3.66	56	10	6
	Cluster 5	7,880				
	L Frontal Pole		6.03	-30	52	28
	L Middle Frontal Gyrus		5.73	-34	34	38
	Cluster 6	5,616				
	R Frontal Pole		6.39	34	44	28
	R Middle Frontal Gyrus		6.35	30	32	34
	Cluster 7	5,536				
	L Frontal Operculum Cortex		7.52	-36	12	6
	L Central Opercular Cortex		5.93	-42	8	2
	L Insular Cortex		5.57	-30	26	6
	L Inferior Frontal Gyrus, pars opercularis		5.03	-52	14	2
	L Frontal Orbital Cortex		4.65	-30	28	0
	L Temporal Pole		4.21	-52	12	-6
	L Precentral Gyrus		3.35	-52	8	4
	L Inferior Frontal Gyrus, pars triangularis		2.82	-52	24	-4
	Cluster 8	1,224				
	L Cingulate Gyrus, posterior division		4.52	-14	-28	38
	L Precuneus Cortex		4.22	-10	-44	50
	L Precentral Gyrus		4.20	-16	-32	42
	Cluster 9	856				
	R Thalamus		4.39	16	-18	6
	Cluster 10	832				
	R Lateral Occipital Cortex, inferior division		4.57	44	-62	-12
	R Inferior Temporal Gyrus, temporooccipital part		3.97	52	-60	-12
	R Middle Temporal Gyrus, temporooccipital part		3.22	48	-56	2
	Cluster 11	664				
	R Putamen		5.23	30	-18	2

	R Amygdala (basolateral nucleus)		5.11	30	-8	-14
	R Hippocampus		3.34	26	-16	-12
	Cluster 12	424				
	R Occipital Pole		4.07	24	-92	10
	R Lateral Occipital Cortex, superior division		3.30	30	-84	18
	Cluster 13	376				
	L Cingulate Gyrus, posterior division		3.69	-2	-28	26
	R Cingulate Gyrus, posterior division		3.83	8	-26	28
	Cluster 14	360				
	L Lingual Gyrus		4.50	-10	-84	-8
	L Occipital Fusiform Gyrus		3.42	-16	-78	-10
	Cluster 15	304				
	L Putamen		5.68	-32	-12	-10
	L Amygdala (central nucleus)		4.14	-24	-12	-10
	L Hippocampus		3.58	-30	-16	-14
	Cluster 16	296				
	L Hippocampus		4.17	-20	-42	2
	L Thalamus		3.83	-22	-36	0
	Cluster 17	296				
	L Postcentral Gyrus		3.53	-66	-22	22
	Cluster 18	264				
	R Hippocampus		3.98	24	-36	4
	R Thalamus		3.75	20	-34	6
	Cluster 19	184				
	L Frontal Pole		4.18	-30	50	-14
	Cluster 20	176				
	L Brain-Stem		3.74	-6	-38	-44
	Cluster 21	168				
	R Brain-Stem		3.87	12	-26	-14
	Cluster 22	168				
	L Lateral Occipital Cortex, inferior division		4.32	-42	-80	-4
	Cluster 23	160				
	R Cingulate Gyrus, anterior division		3.93	4	-8	40
	Cluster 24	144				
	L Postcentral Gyrus		3.85	-56	-18	30
	Cluster 25	136				
	R Superior Frontal Gyrus		4.34	4	56	34
	Cluster 26	128				

	R Hippocampus		4.83	34	-34	-6
	Cluster 27	128				
	L Supramarginal Gyrus, posterior division		3.60	-52	-48	12
	Cluster 28	128				
	R Inferior Frontal Gyrus, pars opercularis		3.33	38	12	26
	Cluster 29	120				
	L Paracingulate Gyrus		3.64	-10	50	8
	Cluster 30	112				
	R Lateral Occipital Cortex, inferior division		3.84	40	-80	-4
	Cluster 31	104				
	R Brain-Stem		3.62	8	-38	-48
	Cluster 32	104				
	R Lateral Occipital Cortex, inferior division		2.99	50	-66	6
	Cluster 33	96				
	R Lateral Occipital Cortex, inferior division		3.78	42	-68	10
	R Lateral Occipital Cortex, superior division		3.60	40	-66	22
	Cluster 34	88				
	R Temporal Pole		4.02	36	8	-36
	Cluster 35	88				
	L Heschls Gyrus (includes H1 and H2)		4.22	-38	-28	12
	Cluster 36	88				
	L Central Opercular Cortex		3.38	-54	-20	18
	Cluster 37	88				
	R Postcentral Gyrus		3.27	22	-36	70
	Cluster 38	88				
	L Superior Frontal Gyrus		3.57	-4	20	64
	Cluster 39	80				
	L Middle Temporal Gyrus, temporooccipital part		3.49	-66	-50	6
	Cluster 40	80				
	L Lateral Occipital Cortex, inferior division		3.25	-40	-70	14
	Cluster 41	80				
	L Cingulate Gyrus, posterior division		3.62	-4	-18	28
	R Cingulate Gyrus, posterior division		3.38	2	-22	30
	Cluster 42	80				
	L Superior Frontal Gyrus		3.85	-12	32	52

	Cluster 43	72				
	L Hippocampus		3.64	-34	-30	-8
	Cluster 44	72				
	L Middle Temporal Gyrus, temporooccipital part		2.95	-58	-50	-4
	Cluster 45	72				
	R Frontal Pole		3.24	42	50	2
	Cluster 46	72				
	L Precentral Gyrus		5.19	-56	0	14
	Cluster 47	64				
	L Putamen		4.08	-32	-20	-4
	Cluster 48	64				
	L Lingual Gyrus		3.68	-22	-50	-2
	Cluster 49	64				
	R Lateral Occipital Cortex, inferior division		3.28	58	-62	6
	Cluster 50	64				
	L Occipital Pole		3.25	-20	-94	10
	Cluster 51	64				
	L Central Opercular Cortex		4.40	-44	0	12
	Cluster 52	64				
	L Precentral Gyrus		3.65	-60	2	20
	Cluster 53	64				
	R Postcentral Gyrus		3.50	52	-16	32
	Cluster 54	56				
	R Brain-Stem		3.43	2	-34	-48
	Cluster 55	56				
	L Brain-Stem		3.39	-10	-38	-30
	Cluster 56	56				
	R Brain-Stem		3.27	4	-26	-22
	Cluster 57	56				
	L Lateral Occipital Cortex, inferior division		3.40	-48	-74	-10
	Cluster 58	56				
	L Hippocampus		3.74	-34	-22	-10
	Cluster 59	56				
	L Frontal Pole		3.79	-32	38	-12
	Cluster 60	56				
	R Middle Temporal Gyrus, temporooccipital part		3.10	56	-56	6
	Cluster 61	56				

	L Frontal Pole		3.88	-38	60	6
	Cluster 62	56				
	L Lateral Occipital Cortex, inferior division		2.96	-56	-66	8
	Cluster 63	56				
	R Occipital Pole		3.61	20	-98	10
	Cluster 64	56				
	L Angular Gyrus		3.11	-46	-56	14
	Cluster 65	56				
	R Middle Temporal Gyrus, temporooccipital part		3.48	54	-52	10
	Cluster 66	56				
	R Cingulate Gyrus, anterior division		3.52	6	28	18
	Cluster 67	56				
	L Cingulate Gyrus, anterior division		3.85	-2	-6	38
	Cluster 68	56				
	R Precentral Gyrus		3.36	24	-18	74
	Cluster 69	48				
	L Inferior Temporal Gyrus, temporooccipital part		3.45	-44	-48	-12
	Cluster 70	48				
	R Middle Temporal Gyrus, posterior division		3.59	68	-20	-4
	Cluster 71	48				
	L Lateral Occipital Cortex, inferior division		3.65	-48	-66	2
	Cluster 72	48				
	R Lateral Occipital Cortex, inferior division		3.69	40	-88	2
	Cluster 73	48				
	L Supramarginal Gyrus, posterior division		2.93	-64	-46	8
	Cluster 74	48				
	L Central Opercular Cortex		2.88	-34	4	14
	Cluster 75	48				
	R Inferior Frontal Gyrus, pars opercularis		3.21	48	14	20
	Cluster 76	48				
	R Inferior Frontal Gyrus, pars opercularis		4.38	56	16	20
	R Precentral Gyrus		2.80	56	10	20
	Cluster 77	48				
	R Superior Frontal Gyrus		4.36	12	28	60
	Cluster 78	40				

	R Brain-Stem		4.06	8	-46	-54
	Cluster 79	40				
	L Brain-Stem		3.36	-2	-32	-24
	Cluster 80	40				
	L Middle Temporal Gyrus, posterior division		3.29	-62	-34	-18
	Cluster 81	40				
	L Lateral Occipital Cortex, inferior division		3.13	-38	-72	-4
	Cluster 82	40				
	R Paracingulate Gyrus		3.56	14	52	6
	Cluster 83	40				
	R Middle Temporal Gyrus, temporooccipital part		3.16	62	-54	12
	Cluster 84	40				
	R Thalamus		3.73	8	-20	16
	Cluster 85	40				
	L Caudate		3.67	-18	-16	24
	Cluster 86	40				
	R Frontal Pole		2.80	14	58	28
	Cluster 87	40				
	R Angular Gyrus		3.20	52	-52	46

Note: Suprathreshold activation was also evident in the L Dorsal Amygdala in the region of the Ce.

Supplemental Table 4. Descriptive statistics for clusters and local extrema showing greater activity during the anticipation of Angry/Fearful Faces relative to Houses (FDR $q < 0.05$, whole-brain corrected).

	mm^3	***t***	**x**	**y**	**z**
Cluster 1	648,072				
L Postcentral Gyrus		15.78	-34	-28	60
L Amygdala (cortical, amygdalohippocampal area)		14.14	-16	-4	-16
L Precentral Gyrus		13.73	-12	-32	68
L Superior Parietal Lobule		12.92	-36	-42	64
L Intracalcarine Cortex		12.78	-6	-72	12
L Superior Frontal Gyrus		12.55	-6	-8	74
L Supramarginal Gyrus, anterior division		11.40	-54	-30	52
L Temporal Occipital Fusiform Cortex		11.40	-44	-48	-20

	L Lateral Occipital Cortex, inferior division		11.18	-56	-70	10
	L Middle Frontal Gyrus		10.76	-44	0	58
	L Juxtapositional Lobule Cortex		10.56	-2	-8	66
	L Supracalcarine Cortex		10.37	-2	-84	10
	L Middle Temporal Gyrus, temporooccipital part		9.39	-58	-60	8
	L Angular Gyrus		9.33	-60	-52	12
	L Thalamus		9.29	-8	-2	10
	L Lingual Gyrus		9.10	-8	-78	-14
	L Cingulate Gyrus, posterior division		8.97	-6	-52	32
	L Lateral Occipital Cortex, superior division		8.69	-36	-58	58
	L Supramarginal Gyrus, posterior division		8.65	-52	-48	10
	L Paracingulate Gyrus		8.39	-4	16	50
	L Caudate		8.20	-12	-6	18
	L Cingulate Gyrus, anterior division		8.05	-8	16	36
	L Precuneus Cortex		7.83	-6	-56	56
	L Parietal Operculum Cortex		7.74	-58	-40	24
	L Cuneal Cortex		7.71	-10	-80	30
	L Insular Cortex		7.36	-40	0	-16
	L Occipital Pole		7.23	-6	-90	16
	L Pallidum		7.02	-16	2	0
	L Temporal Pole		6.97	-36	4	-20
	L Central Opercular Cortex		6.95	-56	-18	20
	L Frontal Orbital Cortex		6.72	-38	30	-16
	L Bed Nucleus of the Stria Terminalis		6.38	-4	4	-2
	L Planum Polare		6.28	-42	-2	-14
	L Inferior Frontal Gyrus, pars triangularis		6.21	-50	24	4
	L Inferior Frontal Gyrus, pars opercularis		6.16	-58	14	24
	L Putamen		5.96	-30	-22	2
	L Frontal Medial Cortex		5.94	-2	54	-12
	L Frontal Pole		5.87	-18	40	42
	L Middle Temporal Gyrus, posterior division		5.76	-66	-32	0
	L Temporal Fusiform Cortex, posterior division		5.60	-42	-30	-18
	L Planum Temporale		5.52	-42	-32	8
	L Frontal Operculum Cortex		5.30	-42	22	4
	L Heschls Gyrus (includes H1 and H2)		5.27	-52	-24	10

	L Temporal Fusiform Cortex, anterior division		5.17	-30	0	-36
	L Accumbens		5.05	-8	16	-6
	L Occipital Fusiform Gyrus		4.89	-40	-70	-16
	L Superior Temporal Gyrus, posterior division		4.89	-62	-30	0
	L Hippocampus		4.85	-26	-34	-6
	L Brainstem		4.35	-6	-18	-20
	L Inferior Temporal Gyrus, posterior division		4.24	-46	-24	-22
	L Subcallosal Cortex		4.10	-2	30	-10
	L Superior Temporal Gyrus, anterior division		3.30	-62	0	-8
	L Middle Temporal Gyrus, anterior division		3.00	-62	0	-22
	R Amygdala (cortical, amygdalohippocampal area)		16.14	16	-4	-18
	R Intracalcarine Cortex		14.97	10	-72	14
	R Precentral Gyrus		12.96	14	-32	64
	R Postcentral Gyrus		12.85	16	-30	68
	R Supracalcarine Cortex		12.40	2	-74	12
	R Middle Frontal Gyrus		12.18	44	0	58
	R Middle Temporal Gyrus, temporooccipital part		12.10	48	-58	6
	R Supramarginal Gyrus, posterior division		12.05	48	-40	10
	R Cingulate Gyrus, posterior division		11.79	6	-52	24
	R Superior Parietal Lobule		11.39	26	-42	66
	R Lateral Occipital Cortex, inferior division		11.31	56	-62	6
	R Central Opercular Cortex		10.80	40	-2	14
	R Superior Frontal Gyrus		10.79	18	-8	72
	R Inferior Temporal Gyrus, temporooccipital part		10.68	46	-42	-20
	R Juxtapositional Lobule Cortex		10.17	4	4	56
	R Precuneus Cortex		10.11	2	-62	34
	R Cuneal Cortex		10.08	6	-78	22
	R Lingual Gyrus		10.07	6	-66	2
	R Temporal Occipital Fusiform Cortex		9.69	48	-48	-24
	R Supramarginal Gyrus, anterior division		9.41	62	-28	24
	R Thalamus		9.38	10	-2	12
	R Paracingulate Gyrus		8.97	0	16	48
	R Caudate		8.69	14	-8	20
	R Angular Gyrus		8.58	52	-56	22

	R Thalamus		8.56	0	-8	10
	R Putamen		8.21	30	-18	0
	R Cingulate Gyrus, anterior division		8.04	6	-8	30
	R Inferior Frontal Gyrus, pars opercularis		7.88	52	16	32
	R Middle Temporal Gyrus, posterior division		7.66	66	-36	2
	R Insular Cortex		7.63	40	4	-16
	R Parietal Operculum Cortex		7.53	54	-32	28
	R Frontal Pole		7.46	2	56	-12
	R Superior Temporal Gyrus, posterior division		7.24	52	-16	-6
	R Frontal Medial Cortex		6.91	2	50	-16
	R Inferior Frontal Gyrus, pars triangularis		6.88	54	26	-6
	R Lateral Occipital Cortex, superior division		6.69	58	-60	38
	R Hippocampus		6.36	24	-36	-6
	R Temporal Fusiform Cortex, anterior division		6.15	38	-2	-38
	R Temporal Pole		6.11	32	8	-24
	R Pallidum		6.07	20	2	2
	R Frontal Orbital Cortex		5.91	48	22	-12
	R Planum Temporale		5.80	38	-32	14
	R Heschls Gyrus (includes H1 and H2)		5.57	54	-14	8
	R Frontal Operculum Cortex		5.48	42	26	0
	R Parahippocampal Gyrus, anterior division		5.19	30	-4	-34
	R Bed Nucleus of the Stria Terminalis		5.08	6	4	0
	R Inferior Temporal Gyrus, posterior division		5.06	44	-28	-18
	R Middle Temporal Gyrus, anterior division		4.40	60	2	-16
	R Accumbens		4.16	6	16	-2
	R Planum Polare		4.13	42	-8	-10
	R Brainstem		4.00	4	-42	-22
	R Superior Temporal Gyrus, anterior division		3.88	62	0	-12
	R Subcallosal Cortex		3.53	4	30	-10
	Cluster 2	552				
	L Brainstem		3.75	-10	-36	-44
	R Brainstem		3.86	2	-30	-48
	Cluster 3	296				
	L Brainstem		3.60	-16	-30	-30

	Cluster 4	248				
	L Middle Temporal Gyrus, anterior division		4.22	-50	-4	-28
	L Temporal Pole		3.00	-50	6	-26
	Cluster 5	240				
	R Brainstem		3.82	12	-26	-42
	Cluster 6	224				
	L Temporal Pole		3.85	-52	4	-16
	Cluster 7	160				
	R Brainstem		3.48	12	-22	-36
	Cluster 8	136				
	L Brainstem		3.31	-8	-28	-36
	R Brainstem		2.68	2	-32	-36
	Cluster 9	104				
	L Frontal Pole		4.09	-26	54	-14
	Cluster 10	96				
	L Temporal Pole		3.94	-44	12	-28
	Cluster 11	96				
	R Inferior Temporal Gyrus, posterior division		3.48	62	-30	-18
	R Middle Temporal Gyrus, posterior division		3.18	64	-32	-16
	Cluster 12	88				
	L Temporal Pole		3.13	-48	4	-22
	L Superior Temporal Gyrus, anterior division		2.44	-48	0	-18
	Cluster 13	80				
	R Precentral Gyrus		4.44	62	2	12
	Cluster 14	72				
	L Brainstem		3.27	-8	-38	-32
	Cluster 15	72				
	L Subcallosal Cortex		2.16	-2	24	-26
	R Subcallosal Cortex		3.54	4	24	-26
	Cluster 16	72				
	R Frontal Pole		4.48	22	42	-16
	Cluster 17	64				
	R Brainstem		3.45	6	-36	-48
	Cluster 18	64				
	R Inferior Temporal Gyrus, posterior division		2.86	46	-12	-32
	Cluster 19	64				

	L Frontal Pole		3.23	-14	68	-2
	Cluster 20	64				
	L Caudate		2.84	-18	20	10
	Cluster 21	56				
	L Frontal Pole		2.80	-42	52	0
	Cluster 22	48				
	R Brainstem		3.46	0	-18	-38
	Cluster 23	48				
	L Inferior Temporal Gyrus, posterior division		2.97	-60	-36	-20
	Cluster 24	48				
	L Middle Temporal Gyrus, posterior division		2.51	-64	-28	-18
	L Inferior Temporal Gyrus, posterior division		2.33	-62	-28	-22
	Cluster 25	48				
	L Frontal Pole		3.45	-18	52	-16
	Cluster 26	40				
	L Temporal Pole		3.43	-46	16	-38
	Cluster 27	40				
	R Brainstem		2.96	0	-18	-32
	Cluster 28	40				
	L Frontal Pole		2.11	-26	50	0
	Cluster 29	40				
	L Heschls Gyrus (includes H1 and H2)		2.68	-42	-20	4

Note: Suprathreshold activation was also evident bilaterally in the Dorsal Amygdala in the region of the Ce.

References

Abdellaoui, A., Chen, H. Y., Willemsen, G., Ehli, E. A., Davies, G. E., Verweij, K. J. H., . . . Cacioppo, J. T. (2019). Associations between loneliness and personality are mostly driven by a genetic association with neuroticism. *J Pers, 87*, 386-397. doi:10.1111/jopy.12397

Abdellaoui, A., Nivard, M. G., Hottenga, J. J., Fedko, I., Verweij, K. J. H., Baselmans, B. M. L., . . . Cacioppo, J. T. (2018). Predicting loneliness with polygenic scores of social, psychological and psychiatric traits. *Genes Brain Behav, 17*, e12472. doi:10.1111/gbb.12472

Abdellaoui, A., Sanchez-Roige, S., Sealock, J., Treur, J. L., Dennis, J., Fontanillas, P., . . . Boomsma, D. I. (2019). Phenome-wide investigation of health outcomes associated with genetic predisposition to loneliness. *Human Molecular Genetics, 28*, 3853-3865. doi:10.1093/hmg/ddz219

Abercrombie, H. C., Schaefer, S. M., Larson, C. L., Oakes, T. R., Lindgren, K. A., Holden, J. E., . . . Davidson, R. J. (1998). Metabolic rate in the right amygdala predicts negative affect in depressed patients. *Neuroreport, 9*, 3301-3307.

Acosta-Cabronero, J., Williams, G. B., Pereira, J. M., Pengas, G., & Nestor, P. J. (2008). The impact of skull-stripping and radio-frequency bias correction on grey-matter segmentation for voxel-based morphometry. *Neuroimage, 39*, 1654-1665. doi:10.1016/j.neuroimage.2007.10.051

Adams, M. J., Howard, D. M., Luciano, M., Clarke, T. K., Davies, G., Hill, W. D., . . . McIntosh, A. M. (*in press*). Genetic stratification of depression by neuroticism: revisiting a diagnostic tradition. *Psychol Med*. doi:10.1017/s0033291719002629

Ahrens, S., Wu, M. V., Furlan, A., Hwang, G. R., Paik, R., Li, H., . . . Li, B. (2018). A central extended amygdala circuit that modulates anxiety. *J Neurosci, 38*, 5567-5583. doi:10.1523/JNEUROSCI.0705-18.2018

Akingbuwa, W. A., Hammerschlag, A. R., Jami, E. S., Allegrini, A. G., Karhunen, V., Sallis, H., . . . Middeldorp, C. M. (2020). Genetic associations between childhood psychopathology and adult depression and associated traits in 42 998 Individuals: A meta-analysis. *JAMA Psychiatry, 77*, 1-15. doi:10.1001/jamapsychiatry.2020.0527

Albaugh, M. D., Hudziak, J. J., Orr, C., Spechler, P. A., Chaarani, B., Mackey, S., . . . Consortium, I. (2019). Amygdalar reactivity is associated with prefrontal cortical thickness in a large population-based sample of adolescents. *PLoS One, 14*, e0216152. doi:10.1371/journal.pone.0216152

Alheid, G. F., & Heimer, L. (1988). New perspectives in basal forebrain organization of special relevance for neuropsychiatric disorders: the striatopallidal, amygdaloid, and corticopetal components of substantia innominata. *Neuroscience, 27*, 1-39.

Allen, M. S., & Robson, D. A. (2018). A 10-year prospective study of personality and reproductive success: Testing the mediating role of healthy living. *Psychology & Health, 33*, 1379-1395. doi:10.1080/08870446.2018.1498499

Allen, M. S., & Walter, E. E. (2018). Linking Big Five personality traits to sexuality and sexual health: A meta-analytic review. *Psychological Bulletin, 144*, 1081-1110. doi:10.1037/bul0000157

Allen, M. S., & Walter, E. E. (2018). Linking big five personality traits to sexuality and sexual health: A meta-analytic review. *Psychol Bull, 144*, 1081-1110. doi:10.1037/bul0000157

Allen, T. D., Johnson, R. C., Saboe, K. N., Cho, E., Dumani, S., & Evans, S. (2012). Dispositional variables and work–family conflict: A meta-analysis. *Journal of Vocational Behavior, 80*, 17-26. doi:https://doi.org/10.1016/j.jvb.2011.04.004

Alloy, L. B., & Abramson, L. Y. (1999). The Temple-Wisconsin Cognitive Vulnerability to Depression Project: Conceptual background, design, and methods. *Journal of Cognitive Psychotherapy, 13*, 227-262.

Allport, G. W. (1966). Traits revisited. *American Psychologist, 21*, 1-10.

Altschul, D., Iveson, M., & Deary, I. J. (*in press*). Generational differences in loneliness and its psychological and sociodemographic predictors: an exploratory and confirmatory machine learning study. *Psychological Medicine*. doi:10.1017/S0033291719003933

American College Health Association. (2019). *American College Health Association-National College Health Assessment II: Undergraduate Student Reference Group Data Report Spring 2019*. Hanover, MD: American College Health Association.

Andersson, J. L. R., Skare, S., & Ashburner, J. (2003). How to correct susceptibility distortions in spin-echo echo-planar images: application to diffusion tensor imaging. *Neuroimage, 20*, 870-888.

Anglim, J., Horwood, S., Smillie, L. D., Marrero, R. J., & Wood, J. K. (2020). Predicting psychological and subjective well-being from personality: A meta-analysis. *Psychological Bulletin, 146*, 279-323. doi:10.1037/bul0000226

Arnett, J. J. (2000). Emerging adulthood. A theory of development from the late teens through the twenties. *Am Psychol, 55*, 469-480.

Asselmann, E., & Specht, J. (2020). Taking the ups and downs at the rollercoaster of love: Associations between major life events in the domain of romantic relationships and the Big Five personality traits. *Developmental Psychology, 56*, 1803-1816. doi:10.1037/dev0001047

Auerbach, R. P., Alonso, J., Axinn, W. G., Cuijpers, P., Ebert, D. D., Green, J. G., . . . Bruffaerts, R. (2016). Mental disorders among college students in the World Health Organization World Mental Health Surveys. *Psychol Med, 46*, 1-16. doi:10.1017/S0033291716001665

Auerbach, R. P., Mortier, P., Bruffaerts, R., Alonso, J., Benjet, C., Cuijpers, P., . . . Collaborators, W. W.-I. (2018). WHO world mental health surveys international college student project: Prevalence and distribution of mental disorders. *J Abnorm Psychol, 127*, 623-638. doi:10.1037/abn0000362

Avants, B. B., Tustison, N. J., Song, G., Cook, P. A., Klein, A., & Gee, J. C. (2011). A reproducible evaluation of ANTs similarity metric performance in brain image registration. *Neuroimage, 54*, 2033-2044. doi:10.1016/j.neuroimage.2010.09.025

Avery, S. N., Clauss, J. A., Winder, D. G., Woodward, N., Heckers, S., & Blackford, J. U. (2014). BNST neurocircuitry in humans. *Neuroimage, 91*, 311-323. doi:10.1016/j.neuroimage.2014.01.017

Bach, D. R., Castegnetti, G., Korn, C. W., Gerster, S., Melinscak, F., & Moser, T. (2018). Psychophysiological modeling: Current state and future directions. *Psychophysiology, 55*(11), e13214.

Bach, D. R., Flandin, G., Friston, K. J., & Dolan, R. J. (2010). Modelling event-related skin conductance responses. *Int J Psychophysiol, 75*(3), 349-356. doi:10.1016/j.ijpsycho.2010.01.005

Bach, D. R., Friston, K. J., & Dolan, R. J. (2013). An improved algorithm for model-based analysis of evoked skin conductance responses. *Biological psychology, 94*(3), 490-497.

Ball, T. M., Sullivan, S., Flagan, T., Hitchcock, C. A., Simmons, A., Paulus, M. P., & Stein, M. B. (2012). Selective effects of social anxiety, anxiety sensitivity, and negative affectivity on the neural bases of emotional face processing. *Neuroimage, 59*, 1879-1887. doi:https://doi.org/10.1016/j.neuroimage.2011.08.074

Barch, D. M., Burgess, G. C., Harms, M. P., Petersen, S. E., Schlaggar, B. L., Corbetta, M., . . . Consortium, W. U.-M. H. (2013). Function in the human connectome: task-fMRI and individual differences in behavior. *Neuroimage, 80*, 169-189. doi:10.1016/j.neuroimage.2013.05.033

Barelds, D. P. (2005). Self and Partner Personality in Intimate Relationships. *European Journal of Personality, 19*, 501-518.

Barlow, D. H., Farchione, T. J., Bullis, J. R., Gallagher, M. W., Murray-Latin, H., Sauer-Zavala, S., . . . Cassiello-Robbins, C. (2017). The unified protocol for transdiagnostic treatment of emotional disorders compared with diagnosis-specific protocols for anxiety disorders: A randomized clinical trial. *JAMA Psychiatry, 74*, 875-884. doi:10.1001/jamapsychiatry.2017.2164

Barlow, D. H., Sauer-Zavala, S., Carl, J. R., Bullis, J. R., & Ellard, K. K. (2013). The nature, diagnosis, and treatment of neuroticism: Back to the future. *Clinical Psychological Science, 2*, 344-365. doi:10.1177/2167702613505532

Baselmans, B. M. L., Jansen, R., Ip, H. F., van Dongen, J., Abdellaoui, A., van de Weijer, M. P., . . . Social Science Genetic Association, C. (2019). Multivariate genome-wide analyses of the well-being spectrum. *Nature Genetics, 51*, 445-451. doi:10.1038/s41588-018-0320-8

Bates, D., Mächler, M., Bolker, B., & Walker, S. (2015). Fitting Linear Mixed-Effects Models Using lme4. *2015, 67*(1), 48. doi:10.18637/jss.v067.i01

Bechara, A., Tranel, D., Damasio, H., Adolphs, R., Rockland, C., & Damasio, A. R. (1995). Double dissociation of conditioning and declarative knowledge relative to the amygdala and hippocampus in humans. *Science, 269*, 1115-1118.

Beck, E. D. (2020). *A mega-analysis of personality prediction: Robustness and boundary conditions.* (Doctor of Philosophy), Washington University, St. Louis,

Beesdo, K., Pine, D. S., Lieb, R., & Wittchen, H. U. (2010). Incidence and risk patterns of anxiety and depressive disorders and categorization of generalized anxiety disorder. *Arch Gen Psychiatry, 67*, 47-57. doi:10.1001/archgenpsychiatry.2009.177

Berry, S. C., Wise, R. G., Lawrence, A. D., & Lancaster, T. M. (2021). Extended-amygdala intrinsic functional connectivity networks: A population study. *Hum Brain Mapp, 42*(6), 1594-1616. doi:10.1002/hbm.25314

Binkley, C., & Fenn, L. (2019, Nov 19). Colleges struggle with soaring student demand for counseling. *Associated Press*. Retrieved from https://apnews.com/article/25905a5c3d28454ba0d84dcb958fe32c

Birn, R. M., Shackman, A. J., Oler, J. A., Williams, L. E., McFarlin, D. R., Rogers, G. M., . . . Kalin, N. H. (2014). Evolutionarily conserved dysfunction of prefrontal-amygdalar connectivity in early-life anxiety. *Molecular Psychiatry, 19*, 915-922.

Birn, R. M., Smith, M. A., Jones, T. B., & Bandettini, P. A. (2008). The respiration response function: the temporal dynamics of fMRI signal fluctuations related to changes in respiration. *Neuroimage, 40*(2), 644-654. doi:10.1016/j.neuroimage.2007.11.059

Blackford, J. U., Avery, S. N., Cowan, R. L., Shelton, R. C., & Zald, D. H. (2011). Sustained amygdala response to both novel and newly familiar faces characterizes inhibited temperament. *Soc Cogn Affect Neurosci, 6*, 621-629. doi:nsq073 [pii]
10.1093/scan/nsq073

Blackford, J. U., Avery, S. N., Shelton, R. C., & Zald, D. H. (2009). Amygdala temporal dynamics: temperamental differences in the timing of amygdala response to familiar and novel faces. *BMC Neurosci, 10*, 145. doi:1471-2202-10-145 [pii]
10.1186/1471-2202-10-145

Bleidorn, W., Hill, P. L., Back, M. D., Denissen, J. J. A., Hennecke, M., Hopwood, C. J., . . . Roberts, B. W. (2019). The policy relevance of personality traits. *American Psychologist, 74*, 1056-1067. doi:10.1037/amp0000503

Boe, H. J., Holgersen, K. H., & Holen, A. (2011). Mental health outcomes and predictors of chronic disorders after the North Sea oil rig disaster. *Journal of Nervous and Mental Disease, 199*, 49-54.

Boissy, A. (1995). Fear and fearfulness in animals. *Quarterly Review of Biology, 70*, 165-191.

Bolger, N., & Eckenrode, J. (1991). Social relationships, personality, and anxiety during a major stressful event. *J Pers Soc Psychol, 61*, 440-449.

Botvinik-Nezer, R., Holzmeister, F., Camerer, C. F., Dreber, A., Huber, J., Johannesson, M., . . . Schonberg, T. (2020). Variability in the analysis of a single neuroimaging dataset by many teams. *Nature, 582*, 84-88. doi:10.1038/s41586-020-2314-9

Brandes, C. M., Herzhoff, K., Smack, A. J., & Tackett, J. L. (2019). The p factor and the n factor: Associations between the general factors of psychopathology and neuroticism in children. *Clinical Psychological Science, 7*, 1266-1284.

Brinkmann, L., Buff, C., Feldker, K., Neumeister, P., Heitmann, C. Y., Hofmann, D., . . . Straube, T. (2018). Inter-individual differences in trait anxiety shape the functional connectivity between the bed nucleus of the stria terminalis and the amygdala during brief threat processing. *Neuroimage, 166*, 110-116.

Brislin, S., Martz, M. E., Joshi, S., Duval, E. R., Gard, A. M., Clark, D. A., . . . Sripada, C. (2020). Differentiated nomological networks of internalizing, externalizing, and the general factor of psychopathology ("P factor") in emerging adolescence in the ABCD study. *PsyArXiv*.

Brock, R. L., Dindo, L., Simms, L. J., & Clark, L. A. (2016). Personality and dyadic adjustment: Who you think your partner is really matters. *J Fam Psychol, 30*, 602-613. doi:10.1037/fam0000210

Brouwer, M. E., Williams, A. D., Kennis, M., Fu, Z., Klein, N. S., Cuijpers, P., & Bockting, C. L. H. (2019). Psychological theories of depressive relapse and recurrence: A systematic review and meta-analysis of prospective studies. *Clinical Psychology Review, 74*, 101773. doi:https://doi.org/10.1016/j.cpr.2019.101773

Bucher, M. A., Suzuki, T., & Samuel, D. B. (2019). A meta-analytic review of personality traits and their associations with mental health treatment outcomes. *Clinical Psychology Review, 70*, 51-63.

Buecker, S., Maes, M., Denissen, J. J. A., & Luhmann, M. (2020). Loneliness and the Big Five personality traits: A meta-analysis. *European Journal of Personality, 34*, 8-28. doi:10.1002/per.2229

Calder, A. J., Ewbank, M. P., & Passamonti, L. (2011). Personality influences the neural responses to viewing facial expressions of emotion. *Philosophical Transactions of the Royal Society B: Biological Sciences, 366*, 1684-1701. doi:10.1098/rstb.2010.0362

Calhoon, G. G., & Tye, K. M. (2015). Resolving the neural circuits of anxiety. *Nature Neuroscience, 18*, 1394-1404.

Canli, T., Qiu, M., Omura, K., Congdon, E., Haas, B. W., Amin, Z., . . . Lesch, K. P. (2006). Neural correlates of epigenesis. *Proc Natl Acad Sci U S A, 103*(43), 16033-16038. doi:0601674103 [pii]
10.1073/pnas.0601674103

Cano, M., Alonso, P., Martinez-Zalacain, I., Subira, M., Real, E., Segalas, C., . . . Soriano-Mas, C. (2018). Altered functional connectivity of the subthalamus and the bed nucleus of the stria terminalis in obsessive-compulsive disorder. *Psychol Med, 48*, 919-928. doi:10.1017/S0033291717002288

Casey, B. J., Cannonier, T., Conley, M. I., Cohen, A. O., Barch, D. M., Heitzeg, M. M., . . . Workgroup, A. I. A. (2018). The Adolescent Brain Cognitive Development (ABCD) study: Imaging acquisition across 21 sites. *Dev Cogn Neurosci, 32*, 43-54. doi:10.1016/j.dcn.2018.03.001

Caspi, A., & Moffitt, T. E. (2018). All for one and one for all: Mental disorders in one dimension. *Am J Psychiatry, 175*, 831-844. doi:10.1176/appi.ajp.2018.17121383

Caspi, A., Roberts, B. W., & Shiner, R. L. (2005). Personality development: stability and change. *Annual review of psychology, 56*, 453-484. doi:10.1146/annurev.psych.55.090902.141913

Caughlin, J. P., Huston, T. L., & Houts, R. M. (2000). How does personality matter in marriage? An examination of trait anxiety, interpersonal negativity, and marital satisfaction. *J Pers Soc Psychol, 78*, 326-336.

Cavanagh, J. F., & Shackman, A. J. (2015). Frontal midline theta reflects anxiety and cognitive control: Meta-analytic evidence. *Journal of Physiology, Paris, 109*, 3-15.

Chang, C., Cunningham, J. P., & Glover, G. H. (2009). Influence of heart rate on the BOLD signal: the cardiac response function. *Neuroimage, 44*(3), 857-869. doi:10.1016/j.neuroimage.2008.09.029

Chapman, B. P., & Goldberg, L. R. (2017). Act-frequency signatures of the Big Five. *Personality and Individual Differences, 116*, 201-205.

Chapman, B. P., Huang, A., Horner, E., Peters, K., Sempeles, E., Roberts, B. W., & Lapham, S. (2019). High school personality traits and 48-year all-cause mortality risk: results from a national sample of 26 845 baby boomers. *Journal of Epidemiology and Community Health, 73*, 106-110. doi:10.1136/jech-2018-211076

Chapman, B. P., Huang, A., Peters, K., Horner, E., Manly, J., Bennett, D. A., & Lapham, S. (2020). Association between high school personality phenotype and dementia 54 years later in results from a national US sample. *JAMA Psychiatry, 77*, 148-154. doi:10.1001/jamapsychiatry.2019.3120

Charles, S. T., Gatz, M., Kato, K., & Pedersen, N. L. (2008). Physical health 25 years later: the predictive ability of neuroticism. *Health Psychol, 27*, 369-378. doi:10.1037/0278-6133.27.3.369

Chase, H. W., Eickhoff, S. B., Laird, A. R., & Hogarth, L. (2011). The neural basis of drug stimulus processing and craving: an activation likelihood estimation meta-analysis. *Biol Psychiatry, 70*, 785-793. doi:10.1016/j.biopsych.2011.05.025

Chavanne, A. V., & Robinson, O. J. (2021). The Overlapping Neurobiology of Induced and Pathological Anxiety: A Meta-Analysis of Functional Neural Activation. *Am J Psychiatry, 178*(2), 156-164. doi:10.1176/appi.ajp.2020.19111153

Cheesman, R., Coleman, J., Rayner, C., Purves, K. L., Morneau-Vaillancourt, G., Glanville, K., . . . Eley, T. C. (2020). Familial influences on neuroticism and education in the UK Biobank. *Behavior Genetics, 50*, 84-93. doi:10.1007/s10519-019-09984-5

Choi, J. M., Padmala, S., & Pessoa, L. (2012). Impact of state anxiety on the interaction between threat monitoring and cognition. *NeuroImage, 59*(2), 1912-1923.

Choi, J. M., Padmala, S., & Pessoa, L. (2015). Counteracting effect of threat on reward enhancements during working memory. *Cognition and Emotion, 29*(8), 1517-1526.

Class, Q. A., Van Hulle, C. A., Rathouz, P. J., Applegate, B., Zald, D. H., & Lahey, B. B. (2019a). Socioemotional dispositions of children and adolescents predict general and specific second-order factors of psychopathology in early adulthood: A 12-year prospective study. *J Abnorm Psychol, 128*, 574-584. doi:10.1037/abn0000433

Class, Q. A., Van Hulle, C. A., Rathouz, P. J., Applegate, B., Zald, D. H., & Lahey, B. B. (2019b). Socioemotional dispositions of children and adolescents predict general and specific second-order factors of psychopathology in early adulthood: A 12-year prospective study. *Journal of Abnormal Psychology, 128*, 574-584. doi:10.1037/abn0000433

Cohen, J. R., Thakur, H., Young, J. F., & Hankin, B. L. (*in press*). The development and validation of an algorithm to predict future depression onset in unselected youth. *Psychological Medicine*. doi:10.1017/S0033291719002691

Coryell, W., Mills, J., Dindo, L., & Calarge, C. A. (*in press*). Predictors of depressive symptom trajectories in a prospective follow-up of late adolescents. *Psychological Medicine*. doi:10.1017/S0033291719002551

Costafreda, S. G., Brammer, M. J., David, A. S., & Fu, C. H. (2008). Predictors of amygdala activation during the processing of emotional stimuli: a meta-analysis of 385 PET and fMRI studies. *Brain Research Reviews, 58*, 57-70.

Cox, R. W. (1996). AFNI: Software for analysis and visualization of functional magnetic resonance neuroimages. *Computers and Biomedical Research, 29*, 162-173.

Credé, M., & Niehorster, S. (2012). Adjustment to College as Measured by the Student Adaptation to College Questionnaire: A Quantitative Review of its Structure and Relationships with Correlates and Consequences. *Educational Psychology Review, 24*(1), 133-165. doi:10.1007/s10648-011-9184-5

Cuijpers, P., Smit, F., Penninx, B. W., de Graaf, R., ten Have, M., & Beekman, A. T. (2010). Economic costs of neuroticism: a population-based study. *Arch Gen Psychiatry, 67*, 1086-1093. doi:10.1001/archgenpsychiatry.2010.130

Daldrup, T., Remmes, J., Lesting, J., Gaburro, S., Fendt, M., Meuth, P., . . . Seidenbecher, T. (2015). Expression of freezing and fear-potentiated startle during sustained fear in mice. *Genes Brain Behav, 14*, 281-291. doi:10.1111/gbb.12211

Davis, M., Antoniadis, E. A., Amaral, D. G., & Winslow, J. T. (2008). Acoustic startle reflex in rhesus monkeys: a review. *Rev Neurosci, 19*, 171-185.

Davis, M., Walker, D. L., Miles, L., & Grillon, C. (2010). Phasic vs sustained fear in rats and humans: Role of the extended amygdala in fear vs anxiety. *Neuropsychopharmacology, 35*, 105-135. doi:npp2009109 [pii]
10.1038/npp.2009.109

Day, F. R., Ong, K. K., & Perry, J. R. B. (2018). Elucidating the genetic basis of social interaction and isolation. *Nature Communications, 9*, 2457. doi:10.1038/s41467-018-04930-1

deCampo, D. M., & Fudge, J. L. (2013). Amygdala projections to the lateral bed nucleus of the stria terminalis in the macaque: comparison with ventral striatal afferents. *J Comp Neurol, 521*, 3191-3216. doi:10.1002/cne.23340

Desikan, R. S., Ségonne, F., Fischl, B., Quinn, B. T., Dickerson, B. C., Blacker, D., . . . Killiany, R. J. (2006). An automated labeling system for subdividing the human cerebral cortex on MRI scans into gyral based regions of interest. *Neuroimage, 31*, 968-980.

du Pont, A., Rhee, S. H., Corley, R. P., Hewitt, J. K., & Friedman, N. P. (2019). Are rumination and neuroticism genetically or environmentally distinct risk factors for psychopathology? *Journal of Abnormal Psychology, 128*, 385-396. doi:10.1037/abn0000430

Duvarci, S., Bauer, E. P., & Paré, D. (2009). The bed nucleus of the stria terminalis mediates inter-individual variations in anxiety and fear. *Journal of Neuroscience, 29*(33), 10357-10361.

Ebner, N. C., Riediger, M., & Lindenberger, U. (2010). FACES—A database of facial expressions in young, middle-aged, and older women and men: Development and validation. *Behavior research methods, 42*(1), 351-362.

Ejova, A., Milojev, P., Worthington, E. L., Bulbulia, J., & Sibley, C. G. (2020). The Big Six personality traits and mental distress: Dynamic modeling in a population panel study reveals bidirectional relationships involving neuroticism, extraversion, and conscientiousness. *Personality and Social Psychology Bulletin, 46*, 1287-1302. doi:10.1177/0146167219895349

Ekman, P., & Friesen, W. (1976). Pictures of Facial Affect (Palo Alto, CA: Consulting Psychologists).

Elliott, M. L., Knodt, A. R., Ireland, D., Morris, M. L., Poulton, R., Ramrakha, S., . . . Hariri, A. R. (2019). Poor test-retest reliability of task-fMRI: New empirical evidence and a meta-analysis. *bioRxiv*, 681700. doi:10.1101/681700

Eskildsen, S. F., Coupé, P., Fonov, V., Manjón, J. V., Leung, K. K., Guizard, N., . . . Alzheimer's Disease Neuroimaging Initiative. (2012). BEaST: brain extraction based on nonlocal segmentation technique. *Neuroimage, 59*, 2362-2373.

Everaerd, D., Klumpers, F., van Wingen, G., Tendolkar, I., & Fernández, G. (2015). Association between neuroticism and amygdala responsivity emerges under stressful conditions. *Neuroimage, 112*, 218-224. doi:10.1016/j.neuroimage.2015.03.014

Eysenck, H. J. (1967). *The biological basis of personality*. Springfield, IL: Charles C. Thomas.

Fadok, J. P., Markovic, M., Tovote, P., & Lüthi, A. (2018). New perspectives on central amygdala function. *Current Opinion in Neurobiology, 49*, 141-147.

Fava, M., Hwang, I., Rush, A. J., Sampson, N., Walters, E. E., & Kessler, R. C. (2010). The importance of irritability as a symptom of major depressive disorder: results from the National Comorbidity Survey Replication. *Mol Psychiatry, 15*, 856-867. doi:10.1038/mp.2009.20

Fein, G., Landman, B., Tran, H., Barakos, J., Moon, K., Di Sclafani, V., & Shumway, R. (2006). Statistical parametric mapping of brain morphology: sensitivity is dramatically increased by using brain-extracted images as inputs. *Neuroimage, 30*, 1187-1195. doi:10.1016/j.neuroimage.2005.10.054

Feinstein, J. S., Adolphs, R., Damasio, A., & Tranel, D. (2011). The human amygdala and the induction and experience of fear. *Current Biology, 21*, 1-5.

Feinstein, J. S., Adolphs, R., & Tranel, D. (2016). A tale of survival from the world of Patient S.M. In D. G. Amaral & R. Adolphs (Eds.), *Living without an amygdala*. New York: Guilford.

Finn, C., Mitte, K., & Neyer, F. J. (2013). The relationship-specific interpretation bias mediates the link between neuroticism and satisfaction in couples. *Journal of Personality, 27*, 200-212.

First, M. B., Williams, J. B. W., Karg, R. S., & Spitzer, R. L. (2015). Structured clinical interview for DSM-5—Research version (SCID-5 for DSM-5, research version; SCID-5-RV). *Arlington, VA: American Psychiatric Association*.

Fischmeister, F. P., Hollinger, I., Klinger, N., Geissler, A., Wurnig, M. C., Matt, E., . . . Beisteiner, R. (2013). The benefits of skull stripping in the normalization of clinical fMRI data. *Neuroimage Clin, 3*, 369-380. doi:10.1016/j.nicl.2013.09.007

Fonzo, G. A., Ramsawh, H. J., Flagan, T. M., Sullivan, S. G., Letamendi, A., Simmons, A. N., . . . Stein, M. B. (2015). Common and disorder-specific neural responses to emotional faces in generalised anxiety, social anxiety and panic disorders. *Br J Psychiatry, 206*, 206-215. doi:10.1192/bjp.bp.114.149880

Fox, A. S., & Kalin, N. H. (2014). A translational neuroscience approach to understanding the development of social anxiety disorder and its pathophysiology. *American Journal of Psychiatry, 171*, 1162-1173.

Fox, A. S., Lapate, R. C., Davidson, R. J., & Shackman, A. J. (2018). The nature of emotion: A research agenda for the 21st century. In A. S. Fox, R. C. Lapate, A. J. Shackman, & R. J. Davidson (Eds.), *The nature of emotion. Fundamental questions* (2nd ed., pp. 403-417). New York, NY: Oxford University Press.

Fox, A. S., Oler, J. A., Shackman, A. J., Shelton, S. E., Raveendran, M., McKay, D. R., . . . Kalin, N. H. (2015). Intergenerational neural mediators of early-life anxious temperament. *Proceedings of the National Academy of Sciences USA, 112*, 9118-9122.

Fox, A. S., Oler, J. A., Tromp, D. P., Fudge, J. L., & Kalin, N. H. (2015). Extending the amygdala in theories of threat processing. *Trends Neurosci, 38*, 319-329. doi:10.1016/j.tins.2015.03.002

Fox, A. S., & Shackman, A. J. (2019). The central extended amygdala in fear and anxiety: Closing the gap between mechanistic and neuroimaging research. *Neuroscience letters, 693*, 58-67. doi:https://doi.org/10.1016/j.neulet.2017.11.056

Fox, A. S., Shelton, S. E., Oakes, T. R., Davidson, R. J., & Kalin, N. H. (2008). Trait-like brain activity during adolescence predicts anxious temperament in primates. *PLoS One, 3*, e2570. doi:10.1371/journal.pone.0002570

Fox, A. S., Souaiaia, T., Oler, J. A., Kovner, R., Kim, J. M. H., Nguyen, J., . . . Kalin, N. H. (in press). Dorsal amygdala neurotrophin-3 decreases anxious temperament in primates. *Biol Psychiatry*. doi:10.1016/j.biopsych.2019.06.022

Frazier, J. A., Chiu, S., Breeze, J. L., Makris, N., Lange, N., Kennedy, D. N., . . . Biederman, J. (2005). Structural brain magnetic resonance imaging of limbic and thalamic volumes in pediatric bipolar disorder. *American Journal of Psychiatry, 162*, 1256-1265.

Freese, J. L., & Amaral, D. G. (2009). Neuroanatomy of the primate amygdala. In P. J. Whalen & E. A. Phelps (Eds.), *The human amygdala* (pp. 3-42). NY: Guilford.

Fried, I., MacDonald, K. A., & Wilson, C. L. (1997). Single neuron activity in human hippocampus and amygdala during recognition of faces and objects. *Neuron, 18*, 753-765.

Fudge, J. L., Kelly, E. A., Pal, R., Bedont, J. L., Park, L., & Ho, B. (2017). Beyond the classic VTA: Extended amygdala projections to DA-striatal paths in the primate. *Neuropsychopharmacology, 42*, 1563-1576. doi:10.1038/npp.2017.38

Fullana, M. A., Tortella-Feliu, M., Fernández de la Cruz, L., Chamorro, J., Pérez-Vigil, A., Ioannidis, J. P. A., . . . Radua, J. (2020). Risk and protective factors for anxiety and obsessive-compulsive disorders: an umbrella review of systematic reviews and meta-analyses. *Psychological Medicine, 50*, 1300-1315. doi:10.1017/S0033291719001247

Fusar-Poli, P., Placentino, A., Carletti, F., Landi, P., Allen, P., Surguladze, S., . . . Politi, P. (2009). Functional atlas of emotional faces processing: a voxel-based meta-analysis of 105 functional magnetic resonance imaging studies. *J Psychiatry Neurosci, 34*, 418-432.

Gale, C. R., Cukic, I., Batty, G. D., McIntosh, A. M., Weiss, A., & Deary, I. J. (2017). When is higher neuroticism protective against death? Findings from UK Biobank. *Psychol Sci, 28*, 1345-1357. doi:10.1177/0956797617709813

Gamer, M., Schmitz, A. K., Tittgemeyer, M., & Schilbach, L. (2013). The human amygdala drives reflexive orienting towards facial features. *Current Biology, 23*(20), R917-R918.

Geukes, K., Breil, S. M., Hutteman, R., Nestler, S., Küfner, A. C. P., & Back, M. D. (2019). Explaining the longitudinal interplay of personality and social

relationships in the laboratory and in the field: The PILS and the CONNECT study. *PLoS One, 14*, e0210424.

Global Burden of Disease Collaborators. (2016). Global, regional, and national incidence, prevalence, and years lived with disability for 310 diseases and injuries, 1990-2015: a systematic analysis for the Global Burden of Disease Study 2015. *Lancet, 388*, 1545-1602. doi:10.1016/S0140-6736(16)31678-6

Glover, L. R., McFadden, K. M., Bjorni, M., Smith, S. R., Rovero, N. G., Oreizi-Esfahani, S., . . . Holmes, A. (2020). A prefrontal-bed nucleus of the stria terminalis circuit limits fear to uncertain threat. *Elife, 9*. doi:10.7554/eLife.60812

Goldberg, L. R. (1999). A broad-bandwidth, public domain, personality inventory measuring the lower-level facets of several five-factor models. In I. Mervielde, I. Deary, F. De Fruyt, & F. Ostendorf (Eds.), *Personality Psychology in Europe* (Vol. 7, pp. 7-28). Tilburg, The Netherlands: Tilburg University Press.

Goldberg, L. R., Johnson, J. A., Eber, H. W., Hogan, R., Ashton, M. C., Cloninger, C. R., & Gough, H. C. (2006). The International Personality Item Pool and the future of public-domain personality measures. *Journal of Research in Personality, 40*, 84-96.

Goldsmith, H. H., Buss, A. H., Plomin, R., Rothbart, M. K., Thomas, A., Chess, S., . . . McCall, R. B. (1987). Roundtable: what is temperament? Four approaches. *Child Dev, 58*, 505-529.

Goldstein, B. L., Perlman, G., Eaton, N. R., Kotov, R., & Klein, D. N. (*in press*). Testing explanatory models of the interplay between depression, neuroticism, and stressful life events: a dynamic trait-stress generation approach. *Psychological Medicine*. doi:10.1017/S0033291719002927

Goldstein, B. L., Perlman, G., Eaton, N. R., Kotov, R., & Klein, D. N. (*in press*). Testing explanatory models of the interplay between depression, neuroticism, and stressful life events: a dynamic trait-stress generation approach. *Psychol Med*. doi:10.1017/s0033291719002927

Goodwin, R. D., Hoven, C. W., Lyons, J. S., & Stein, M. B. (2002). Mental health service utilization in the United States. The role of personality factors. *Soc Psychiatry Psychiatr Epidemiol, 37*, 561-566. doi:10.1007/s00127-002-0563-6

Gorka, A. X., Torrisi, S., Shackman, A. J., Grillon, C., & Ernst, M. (2018). Intrinsic functional connectivity of the central nucleus of the amygdala and bed nucleus of the stria terminalis. *Neuroimage, 168*, 392-402.

Gothard, K. M., Battaglia, F. P., Erickson, C. A., Spitler, K. M., & Amaral, D. G. (2007). Neural responses to facial expression and face identity in the monkey amygdala. *J Neurophysiol, 97*, 1671-1683. doi:00714.2006 [pii]
10.1152/jn.00714.2006

Grabner, G., Janke, A. L., Budge, M. M., Smith, D., Pruessner, J., & Collins, D. L. (2006). Symmetric atlasing and model based segmentation: an application to the hippocampus in older adults. *Med Image Comput Comput Assist Interv Int Conf Med Image Comput Comput Assist Interv, 9*, 58–66.

Graham, E. K., Rutsohn, J. P., Turiano, N. A., Bendayan, R., Batterham, P. J., Gerstorf, D., . . . Mroczek, D. K. (2017). Personality predicts mortality risk: An integrative data analysis of 15 international longitudinal studies. *Journal of Research in Personality, 70*, 174-186.

Graham, M. S., Drobnjak, I., & Zhang, H. (2017). Quantitative assessment of the susceptibility artefact and its interaction with motion in diffusion MRI. *PLoS One, 12*, e0185647.

Greenberg, T., Bertocci, M. A., Chase, H. W., Stiffler, R., Aslam, H. A., Graur, S., . . . Phillips, M. L. (2017). Mediation by anxiety of the relationship between amygdala activity during emotion processing and poor quality of life in young adults. *Transl Psychiatry, 7*, e1178. doi:10.1038/tp.2017.127

Greve, D. N., & Fischl, B. (2009). Accurate and robust brain image alignment using boundary-based registration. *Neuroimage, 48*, 63-72.

Griessner, J., Pasieka, M., Bohm, V., Grossl, F., Kaczanowska, J., Pliota, P., . . . Haubensak, W. (*in press*). Central amygdala circuit dynamics underlying the benzodiazepine anxiolytic effect. *Mol Psychiatry*. doi:10.1038/s41380-018-0310-3

Gross, J. J., Sutton, S. K., & Ketelaar, T. (1998). Relations between affect and personality: Support for the affect-level and affective reactivity views. *Personality and Social Psychology Bulletin, 24*, 279-288.

Grupe, D. W., & Nitschke, J. B. (2013). Uncertainty and anticipation in anxiety: an integrated neurobiological and psychological perspective. *Nat Rev Neurosci, 14*, 488-501. doi:nrn3524 [pii]
10.1038/nrn3524

Gungor, N. Z., & Paré, D. (2016). Functional heterogeneity in the bed nucleus of the stria terminalis. *Journal of Neuroscience, 36*, 8038-8049.

Günther, V., Hußlack, A., Weil, A. S., Bujanow, A., Henkelmann, J., Kersting, A., . . . Suslow, T. (2020). Individual differences in anxiety and automatic amygdala

response to fearful faces: A replication and extension of Etkin et al. (2004). *Neuroimage Clin, 28,* 102441. doi:10.1016/j.nicl.2020.102441

Hansson, I., Henning, G., Buratti, S., Lindwall, M., Kivi, M., Johansson, B., & Berg, A. I. (2020). The role of personality in retirement adjustment: Longitudinal evidence for the effects on life satisfaction. *Journal of Personality, 88,* 642-658. doi:10.1111/jopy.12516

Hanzal, A., & Segrin, C. (2009). The role of conflict resolution styles in mediating the relationship between enduring vulnerabilities and marital quality. *Journal of Family Communication, 9,* 150-169.

Harari, M. B., Reaves, A. C., Beane, D. A., Laginess, A. J., & Viswesvaran, C. (2018). Personality and expatriate adjustment: A meta-analysis. *Journal of Occupational and Organizational Psychology, 91,* 486-517. doi:10.1111/joop.12215

Hauner, K. K., Zinbarg, R. E., & Revelle, W. (2014). A latent variable model approach to estimating systematic bias in the oversampling method. *Behav Res, 46,* 786-797.

Hawrylycz, M. J., Lein, E. S., Guillozet-Bongaarts, A. L., Shen, E. H., Ng, L., Miller, J. A., . . . Jones, A. R. (2012). An anatomically comprehensive atlas of the adult human brain transcriptome. *Nature, 489,* 391-399. doi:10.1038/nature11405

Hays, R. B., & Oxley, D. (1986). Social network development and functioning during a life transition. *J Pers Soc Psychol, 50,* 305-313.

Hefner, K. R., Moberg, C. A., Hachiya, L. Y., & Curtin, J. J. (2013). Alcohol stress response dampening during imminent versus distal, uncertain threat. *J Abnorm Psychol, 122*(3), 756-769. doi:10.1037/a0033407

Heller, D., Watson, D., & Ilies, R. (2004). The role of person versus situation in life satisfaction: A critical examination. *Psychological Bulletin, 130,* 574-600.

Henson, R. (2007a). Efficient experimental design for fMRI. *Statistical parametric mapping: The analysis of functional brain images*, 193-210.

Henson, R. (2007b). Efficient experimental design for fMRI. In K. Friston, J. Ashburner, S. Kiebel, T. Nichols, & W. Penny (Eds.), *Statistical parametric mapping: The analysis of functional brain images* (pp. 193-210). New York, NY: Academic Press.

Hoff, K. A., Einarsdóttir, S., Chu, C., Briley, D. A., & Rounds, J. (*in press*). Personality changes predict early career outcomes: Discovery and replication in 12-Year longitudinal studies. *Psychological Science*.

Hoffman, K. L., Gothard, K. M., Schmid, M. C., & Logothetis, N. K. (2007). Facial-expression and gaze-selective responses in the monkey amygdala. *Curr Biol, 17*, 766-772. doi:10.1016/j.cub.2007.03.040

Holmes, A. J., & Patrick, L. M. (2018). The Myth of Optimality in Clinical Neuroscience. *Trends Cogn Sci, 22*(3), 241-257. doi:10.1016/j.tics.2017.12.006

Huang, I. C., Lee, J. L., Ketheeswaran, P., Jones, C. M., Revicki, D. A., & Wu, A. W. (2017). Does personality affect health-related quality of life? A systematic review. *PLoS One, 12*, e0173806. doi:10.1371/journal.pone.0173806

Hudson, M., Seppälä, K., Putkinen, V., Sun, L., Glerean, E., Karjalainen, T., . . . Nummenmaa, L. (*in press*). Dissociable neural systems for unconditioned acute and sustained fear. *Neuroimage*, 116522. doi:https://doi.org/10.1016/j.neuroimage.2020.116522

Hur, J., DeYoung, K. A., Islam, S., Anderson, A. S., Barstead, M. G., & Shackman, A. J. (*2020*). Social context and the real-world consequences of social anxiety. *Psychol Med, 50*(12), 1989-2000. doi:10.1017/S0033291719002022

Hur, J., Kaplan, C. M., Smith, J. F., Bradford, D. E., Fox, A. S., Curtin, J. J., & Shackman, A. J. (2018). Acute alcohol administration dampens central extended amygdala reactivity. *Scientific Reports, 8*, 16702.

Hur, J., Smith, J. F., DeYoung, K. A., Anderson, A. S., Kuang, J., Kim, H. C., . . . Shackman, A. J. (2020). Anxiety and the neurobiology of uncertain threat anticipation. *bioRxiv*, 2020.2002.2025.964734. doi:10.1101/2020.02.25.964734

Hur, J., Stockbridge, M. D., Fox, A. S., & Shackman, A. J. (2019). Dispositional negativity, cognition, and anxiety disorders: An integrative translational neuroscience framework. *Progress in Brain Research, 247*, 375-436.

Indovina, I., Robbins, T. W., Núñez-Elizalde, A. O., Dunn, B. D., & Bishop, S. J. (2011). Fear-conditioning mechanisms associated with trait vulnerability to anxiety in humans. *Neuron, 69*, 563-571. doi:10.1016/j.neuron.2010.12.034

Inman, C. S., Bijanki, K. R., Bass, D. I., Gross, R. E., Hamann, S., & Willie, J. T. (2020). Human amygdala stimulation effects on emotion physiology and emotional experience. *Neuropsychologia, 145*, 106722. doi:10.1016/j.neuropsychologia.2018.03.019

Jeronimus, B. F., Kotov, R., Riese, H., & Ormel, J. (2016). Neuroticism's prospective association with mental disorders halves after adjustment for baseline symptoms and psychiatric history, but the adjusted association hardly decays

with time: a meta-analysis on 59 longitudinal/prospective studies with 443 313 participants. *Psychol Med, 46*, 2883-2906. doi:10.1017/S0033291716001653

Jo, H. J., Gotts, S. J., Reynolds, R. C., Bandettini, P. A., Martin, A., Cox, R. W., & Saad, Z. S. (2013). Effective preprocessing procedures virtually eliminate distance-dependent motion artifacts in resting state FMRI. *Journal of Applied Mathematics, 2013*, 1-9.

Joel, S., Eastwick, P. W., Allison, C. J., Arriaga, X. B., Baker, Z. G., Bar-Kalifa, E., . . . Wolf, S. (*in press*). Machine learning uncovers the most robust self-report predictors of relationship quality across 43 longitudinal couples studies. *Proceedings of the National Academy of Sciences USA*, 201917036. doi:10.1073/pnas.1917036117

John, O. P., Naumann, L. P., & Soto, C. J. (2008). Paradigm shift to the integrative big-five trait taxonomy: History, measurement, and conceptual issues. In O. P. John, R. W. Robins, & L. A. Pervin (Eds.), *Handbook of personality: Theory and research* (pp. 114-158). NY: Guilford.

Jokela, M., Airaksinen, J., Kivimaki, M., & Hakulinen, C. (2018). Is within-individual variation in personality traits associated with changes in health behaviours? Analysis of seven longitudinal cohort studies. *European Journal of Personality, 32*, 642-652.

Jokela, M., Airaksinen, J., Virtanen, M., Batty, G. D., Kivimäki, M., & Hakulinen, C. (*in press*). Personality, disability-free life years, and life expectancy: Individual participant meta-analysis of 131,195 individuals from 10 cohort studies. *Journal of Personality*. doi:10.1111/jopy.12513

Jones, H. J., Heron, J., Hammerton, G., Stochl, J., Jones, P. B., Cannon, M., . . . Me Research, T. (2018). Investigating the genetic architecture of general and specific psychopathology in adolescence. *Translational Psychiatry, 8*, 145. doi:10.1038/s41398-018-0204-9

Judge, T. A., Heller, D., & Mount, M. K. (2002). Five-factor model of personality and job satisfaction: A meta-analysis. *Journal of Applied Psychology, 87*, 530-541.

Kaczkurkin, A. N., Moore, T. M., Ruparel, K., Ciric, R., Calkins, M. E., Shinohara, R. T., . . . Sattherthwaite, T. D. (2016). Elevated amygdala perfusion mediates developmental sex differences in trait anxiety. *Biological Psychiatry, 80*, 775-785.

Kagan, J., Reznick, J. S., & Snidman, N. (1988). Biological bases of childhood shyness. *Science, 240*, 167-171.

Kajonius, P. J., & Carlander, A. (2017). Who gets ahead in life? Personality traits and childhood background in economic success. *Journal of Economic Psychology, 59*, 164-170.

Kalin, N. H. (2017). Mechanisms underlying the early risk to develop anxiety and depression: A translational approach. *Eur Neuropsychopharmacol, 27*, 543-553. doi:10.1016/j.euroneuro.2017.03.004

Kalin, N. H., Fox, A. S., Kovner, R., Riedel, M. K., Fekete, E. M., Roseboom, P. H., . . . Oler, J. A. (2016). Overexpressing corticotropin-releasing hormone in the primate amygdala increases anxious temperament and alters its neural circuit. *Biol Psychiatry, 80*, 345-355. doi:10.1016/j.biopsych.2016.01.010

Kamali, A., Sair, H. I., Blitz, A. M., Riascos, R. F., Mirbagheri, S., Keser, Z., & Hasan, K. M. (2016). Revealing the ventral amygdalofugal pathway of the human limbic system using high spatial resolution diffusion tensor tractography. *Brain Struct Funct, 221*, 3561-3569. doi:10.1007/s00429-015-1119-3

Kamali, A., Yousem, D. M., Lin, D. D., Sair, H. I., Jasti, S. P., Keser, Z., . . . Hasan, K. M. (2015). Mapping the trajectory of the stria terminalis of the human limbic system using high spatial resolution diffusion tensor tractography. *Neurosci Lett, 608*, 45-50. doi:10.1016/j.neulet.2015.09.035

Katz, B. A., Matanky, K., Aviram, G., & Yovel, I. (2020). Reinforcement sensitivity, depression and anxiety: A meta-analysis and meta-analytic structural equation model. *Clinical Psychology Review, 77*, 101842. doi:https://doi.org/10.1016/j.cpr.2020.101842

Kelter, R. (2020). Bayesian alternatives to null hypothesis significance testing in biomedical research: a non-technical introduction to Bayesian inference with JASP. *BMC medical research methodology, 20*, 142-142. doi:10.1186/s12874-020-00980-6

Kendler, K. S., Gardner, C. O., Neale, M. C., Aggen, S., Heath, A., Colodro-Conde, L., . . . Gillespie, N. A. (2019). Shared and specific genetic risk factors for lifetime major depression, depressive symptoms and neuroticism in three population-based twin samples. *Psychological Medicine, 49*, 2745-2753. doi:10.1017/S003329171800377X

Kenwood, M. M., & Kalin, N. H. (2020). Nonhuman primate models to explore mechanisms underlying early-life temperamental anxiety. *Biological Psychiatry*. doi:https://doi.org/10.1016/j.biopsych.2020.08.028

Kessler, R. C., Amminger, G. P., Aguilar-Gaxiola, S., Alonso, J., Lee, S., & Ustun, T. B. (2007). Age of onset of mental disorders: A review of recent literature. *Current Opinion in Psychiatry, 20*, 359-364.

Kessler, R. C., Petukhova, M., Sampson, N. A., Zaslavsky, A. M., & Wittchen, H. U. (2012). Twelve-month and lifetime prevalence and lifetime morbid risk of anxiety and mood disorders in the United States. *Int J Methods Psychiatr Res, 21*, 169-184. doi:10.1002/mpr.1359

Khoo, S., Stanton, K., Clark, L. A., & Watson, D. (2020). Facet-level personality relations of the symptom dimensions of the tripartite model. *Journal of Psychopathology and Behavioral Assessment, 42*, 160-177. doi:10.1007/s10862-019-09763-w

Kirlic, N., Aupperle, R. L., Rhudy, J. L., Misaki, M., Kuplicki, R., Sutton, A., & Alvarez, R. P. (2019). Latent variable analysis of negative affect and its contributions to neural responses during shock anticipation. *Neuropsychopharmacology, 44*, 695-702. doi:10.1038/s41386-018-0187-5

Klein, A., Andersson, J., Ardekani, B. A., Ashburner, J., Avants, B., Chiang, M. C., . . . Parsey, R. V. (2009). Evaluation of 14 nonlinear deformation algorithms applied to human brain MRI registration. *Neuroimage, 46*, 786-802. doi:10.1016/j.neuroimage.2008.12.037

Klimstra, T. A., Noftle, E. E., Luyckx, K., Goossens, L., & Robins, R. W. (2018). Personality development and adjustment in college: A multifaceted, cross-national view. *J Pers Soc Psychol, 115*, 338-361. doi:10.1037/pspp0000205

Klumpers, F., Kroes, M. C. W., Baas, J., & Fernandez, G. (2017). How human amygdala and bed nucleus of the stria terminalis may drive distinct defensive responses. *J Neurosci, 37*, 9645-9656. doi:10.1523/JNEUROSCI.3830-16.2017

Klumpers, F., Morgan, B., Terburg, D., Stein, D. J., & van Honk, J. (2015). Impaired acquisition of classically conditioned fear-potentiated startle reflexes in humans with focal bilateral basolateral amygdala damage. *Social cognitive and affective neuroscience, 10*, 1161-1168.

Knowles, K. A., & Olatunji, B. O. (*in press*). Specificity of trait anxiety in anxiety and depression: Meta-analysis of the State-Trait Anxiety Inventory. *Clinical Psychology Review*, 101928. doi:https://doi.org/10.1016/j.cpr.2020.101928

Kööts-Ausmees, L., Schmidt, M., Esko, T., Metspalu, A., Alliki, J., & Realo, A. (2016). The role of the five-factor personality traits in general self-rated health. *European Journal of Personality, 30*, 492-504.

Korn, C. W., Vunder, J., Miró, J., Fuentemilla, L., Hurlemann, R., & Bach, D. R. (2017). Amygdala lesions reduce anxiety-like behavior in a human

benzodiazepine-sensitive approach-avoidance conflict test. *Biological Psychiatry, 82*, 522-531.

Kornadt, A. E., Hagemeyer, B., Neyer, F. J., & Kandler, C. (2018). Sound body, sound mind? The interrelation between health change and personality change in old age. *European Journal of Personality, 32,* 30-45.

Kostyrka-Allchorne, K., Wass, S. V., & Sonuga-Barke, E. J. S. (2020). Research Review: Do parent ratings of infant negative emotionality and self-regulation predict psychopathology in childhood and adolescence? A systematic review and meta-analysis of prospective longitudinal studies. *Journal of Child Psychology and Psychiatry, 61*, 401-416. doi:10.1111/jcpp.13144

Kroencke, L., Kuper, N., Bleidorn, W., & Denissen, J. J. A. (*in press*). How does substance use affect personality development? Disentangling between- and within-person effects. *Social Psychological and Personality Science*, 1948550620921702. doi:10.1177/1948550620921702

Kuhn, S., & Gallinat, J. (2011). Common biology of craving across legal and illegal drugs - a quantitative meta-analysis of cue-reactivity brain response. *Eur J Neurosci, 33*, 1318-1326. doi:10.1111/j.1460-9568.2010.07590.x

Lahey, B. B. (2009). Public health significance of neuroticism. *American Psychologist, 64*, 241-256. doi:10.1037/a0015309

Lang, P. J., Bradley, M. M., & Cuthbert, B. N. (2008). *International affective picture system (IAPS): Affective ratings of pictures and instruction manual. Technical Report A-8*. Retrieved from Gainesville, FL:

Lange, M. D., Daldrup, T., Remmers, F., Szkudlarek, H. J., Lesting, J., Guggenhuber, S., . . . Pape, H. C. (2017). Cannabinoid CB1 receptors in distinct circuits of the extended amygdala determine fear responsiveness to unpredictable threat. *Mol Psychiatry, 22*, 1422-1430. doi:10.1038/mp.2016.156

Lavner, J. A., Weiss, B., Miller, J. D., & Karney, B. R. (2018). Personality change among newlyweds: Patterns, predictors, and associations with marital satisfaction over time. *Dev Psychol, 54*, 1172-1185. doi:10.1037/dev0000491

Leckelt, M., Richter, D., Schröder, C., Küfner, A. C. P., Grabka, M. M., & Back, M. D. (2019). The rich are different: Unravelling the perceived and self-reported personality profiles of high-net-worth individuals. *British Journal of Psychology, 110*, 769-789. doi:10.1111/bjop.12360

LeDoux, J. E. (2015). *Anxious. Using the brain to understand and treat fear and anxiety*. New York, NY: Viking.

LeDoux, J. E., & Pine, D. S. (2016). Using Neuroscience to Help Understand Fear and Anxiety: A Two-System Framework. *Am J Psychiatry, 173*(11), 1083-1093. doi:10.1176/appi.ajp.2016.16030353

Lenhausen, M. R., van Scheppingen, M. A., & Bleidorn, W. (2020). Self-other agreement in personality development in romantic couples. *PsyArXiv*.

Leskela, U., Melartin, T., Rytsala, H., Jylha, P., Sokero, P., Lestela-Mielonen, P., & Isometsa, E. (2009). Influence of personality on objective and subjective social support among patients with major depressive disorder: a prospective study. *J Nerv Ment Dis, 197*, 728-735. doi:10.1097/NMD.0b013e3181b97960

Levin-Aspenson, H., Khoo, S., & Kotelnikova, Y. (2019). Hierarchical taxonomy of psychopathology across development: Associations with personality. *Journal of Research in Personality, 81*, 72-78.

Li, J. J., Hilton, E. C., Lu, Q., Hong, J., Greenberg, J. S., & Mailick, M. R. (2019). Validating psychosocial pathways of risk between neuroticism and late life depression using a polygenic score approach. *Journal of Abnormal Psychology, 128*, 200-211.

Lindquist, K. A., Wager, T. D., Kober, H., Bliss-Moreau, E., & Barrett, L. F. (2012). The brain basis of emotion: A meta-analytic review. *Behavioral and Brain Sciences, 35*, 121-143.

Lipson, S. K., Lattie, E. G., & Eisenberg, D. (2019). Increased rates of mental health service utilization by U.S. college students: 10-Year population-level trends (2007-2017). *Psychiatr Serv, 70*, **60-63**. doi:10.1176/appi.ps.201800332

Liu, C. H., Stevens, C., Wong, S. H. M., Yasui, M., & Chen, J. A. (2019). The prevalence and predictors of mental health diagnoses and suicide among U.S. college students: Implications for addressing disparities in service use. *Depress Anxiety, 36*, 8-17. doi:10.1002/da.22830

Liu, M., Jiang, Y., Wedow, R., Li, Y., Brazel, D. M., Chen, F., . . . Hunt All-In Psychiatry. (2019). Association studies of up to 1.2 million individuals yield new insights into the genetic etiology of tobacco and alcohol use. *Nature Genetics, 51*, 237-244. doi:10.1038/s41588-018-0307-5

Long, J. A. (2019). interactions: Comprehensive, User-Friendly Toolkit for Probing Interactions. In.

Lorio, S., Fresard, S., Adaszewski, S., Kherif, F., Chowdhury, R., Frackowiak, R. S., . . . Draganski, B. (2016). New tissue priors for improved automated classification of subcortical brain structures on MRI. *Neuroimage, 130*, 157-166. doi:10.1016/j.neuroimage.2016.01.062

Lowery-Gionta, E. G., DiBerto, J., Mazzone, C. M., & Kash, T. L. (2018). GABA neurons of the ventral periaqueductal gray area modulate behaviors associated with anxiety and conditioned fear. *Brain Struct Funct, 223*, 3787-3799. doi:10.1007/s00429-018-1724-z

MacDuffie, K. E., Knodt, A. R., Radtke, S. R., Strauman, T. J., & Hariri, A. R. (2019). Self-rated amygdala activity: an auto-biological index of affective distress. *Personal Neurosci, 2*, e1. doi:10.1017/pen.2019.1

Mai, J. K., Majtanik, M., & Paxinos, G. (2015). *Atlas of the human brain* (4th ed.). San Diego, CA: Academic Press.

Makowski, D., Ben Shachar, M., & Lüdecke, D. (2019). bayestestR: Describing Effects and their Uncertainty, Existence and Significance within the Bayesian Framework. *The Journal of Open Source Software, 4*, 1541. doi:10.21105/joss.01541

Makris, N., Goldstein, J. M., Kennedy, D., Hodge, S. M., Caviness, V. S., Faraone, S. V., . . . Seidman, L. J. (2006). Decreased volume of left and total anterior insular lobule in schizophrenia. *Schizophrenia Research, 83*, 155-171.

Mann, F. D., Atherton, O. E., DeYoung, C. G., Krueger, R. F., & Robins, R. W. (*in press*). Big five personality traits and common mental disorders within a hierarchical taxonomy of psychopathology: A longitudinal study of Mexican-origin youth. *Journal of Abnormal Psychology*. doi:10.1037/abn0000633

Maus, B., van Breukelen, G. J., Goebel, R., & Berger, M. P. (2010). Optimization of blocked designs in fMRI studies. *Psychometrika, 75*(2), 373-390.

McHugh, J. E., & Lawlor, B. A. (2012). Social support differentially moderates the impact of neuroticism and extraversion on mental wellbeing among community-dwelling older adults. *J Ment Health, 21*, 448-458. doi:10.3109/09638237.2012.689436

Meng, W., Adams, M. J., Reel, P., Rajendrakumar, A., Huang, Y., Deary, I. J., . . . Smith, B. H. (2020). Genetic correlations between pain phenotypes and depression and neuroticism. *European Journal of Human Genetics, 28*, 358-366. doi:10.1038/s41431-019-0530-2

Michelini, G., Perlman, G., Tian, Y., Mackin, D., Nelson, B., Klein, D., & Kotov, R. (2020). Multiple domains of risk factors for first onset of depression in adolescent girls. *PsyArXiv*. doi:doi:10.31234/osf.io/8m9ga

Miles, L., Davis, M., & Walker, D. (2011). Phasic and sustained fear are pharmacologically dissociable in rats. *Neuropsychopharmacology, 36*, 1563-1574. doi:10.1038/npp.2011.29

Miller, K. L., Alfaro-Almagro, F., Bangerter, N. K., Thomas, D. L., Yacoub, E., Xu, J., . . . Smith, S. M. (2016). Multimodal population brain imaging in the UK Biobank prospective epidemiological study. *Nat Neurosci, 19*, 1523-1536. doi:10.1038/nn.4393

Mineka, S., Williams, A. L., Wolitzky-Taylor, K., Vrshek-Schallhorn, S., Craske, M. G., Hammen, C., & Zinbarg, R. E. (*in press*). Five-year prospective neuroticism-stress effects on major depressive episodes: Primarily additive effects of the general neuroticism factor and stress. *J Abnorm Psychol*. doi:10.1037/abn0000530

Mobbs, D., Adolphs, R., Fanselow, M. S., Barrett, L. F., LeDoux, J. E., Ressler, K., & Tye, K. M. (2019). Viewpoints: Approaches to defining and investigating fear. *Nat Neurosci, 22*(8), 1205-1216. doi:10.1038/s41593-019-0456-6

Mobbs, D., Yu, R., Rowe, J. B., Eich, H., FeldmanHall, O., & Dalgleish, T. (2010). Neural activity associated with monitoring the oscillating threat value of a tarantula. *Proceedings of the National Acadademy of Sciences USA, 107*, 20582-20586.

Mueller, S., Wagner, J., Smith, J., Voelkle, M. C., & Gerstorf, D. (2018). The interplay of personality and functional health in old and very old age: Dynamic within-person interrelations across up to 13 years. *J Pers Soc Psychol, 115*, 1127-1147. doi:10.1037/pspp0000173

Mumper, E. E., Dyson, M. W., Finsaas, M. C., Olino, T. M., & Klein, D. N. (2020). Life stress moderates the effects of preschool behavioral inhibition on anxiety in early adolescence. *Journal of Child Psychology and Psychiatry, 61*, 167-174. doi:10.1111/jcpp.13121

Munafò, M. R., Nosek, B. A., Bishop, D. V. M., Button, K. S., Chambers, C. D., du Sert, N. P., . . . Ioannidis, J. P. A. (2017). A manifesto for reproducible science. *Nature Human Behaviour, 1*, 21.

Newton-Howes, G., Horwood, J., & Mulder, R. (2015). Personality characteristics in childhood and outcomes in adulthood: findings from a 30 year longitudinal study. *Aust N Z J Psychiatry, 49*, 377-386. doi:10.1177/0004867415569796

O'Meara, M. S., & South, S. C. (2019). Big Five personality domains and relationship satisfaction: Direct effects and correlated change over time. *J Pers, 87*, 1206-1220. doi:10.1111/jopy.12468

Oler, J. A., Birn, R. M., Patriat, R., Fox, A. S., Shelton, S. E., Burghy, C. A., . . . Kalin, N. H. (2012). Evidence for coordinated functional activity within the extended amygdala of non-human and human primates. *Neuroimage, 61*, 1059-1066. doi:S1053-8119(12)00326-6 [pii]
10.1016/j.neuroimage.2012.03.045

Oler, J. A., Fox, A. S., Shackman, A. J., & Kalin, N. H. (2016). The central nucleus of the amygdala is a critical substrate for individual differences in anxiety. In D. G. Amaral & R. Adolphs (Eds.), *Living without an amygdala* (pp. 218-251). NY: Guilford.

Oler, J. A., Tromp, D. P., Fox, A. S., Kovner, R., Davidson, R. J., Alexander, A. L., . . . Fudge, J. L. (2017). Connectivity between the central nucleus of the amygdala and the bed nucleus of the stria terminalis in the non-human primate: neuronal tract tracing and developmental neuroimaging studies. *Brain Struct Funct, 222*, 21-39. doi:10.1007/s00429-016-1198-9

Oltmanns, J. R., Jackson, J. J., & Oltmanns, T. F. (2020). Personality change: Longitudinal self-other agreement and convergence with retrospective-reports. *J Pers Soc Psychol, 118*, 1065-1079. doi:10.1037/pspp0000238

Orem, T. R., Wheelock, M. D., Goodman, A. M., Harnett, N. G., Wood, K. H., Gossett, E. W., . . . Knight, D. C. (2019). Amygdala and prefrontal cortex activity varies with individual differences in the emotional response to psychosocial stress. *Behavioral neuroscience, 133*, 203-211. doi:10.1037/bne0000305

Pancer, S. M., Hunsberger, B., Pratt, M. W., & Alisat, S. (2000). Cognitive complexity of expectations and adjustment to university in the first year. *Journal of Adolescent Research, 15*, 38-57.

Pedersen, W. S., Schaefer, S. M., Gresham, L. K., Lee, S. D., Kelly, M. P., Mumford, J. A., . . . Davidson, R. J. (2020). Higher resting-state BNST-CeA connectivity is associated with greater corrugator supercilii reactivity to negatively valenced images. *Neuroimage, 207*, 116428. doi:10.1016/j.neuroimage.2019.116428

Plichta, M. M., Grimm, O., Morgen, K., Mier, D., Sauer, C., Haddad, L., . . . Schwarz, A. J. (2014). Amygdala habituation: a reliable fMRI phenotype. *Neuroimage, 103*, 383-390.

Pomrenze, M. B., Giovanetti, S. M., Maiya, R., Gordon, A. G., Kreeger, L. J., & Messing, R. O. (2019). Dissecting the roles of GABA and neuropeptides from rat central amygdala CRF neurons in anxiety and fear learning. *Cell Rep, 29*, 13-21 e14. doi:10.1016/j.celrep.2019.08.083

Pomrenze, M. B., Tovar-Diaz, J., Blasio, A., Maiya, R., Giovanetti, S. M., Lei, K., . . . Messing, R. O. (2019). A corticotropin releasing factor network in the extended

amygdala for anxiety. *J Neurosci, 39*, 1030-1043. doi:10.1523/JNEUROSCI.2143-18.2018

Power, J. D., Schlaggar, B. L., & Petersen, S. E. (2015). Recent progress and outstanding issues in motion correction in resting state fMRI. *Neuroimage, 105*, 536-551.

Pruim, R. H. R., Mennes, M., van Rooij, D., Llera, A., Buitelaar, J. K., & Beckmann, C. F. (2015). ICA-AROMA: a robust ICA-based strategy for removing motion artifacts from fMRI data. *Neuroimage, 112*, 267-277.

Puterman, E., Weiss, J., Hives, B. A., Gemmill, A., Karasek, D., Mendes, W. B., & Rehkopf, D. H. (2020). Predicting mortality from 57 economic, behavioral, social, and psychological factors. *Proceedings of the National Academy of Sciences USA, 117*, 16273-16282. doi:10.1073/pnas.1918455117

Quach, B. C., Bray, M. J., Gaddis, N. C., Liu, M., Palviainen, T., Minica, C. C., . . . Hancock, D. B. (2020). Expanding the genetic architecture of nicotine dependence and its shared genetics with multiple traits: Findings from the Nicotine Dependence GenOmics (iNDiGO) consortium. *bioRxiv*, 2020.2001.2015.898858. doi:10.1101/2020.01.15.898858

Quintana, D. S., & Williams, D. R. (2018). Bayesian alternatives for common null-hypothesis significance tests in psychiatry: a non-technical guide using JASP. *BMC Psychiatry, 18*, 178. doi:10.1186/s12888-018-1761-4

Rapee, R. M., & Bayer, J. K. (2018). Behavioural inhibition and the prevention of internalising distress in early childhood. In K. Pérez-Edgar & N. A. Fox (Eds.), *Behavioral inhibition: Integrating theory, research, and clinical perspectives* (pp. 337-355). Cham, Switzerland: Springer.

Reddan, M. C., Wager, T. D., & Schiller, D. (2018). Attenuating neural threat expression with imagination. *Neuron, 100*, 994-1005.e1004. doi:10.1016/j.neuron.2018.10.047

Reiss, S. (1997). Trait anxiety: it's not what you think it is. *J Anxiety Disord, 11*, 201-214.

Ressler, R. L., Goode, T. D., Evemy, C., & Maren, S. (2020). NMDA receptors in the CeA and BNST differentially regulate fear conditioning to predictable and unpredictable threats. *Neurobiology of Learning and Memory, 174*, 107281. doi:https://doi.org/10.1016/j.nlm.2020.107281

Roberts, B. W., Luo, J., Briley, D. A., Chow, P. I., Su, R., & Hill, P. L. (2017). A systematic review of personality trait change through intervention. *Psychol Bull, 143*(2), 117-141. doi:10.1037/bul0000088

Roohafza, H., Feizi, A., Afshar, H., Mazaheri, M., Behnamfar, O., Hassanzadeh-Keshteli, A., & Adibi, P. (2016). Path analysis of relationship among personality, perceived stress, coping, social support, and psychological outcomes. *World J Psychiatry, 6*, 248-256. doi:10.5498/wjp.v6.i2.248

Røysamb, E., Nes, R. B., Czajkowski, N. O., & Vassend, O. (2018). Genetics, personality and wellbeing. A twin study of traits, facets and life satisfaction. *Sci Rep, 8*, 12298. doi:10.1038/s41598-018-29881-x

Sabatinelli, D., Fortune, E. E., Li, Q., Siddiqui, A., Krafft, C., Oliver, W. T., . . . Jeffries, J. (2011). Emotional perception: Meta-analyses of face and natural scene processing. *Neuroimage, 54*, 2524-2533. doi:S1053-8119(10)01303-0 [pii]
10.1016/j.neuroimage.2010.10.011

Sadeh, N., Miller, M. W., Wolf, E. J., & Harkness, K. L. (2015). Negative emotionality and disconstraint influence PTSD symptom course via exposure to new major adverse life events. *Journal of Anxiety Disorders, 31*, 20-27. doi:https://doi.org/10.1016/j.janxdis.2015.01.003

Sallis, H. M., Davey Smith, G., & Munafo, M. R. (2019). Cigarette smoking and personality: interrogating causality using Mendelian randomisation. *Psychol Med, 49*, 2197-2205. doi:10.1017/S0033291718003069

Satterthwaite, T. D., Connolly, J. J., Ruparel, K., Calkins, M. E., Jackson, C., Elliott, M. A., . . . Gur, R. E. (2016). The Philadelphia Neurodevelopmental Cohort: A publicly available resource for the study of normal and abnormal brain development in youth. *Neuroimage, 124*, 1115-1119. doi:10.1016/j.neuroimage.2015.03.056

Sauer-Zavala, S., Fournier, J. C., Jarvi Steele, S., Woods, B. K., Wang, M., Farchione, T. J., & Barlow, D. H. (2020). Does the unified protocol really change neuroticism? Results from a randomized trial. *Psychol Med*, 1-10. doi:10.1017/s0033291720000975

Sauer-Zavala, S. E., Fournier, J. C., Jarvi Steele, S., Woods, B. K., Wang, M., Farchione, T. J., & Barlow, D. H. (*in press*). Does the unified protocol really change neuroticism? Results from a randomized trial. *Psychological Medicine*. doi:10.1017/S0033291720000975

Scheller, E., Büchel, C., & Gamer, M. (2012). Diagnostic features of emotional expressions are processed preferentially. *PLoS One, 7*(7), e41792.

Schuyler, B. S., Kral, T. R., Jacquart, J., Burghy, C. A., Weng, H. Y., Perlman, D. M., . . . Davidson, R. J. (2012). Temporal dynamics of emotional responding:

amygdala recovery predicts emotional traits. *Soc Cogn Affect Neurosci, 9*, 176-181. doi:nss131 [pii]
10.1093/scan/nss131

Sen, S., Kranzler, H. R., Krystal, J. H., Speller, H., Chan, G., Gelernter, J., & Guille, C. (2010). A prospective cohort study investigating factors associated with depression during medical internship. *Archives of General Psychiatry, 67*, 557-565. doi:10.1001/archgenpsychiatry.2010.41

Sergerie, K., Chochol, C., & Armony, J. L. (2008). The role of the amygdala in emotional processing: a quantitative meta-analysis of functional neuroimaging studies. *Neurosci Biobehav Rev, 32*, 811-830. doi:S0149-7634(08)00007-9 [pii]
10.1016/j.neubiorev.2007.12.002

Sescousse, G., Caldu, X., Segura, B., & Dreher, J. C. (2013). Processing of primary and secondary rewards: a quantitative meta-analysis and review of human functional neuroimaging studies. *Neurosci Biobehav Rev, 37*, 681-696. doi:10.1016/j.neubiorev.2013.02.002

Shackman, A. J., & Fox, A. S. (2016). Contributions of the central extended amygdala to fear and anxiety. *Journal of Neuroscience, 36*, 8050-8063. doi:10.1523/JNEUROSCI.0982-16.2016

Shackman, A. J., & Fox, A. S. (2018). Getting serious about variation: Lessons for clinical neuroscience. *Trends in cognitive sciences, 22*, 368-369.

Shackman, A. J., & Fox, A. S. (2021). Two Decades of Anxiety Neuroimaging Research: New Insights and a Look to the Future. *Am J Psychiatry, 178*(2), 106-109. doi:10.1176/appi.ajp.2020.20121733

Shackman, A. J., Fox, A. S., Oler, J. A., Shelton, S. E., Oakes, T. R., Davidson, R. J., & Kalin, N. H. (2017). Heightened extended amygdala metabolism following threat characterizes the early phenotypic risk to develop anxiety-related psychopathology. *Mol Psychiatry, 22*(5), 724-732. doi:10.1038/mp.2016.132

Shackman, A. J., Salomons, T. V., Slagter, H. A., Fox, A. S., Winter, J. J., & Davidson, R. J. (2011). The integration of negative affect, pain and cognitive control in the cingulate cortex. *Nat Rev Neurosci, 12*, 154-167. doi:nrn2994 [pii]
10.1038/nrn2994

Shackman, A. J., Stockbridge, M. D., LeMay, E. P., & Fox, A. S. (2018). The psychological and neurobiological bases of dispositional negativity. In A. S. Fox, R. C. Lapate, A. J. Shackman, & R. J. Davidson (Eds.), *The nature of emotion. Fundamental questions* (2nd ed., pp. 67-71). New York, NY: Oxford University Press.

Shackman, A. J., Tromp, D. P. M., Stockbridge, M. D., Kaplan, C. M., Tillman, R. M., & Fox, A. S. (2016). Dispositional negativity: An integrative psychological and neurobiological perspective. *Psychological Bulletin, 142,* 1275-1314.

Shackman, A. J., Weinstein, J. S., Hudja, S. N., Bloomer, C. D., Barstead, M. G., Fox, A. S., & Lemay, E. P., Jr. (2018). Dispositional negativity in the wild: Social environment governs momentary emotional experience. *Emotion, 18*, 707-724. doi:10.1037/emo0000339
10.1037/emo0000339.supp (Supplemental)

Shaver, P. R., & Brennan, K. A. (1992). Attachment styles and the "Big Five" personality traits: Their connections with each other and with romantic relationship outcomes. *Personality and Social Psychology Bulletin, 18*, 536-545.

Siegel, J. S., Power, J. D., Dubis, J. W., Vogel, A. C., Church, J. A., Schlaggar, B. L., & Petersen, S. E. (2014). Statistical improvements in functional magnetic resonance imaging analyses produced by censoring high-motion data points. *Human Brain Mapping, 35*, 1981-1996.

Siless, V., Hubbard, N. A., Jones, R., Wang, J., Lo, N., Bauer, C. C. C., . . . Yendiki, A. (2020). Image acquisition and quality assurance in the Boston Adolescent Neuroimaging of Depression and Anxiety study. *Neuroimage Clin, 26*, 102242. doi:10.1016/j.nicl.2020.102242

Silverman, M. H., Wilson, S., Ramsay, I. S., Hunt, R. H., Thomas, K. M., Krueger, R. F., & Iacono, W. G. (2019). Trait neuroticism and emotion neurocircuitry: Functional magnetic resonance imaging evidence for a failure in emotion regulation. *Development and Psychopathology, 31*, 1085-1099. doi:10.1017/S0954579419000610

Singmann, H., Bolker, B., Westfall, J., & Aust, F. (2021). afex: analysis of factorial experiments. In.

Sjouwerman, R., Scharfenort, R., & Lonsdorf, T. B. (2020). Individual differences in fear acquisition: multivariate analyses of different emotional negativity scales, physiological responding, subjective measures, and neural activation. *Sci Rep, 10*(1), 15283. doi:10.1038/s41598-020-72007-5

Slatcher, R. B., & Vazire, S. (2009). Effects of global and contextualized personality on relationship satisfaction. *Journal of Research in Personality, 43*, 624-633.

Slee, A., Nazareth, I., Freemantle, N., & Horsfall, L. (*in press*). Trends in generalised anxiety disorders and symptoms in primary care: UK population-based cohort study. *Br J Psychiatry*. doi:10.1192/bjp.2020.159

Smith, J. F., Hur, J., Kaplan, C. M., & Shackman, A. J. (2018). The Impact of Spatial Normalization for Functional Magnetic Resonance Imaging Data Analyses Revisited. *bioRxiv*, 272302. doi:10.1101/272302

Smith, S. M., Jenkinson, M., Woolrich, M. W., Beckmann, C. F., Behrens, T. E. J., Johansen-Berg, H., . . . Matthews, P. M. (2004). Advances in functional and structural MR image analysis and implementation as FSL. *Neuroimage, 23(S1)*, 208-219.

Somerville, L. H., Bookheimer, S. Y., Buckner, R. L., Burgess, G. C., Curtiss, S. W., Dapretto, M., . . . Barch, D. M. (2018). The Lifespan Human Connectome Project in Development: A large-scale study of brain connectivity development in 5–21 year olds. *Neuroimage, 183*, 456-468. doi:https://doi.org/10.1016/j.neuroimage.2018.08.050

Somerville, L. H., Whalen, P. J., & Kelley, W. M. (2010). Human bed nucleus of the stria terminalis indexes hypervigilant threat monitoring. *Biol Psychiatry, 68*, 416-424. doi:10.1016/j.biopsych.2010.04.002

Soto, C. J. (2019). How replicable are links between personality traits and consequential life outcomes? The life outcomes of personality replication project. *Psychological Science, 30*, 711-727.

Soto, C. J. (*in press*). Do links between personality and life outcomes generalize? Testing the robustness of trait–outcome associations across gender, age, ethnicity, and analytic approaches. *Social Psychological and Personality Science*. doi:10.1177/1948550619900572

Soto, C. J., & John, O. P. (2017). The next Big Five Inventory (BFI-2): Developing and assessing a hierarchical model with 15 facets to enhance bandwidth, fidelity, and predictive power. *Journal of Personality and Social Psychology, 113*(1), 117.

Spengler, M., Roberts, B. W., Ludtke, O., Martin, R., & Brunner, M. (2016). The kind of student you were in elementary school predicts mortality. *J Pers, 84*, 547-553. doi:10.1111/jopy.12180

Spielberger, C. D. (1966). Theory and research on anxiety. In C. D. Spielberger (Ed.), *Anxiety and behavior* (pp. 3-22). NY: Academic Press.

Stein, M. B., Simmons, A. N., Feinstein, J. S., & Paulus, M. P. (2007). Increased amygdala and insula activation during emotion processing in anxiety-prone subjects. *Am J Psychiatry, 164*, 318-327. doi:164/2/318 [pii]
10.1176/appi.ajp.164.2.318

Stelzer, J., Lohmann, G., Mueller, K., Buschmann, T., & Turner, R. (2014). Deficient approaches to human neuroimaging. *Front Hum Neurosci, 8*, 462. doi:10.3389/fnhum.2014.00462

Stieger, M., Flückiger, C., Rüegger, D., Kowatsch, T., Roberts, B. W., & Allemand, M. (2021). Changing personality traits with the help of a digital personality change intervention. *Proc Natl Acad Sci U S A, 118*(8). doi:10.1073/pnas.2017548118

Stout, D. M., Shackman, A. J., Pedersen, W. S., Miskovich, T. A., & Larson, C. L. (2017). Neural circuitry governing anxious individuals' mis-allocation of working memory to threat. *Scientific reports, 7*(1), 8742.

Stout, D. M., Shackman, A. J., Pedersen, W. S., Miskovich, T. A., & Larson, C. L. (2017). Neural circuitry governing anxious individuals' mis-allocation of working memory to threat. *Scientific Reports, 7*, 8742.

Substance Abuse and Mental Health Services Administration. (2019). *Key substance use and mental health indicators in the United States: Results from the 2018 National Survey on Drug Use and Health*. Rockville, MD: Center for Behavioral Health Statistics and Quality.

Sutin, A. R., Stephan, Y., Luchetti, M., Artese, A., Oshio, A., & Terracciano, A. (2016). The Five Factor model of personality and physical inactivity: A meta-analysis of 16 samples. *Journal of Research in Personality, 63*, 22-28.

Swickert, R. J., Hittner, J. B., & Foster, A. (2010). Big Five traits interact to predict perceived social support. *Personality and Individual Differences, 48*, 736-741.

Swider, B. W., & Zimmerman, R. D. (2010). Born to burnout: A meta-analytic path model of personality, job burnout, and work outcomes. *Journal of Vocational Behavior, 76*, 487-506. doi:https://doi.org/10.1016/j.jvb.2010.01.003

Tackett, J. L., & Lahey, B. (2017). Neuroticism. In T. A. Widiger (Ed.), *The Oxford handbook of the five factor model* (pp. 39-56). New York, NY: Oxford University Press.

Tackman, A. M., Baranski, E. N., Danvers, A. F., Sbarra, D. A., Raison, C. L., Moseley, S. A., . . . Mehl, M. R. (*in press*). 'Personality in its natural habitat' Revisited: A pooled, multi-sample examination of the relationships between the Big Five personality traits and daily behaviour and language use. *European Journal of Personality*. doi:10.1002/per.2283

Tang, A., Crawford, H., Morales, S., Degnan, K. A., Pine, D. S., & Fox, N. A. (2020). Infant behavioral inhibition predicts personality and social outcomes three

decades later. *Proceedings of the National Academy of Sciences USA, 117*, 9800-9807. doi:10.1073/pnas.1917376117

Tang, D. W., Fellows, L. K., Small, D. M., & Dagher, A. (2012). Food and drug cues activate similar brain regions: a meta-analysis of functional MRI studies. *Physiol Behav, 106*, 317-324. doi:10.1016/j.physbeh.2012.03.009

Team, R. C. (2020). R: A language and environment for statistical computing. Version 4.0. 2 (Taking Off Again). *R Foundation for Statistical Computing, Vienna, Austria*.

ten Donkelaar, H. J., Tzourio-Mazoyer, N., & Mai, J. K. (2018). Toward a common terminology for the gyri and sulci of the human cerebral cortex. *Frontiers in Neuroanatomy, 12*. doi:10.3389/fnana.2018.00093

ten Have, M., Oldehinkel, A., Vollebergh, W., & Ormel, J. (2005). Does neuroticism explain variations in care service use for mental health problems in the general population? Results from the Netherlands Mental Health Survey and Incidence Study (NEMESIS). *Soc Psychiatry Psychiatr Epidemiol, 40*, 425-431. doi:10.1007/s00127-005-0916-z

Thake, J., & Zelenski, J. M. (2013). Neuroticism, BIS, and reactivity to discrete negative mood inductions. *Personality and Individual Differences, 54*, 208-213. doi:https://doi.org/10.1016/j.paid.2012.08.041

Theiss, J. D., Ridgewell, C., McHugo, M., Heckers, S., & Blackford, J. U. (2017). Manual segmentation of the human bed nucleus of the stria terminalis using 3T MRI. *Neuroimage, 146*, 288-292. doi:10.1016/j.neuroimage.2016.11.047

Thorp, J. G., Campos, A. I., Grotzinger, A. D., Gerring, Z., An, J., Ong, J.-S., . . . Derks, E. M. (2020). Symptom-level genetic modelling identifies novel risk loci and unravels the shared genetic architecture of anxiety and depression. *medRxiv*, 2020.2004.2008.20057653. doi:10.1101/2020.04.08.20057653

Tillman, R. M., Stockbridge, M. D., Nacewicz, B. M., Torrisi, S., Fox, A. S., Smith, J. F., & Shackman, A. J. (2018). Intrinsic functional connectivity of the central extended amygdala. *Human brain mapping, 39*, 1291-1312.

Torrisi, S., Gorka, A. X., Gonzalez-Castillo, J., O'Connell, K., Balderston, N., Grillon, C., & Ernst, M. (2018). Extended amygdala connectivity changes during sustained shock anticipation. *Transl Psychiatry, 8*, 33. doi:10.1038/s41398-017-0074-6

Torrisi, S., O'Connell, K., Davis, A., Reynolds, R., Balderston, N., Fudge, J. L., . . . Ernst, M. (2015). Resting state connectivity of the bed nucleus of the stria

terminalis at ultra-high field. *Hum Brain Mapp, 36*, 4076-4088. doi:10.1002/hbm.22899

Tovote, P., Fadok, J. P., & Luthi, A. (2015). Neuronal circuits for fear and anxiety. *Nat Rev Neurosci, 16*, 317-331. doi:10.1038/nrn3945

Tozzi, L., Staveland, B., Holt-Gosselin, B., Chesnut, M., Chang, S. E., Choi, D., . . . Williams, L. M. (2020). The human connectome project for disordered emotional states: Protocol and rationale for a research domain criteria study of brain connectivity in young adult anxiety and depression. *Neuroimage, 214*, 116715. doi:10.1016/j.neuroimage.2020.116715

Tozzi, L., Staveland, B., Holt-Gosselin, B., Chesnut, M., Chang, S. E., Choi, D., . . . Williams, L. M. (*in press*). The human connectome project for disordered emotional states: Protocol and rationale for a research domain criteria study of brain connectivity in young adult anxiety and depression. *Neuroimage*, 116715. doi:https://doi.org/10.1016/j.neuroimage.2020.116715

Tranel, D., Gullickson, G., Koch, M., & Adolphs, R. (2006). Altered experience of emotion following bilateral amygdala damage. *Cognitive Neuropsychiatry, 11*, 219–232.

Turner, R., & Geyer, S. (2014). Comparing like with like: the power of knowing where you are. *Brain Connect, 4*(7), 547-557. doi:10.1089/brain.2014.0261

Tustison, N. J., Avants, B. B., Cook, P. A., Zheng, Y. J., Egan, A., Yushkevich, P. A., & Gee, J. C. (2010). N4ITK: Improved N3 bias correction. *IEEE Transactions on Medical Imaging, 29*, 1310-1320. doi:10.1109/tmi.2010.2046908

Twenge, J. M., Cooper, A. B., Joiner, T. E., Duffy, M. E., & Binau, S. G. (2019). Age, period, and cohort trends in mood disorder indicators and suicide-related outcomes in a nationally representative dataset, 2005–2017. *Journal of Abnormal Psychology, 128*, 185-199. doi:10.1037/abn0000410

Uliaszek, A. A., Hauner, K. K., Zinbarg, R. E., Craske, M. G., Mineka, S., Griffith, J. W., & Rose, R. D. (2009). An examination of content overlap and disorder-specific predictions in the associations of neuroticism with anxiety and depression. *J Res Pers, 43*, 785-794. doi:10.1016/j.jrp.2009.05.009

Valk, S. L., Hoffstaedter, F., Camilleri, J. A., Kochunov, P., Yeo, B. T. T., & Eickhoff, S. B. (2020). A shared genetic basis for personality traits and local cortical grey matter structure? *bioRxiv*, 645945. doi:10.1101/645945

van Doorn, J., van den Bergh, D., Böhm, U., Dablander, F., Derks, K., Draws, T., . . . Wagenmakers, E.-J. (*in press*). The JASP guidelines for conducting and

reporting a Bayesian analysis. *Psychonomic Bulletin & Review*. doi:10.3758/s13423-020-01798-5

van Eeden, W. A., van Hemert, A. M., Carlier, I. V. E., Penninx, B. W., Spinhoven, P., & Giltay, E. J. (2019). Neuroticism and chronicity as predictors of 9-year course of individual depressive symptoms. *J Affect Disord, 252*, 484-492. doi:10.1016/j.jad.2019.04.052

Villalta-Gil, V., Hinton, K. E., Landman, B. A., Yvernault, B. C., Perkins, S. F., Katsantonis, A. S., . . . Zald, D. H. (2017). Convergent individual differences in visual cortices, but not the amygdala across standard amygdalar fMRI probe tasks. *Neuroimage, 146*, 312-319. doi:10.1016/j.neuroimage.2016.11.038

von Soest, T., Wagner, J., Hansen, T., & Gerstorf, D. (2018). Self-esteem across the second half of life: The role of socioeconomic status, physical health, social relationships, and personality factors. *Journal of Personality and Social Psychology, 114*, 945-958. doi:10.1037/pspp0000123

Wager, T. D., Keller, M. C., Lacey, S. C., & Jonides, J. (2005). Increased sensitivity in neuroimaging analyses using robust regression. *Neuroimage, 26*(1), 99-113. doi:https://doi.org/10.1016/j.neuroimage.2005.01.011

Wang, S., Tudusciuc, O., Mamelak, A. N., Ross, I. B., Adolphs, R., & Rutishauser, U. (2014). Neurons in the human amygdala selective for perceived emotion. *Proc Natl Acad Sci U S A, 111*, E3110-3119. doi:10.1073/pnas.1323342111

Watson, D., Stanton, K., & Clark, L. A. (2017). Self-report indicators of negative valence constructs within the research domain criteria (RDoC): A critical review. *J Affect Disord, 216*, 58-69. doi:10.1016/j.jad.2016.09.065

West, H. V., Burgess, G. C., Dust, J., Kandala, S., & Barch, D. M. (2021). Amygdala Activation in Cognitive Task fMRI Varies with Individual Differences in Cognitive Traits. *Cogn Affect Behav Neurosci, 21*(1), 254-264. doi:10.3758/s13415-021-00863-3

Weston, S. J., & Jackson, J. J. (2018). The role of vigilance in the relationship between neuroticism and health: A registered report. *Journal of Research in Personality, 73*, 27-34.

Wettstein, M., Wahl, H. W., & Siebert, J. S. (*in press*). 20-year trajectories of health in midlife and old age: Contrasting the impact of personality and attitudes toward own aging. *Psychol Aging*. doi:10.1037/pag0000464

Widiger, T. A., & Oltmanns, J. R. (2017). Neuroticism is a fundamental domain of personality with enormous public health implications. *World Psychiatry, 16*, 144-145. doi:10.1002/wps.20411

Woo, C. W., Chang, L. J., Lindquist, M. A., & Wager, T. D. (2017). Building better biomarkers: brain models in translational neuroimaging. *Nat Neurosci, 20*(3), 365-377. doi:10.1038/nn.4478

Yilmazer-Hanke, D. M. (2012). Amygdala. In J. K. Mai & G. Paxinos (Eds.), *The human nervous system* (pp. 759-834). San Diego: Academic Press.

You, X., Huang, J., Wang, Y., & Bao, X. (2015). Relationships between individual-level factors and burnout: A meta-analysis of Chinese participants. *Personality and Individual Differences, 74*, 139-145. doi:https://doi.org/10.1016/j.paid.2014.09.048

Zemestani, M., Ommati, P., Rezaei, F., & Gallagher, M. W. (2021). Changes in neuroticism-related constructs over the Unified Protocol for Transdiagnostic Treatment of Emotional Disorders in patients on an optimal dose of SSRI. *Personal Disord*. doi:10.1037/per0000482

Zentner, M., & Shiner, R. L. (2012). Fifty years of progress in temperament research: A synthesis of major themes, findings, and challenges and a look forward. In M. Zentner & R. L. Shiner (Eds.), *Handbook of temperament* (pp. 673-700). New York, NY: Guilford Press.

Zhang, Y., Brady, M., & Smith, S. (2001). Segmentation of brain MR images through a hidden Markov random field model and the expectation-maximization algorithm. *IEEE Transactions in Medical Imaging, 20*, 45-57.

Zuckerman, M. (1976). General and situation-specific traits and states: new approaches to assessment of anxiety and other constructs. In M. Zuckerman & C. D. Spielberger (Eds.), *Emotions and anxiety: new concepts, methods and applications* (pp. 133-174). Hillsdale, NJ: Lawrence Erlbaum.